Title

Activation of Aryl C—H Bonds Through the Utilization of Iron and Cobalt Catalytic Systems

Author

Crowley III, Robert Thomas

Publication Date

2024

Peer reviewed|Thesis/dissertation

UNIVERSITY OF CALIFORNIA
RIVERSIDE

Activation of Aryl C–H Bonds Through the Utilization of Iron and Cobalt Catalytic Systems

A Dissertation submitted in partial satisfaction
of the requirements for the degree of

Doctor of Philosophy

in

Chemistry

by

Robert Thomas Crowley III

March 2025

Dissertation Committee:
Dr. Kevin Kou, Chairperson
Dr. Michael Pirrung
Dr. Christopher Switzer

The Dissertation of Robert Thomas Crowley III is approved:

_____

_____

_____

Committee Chairperson

University of California, Riverside

Acknowledgements:

The text of this dissertation, in part or in full, is a reprint of the material as it appears in the following publications:

Chapter 2: Crowley, R. III; Lujan, B.; Martinez, A.; Manasi, R.; DeBow, J. D.; Kou, K. G. M., A Fenton approach to aromatic radical cations and diarylmethane synthesis. *Journal of Organic Chemistry* **2023**, *88*, 15060–15066.

Chapter 3: Pan, A.; Chojnacka, M.; Crowley III, R.; Gottemann, L.; Haines, B.; Kou, K. G. M., Synergistic Brønsted/Lewis acid catalyzed aromatic alkylation with unactivated tertiary alcohols or di-*tert*-butylperoxide to synthesize quaternary carbon centers. *Chemical Science* **2022**, *13*, 3539–3548.

The co-author Kevin G. M. Kou listed in these publications directed and supervised the research which forms the basis for this dissertation. All other co-authors listed in these publications contributed technical expertise.

I acknowledge,

Dr. Kevin Kou for taking me in when my previous mentor left the university and many years of mentorship and guidance. For allowing me the opportunity to gain experience in a variety of analytical techniques, and for always pushing me to do more than was required, teaching me to value intellectual challenges for the sake of the challenge.

Dr. Lingchao Zhu for his help with deuterium NMR and EPR experiments, which were essential for the mechanistic studies in **Chapter 2**.

Dr. Jie Zhou for teaching me to use MALDI-TOF instrumentation and how to manipulate parameters on the HRMS to observe weakly-ionizing compounds.

Dedication:

This dissertation is dedicated to my parents, Robert Crowley Jr. and Lucille Crowley, and to my sister Maria Crowley whose constant support and encouragement made this entire process possible. It is also dedicated to my darling boyfriend Christopher Drozd who was by my side through the more challenging moments both in the writing of this document and the performance of the research that these pages describe.

ABSTRACT OF THE DISSERTATION

Activation of Aryl C–H Bonds Through the Utilization of Iron and Cobalt Catalytic Systems

by

Robert Thomas Crowley III

Doctor of Philosophy, Graduate Program in Chemistry
University of California, Riverside, March 2025
Dr. Kevin Kou, Chairperson

The ability to create new carbon–carbon bonds impacts pharmaceutical, agrochemical, and materials development. While this field has progressed significantly, the most common methods rely heavily on the usage of expensive, precious metal catalysts. In this dissertation, three methods will be presented that expand the synthetic toolbox for forging C–C bonds through use of inexpensive, readily-accessible metals.

Iron is a particularly attractive catalyst due to its earth-abundance and ease of handling. Fenton's reagent, a mixture of Fe(II), hydrogen peroxide, and sulfuric acid that catalyzes the radical alkylation of pyridines (*i.e.*, the Minisci reaction), was inspiration for our synthesis of diarylmethanes, which involves C–H abstraction of methanol, coupling of the resultant hydroxymethyl radical with an arene to form benzylic alcohol intermediates, followed by electrophilic aromatic substitution. Iron was also used to expand the utility of the Friedel–Crafts reaction. Here, a dual Brønsted/Lewis acid catalytic system was

developed, enabling arene alkylation with unactivated tertiary alcohols, reactants that previously required heterogeneous superacids to achieve reactivity.

The final part of the dissertation focuses on using cobalt to replace rhodium for directed C–H activation. Departing from conventional reactivity with electron-poor alkenes and alkynes, our lab develops novel methods using electron-rich coupling partners, ultimately expanding the types of products that can be synthesized. Specifically, exploiting cobalt for C–H activation of arenes bearing a simple amide directing group and its subsequent coupling with electron-rich alkynes, an underexplored substrate class, will be presented.

Table of Contents

List of figures

List of tables

List of abbreviations

SAR……Structure activity relationship

DYRK1A……..……..Dual-specificity tyrosine phosphorylation–regulated kinase 1A

MAO-A……..Monoamine oxidase A

EAS…….....Electrophilic aromatic substitution

NBS…….*N*-bromosuccinamide

NCS…….*N*-chlorosuccinamine

EDG……Electron-donating group

BOX……..Bisoxazoline

BINOL……1,1’-Bi-2-napthol

PYBOX……Bisoxazolinyl-pyridine

BINAP……...2,2′-bis(diphenylphosphino)-1,1′-binaphthyl

dppf.…..bis(diphenylphosphino)ferrocene

coe……...cyclooctene

TFA……..trifluoroacetic acid

DCE……1,2-dichloroethane

TPP…….*meso*-tetraphenylporphyrin

HFIP……...1,1,1,3,3,3-Hexafluoro-2-propanol

TEMPO……..(2,2,6,6-Tetramethylpiperidin-1-yl)oxyl

KIE……...Kinetic isotope effect

NMR……..Nuclear magnetic resonance

SFC……...Supercritical fluid chromatography

DFT……Density functional theory

DTBP……..Di-*tert*-butyl peroxide

Chapter 1: Reactions for the functionalization of arenes

1.1 Arene functionalization for medicinal chemistry

In the world of commodity products, the pharmaceutical industry is one that commands a $1.6 trillion value, and is essential for the health and well-being of people worldwide. For this reason, a large body of research has been dedicated to analyzing the ways that the structure of a molecule informs its pharmacological activity. These studies go back to 1997 when Lipinski published the "rule of five", one of the important aspects of which is the presence of more than five H-bond donors on a molecule would hinder its absorption/permeability.[1] In the years following, studies have been published examining everything from molecular weight[2] to how the number of aromatic rings affects permeability.[3] To facilitate these studies, much of the efforts devoted to synthetic methods development targeted new ways to synthesize potential drug targets.

A survey of papers published by Pfizer, AstraZeneca, and GlaxoSmithKline containing 3,500 potential drug targets found that 99% of the molecules contained at least one aromatic ring.[4] For this reason, methods that allow for the construction or functionalization of aromatic compounds is of particular interest as they facilitate the creation of deep compound libraries. In particular, the ability to perform late-stage functionalization is a powerful strategy as it means a scaffold with known pharmacological properties can be constructed and then modified to perform SAR studies, helping to identify the ideal drug candidate.[5–6] One recently published example was the synthesis of male gamete formation inhibitor for the blockage of malaria transmission.[7] The

development (**Figure 1.1**) began with compound **1** which had been discovered in a high throughput screen with the concentration needed to reach 50% effectiveness (EC_{50}) being 292±38 nM.[8] Modifications of the arenes associated with the chromane and sulfonamide functional groups led to structure **2** with EC_{50} = 79±18 nM, which corresponds to a 3.7 times enhancement in potency.

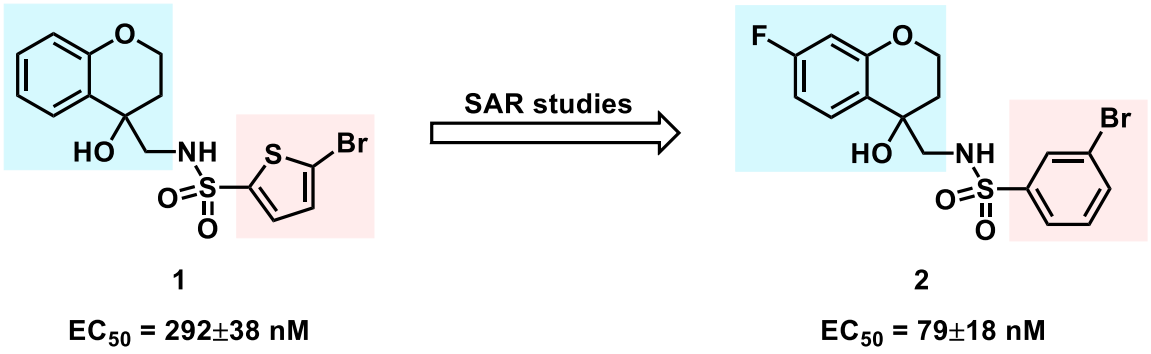

Figure 1.1 Structure-activity relationship studies to improve a male gamete formation inhibitor.
Through fluorination of the chromane (blue) ring and swapping of the sulfonamide bromo-arene (red) the required dosage can drop substantially

Late-stage arene functionalization is particularly powerful when the structure of the target enzyme is known.[9] While the risk of overinterpretation of these structures is a problem, modeling of target enzymes can help to guide lead optimization when used correctly without the need for vast compound libraries to be synthesized in advance.[10] In 2007, the β-carboline alkaloid harmine (**3**) was identified as a DYRK1A inhibitor, however it's usage as a potential therapeutic is limited as it also inhibits MAO-A, an enzyme that maintains neurotransmitter homeostasis, at an even lower concentration.[11–12] DYRK1A plays an important role in neuronal development, and there is significant evidence that overexpression of this gene is tied to altered brain development in individuals with Down

syndrome.[13] To address this, a recent study utilized protein modeling simulations to discover a more selective derivative of harmine (**Figure 1.2**).[14]

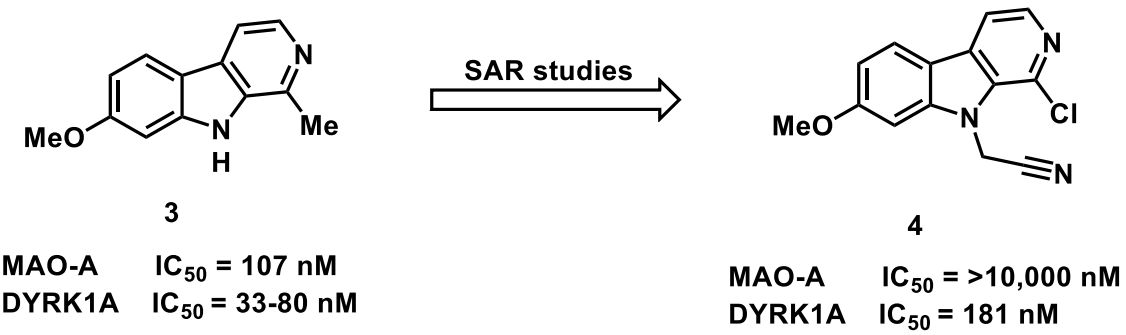

Figure 1.2 Structures of harmine and the modified structure.

Through analysis of the binding models (**Figure 1.3**), an interaction that can easily be targeted is observed, namely a favorable H-bond between the indole nitrogen and two amino acid residues (Ile 207 and Asn181), which is not present in DYRK1A.

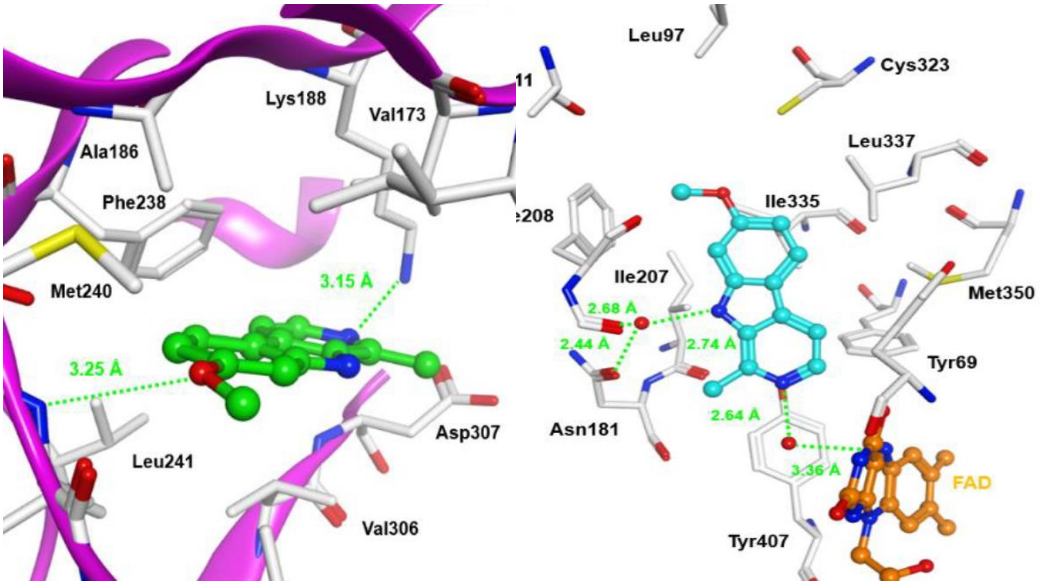

Figure 1.3 Binding modes of harmine in DYRK1A and MAO-A.
Calculated binding modes of harmine in DYRK1A (left) and MAO-A (right) with the H-bonding interactions shown

A series of arene alkylations/halogenations and indole *N*–alkylation arrived at compound **4**, which maintained the DYRK1A inhibition while being devoid of MAO-A inhibition activity. The main modification involved the swapping of the methyl group on the pyridyl component for chlorine, and attaching a cyanomethyl group to the indole nitrogen.

In both above examples, the optimized compounds were discovered through a mix of starting material swapping and late-stage functionalization. The latter has the advantage of allowing for "on-the-fly" modification as information is gained through biological testing of compounds. When late-stage modification is not possible, a new synthesis plan is required, adding additional time and resource requirements to discover potential drug candidates. For example, in optimizing harmine (**3**), the installation of the chlorine to the pyridyl component could not be accomplished via direct modification as no methods existed to substitute an alkyl group for a chlorine. To accomplish this transformation, a five-step sequence was required, starting from *meta*-anisidine.[15] In order to facilitate the sort of transformations that would allow for late-stage modifications, a great body of research has been dedicated to methods for direct functionalization of activated aromatic rings. This chapter focuses on direct arene functionalization methods which is divided into four main reaction types for clarity.

1.2 Electrophilic aromatic substitution (EAS) reactions

One of the reported methods for benzene functionalization dates back to the 19th century when Henry Armstrong reported the first electrophilic aromatic substitution reaction (EAS).[16] This reaction employs arene nucleophiles to form new bonds with a

variety of different electrophiles. This reaction (**Scheme 1.4**) proceeds through σ-complex **5**, proposed by George Wheland, which has come to be known as the Wheland intermediate.[17] Rearomatization yields functionalized product **6**.

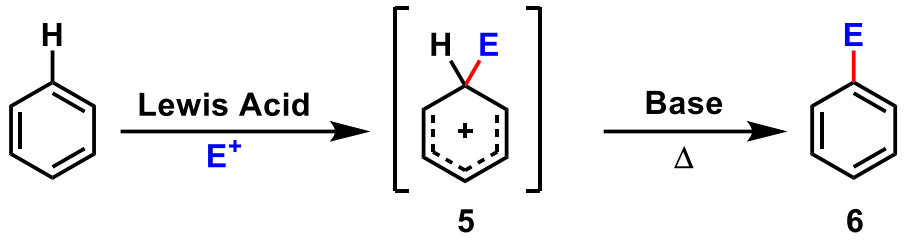

Figure 1.4 General mechanism of the EAS reaction

With reactions of this type, the selectivity needs to be carefully considered. For example, the preparation of 2-bromotoluene (**9**) via EAS would not proceed directly from toluene as steric effects would favor formation of 4-bromotoluene (**10**). If, instead, an alkylation was performed (**Figure 1.5**) to yield 4-*tert*-butyltoluene (**7**), the subsequent halogenation would yield 2-bromo-4-*tert*-butyltoluene (**8**) as an intermediate. A final aluminum-mediated dealkylation would yield the target 2-bromotoluene (**9**), albeit in a more step-intensive manner.[18]

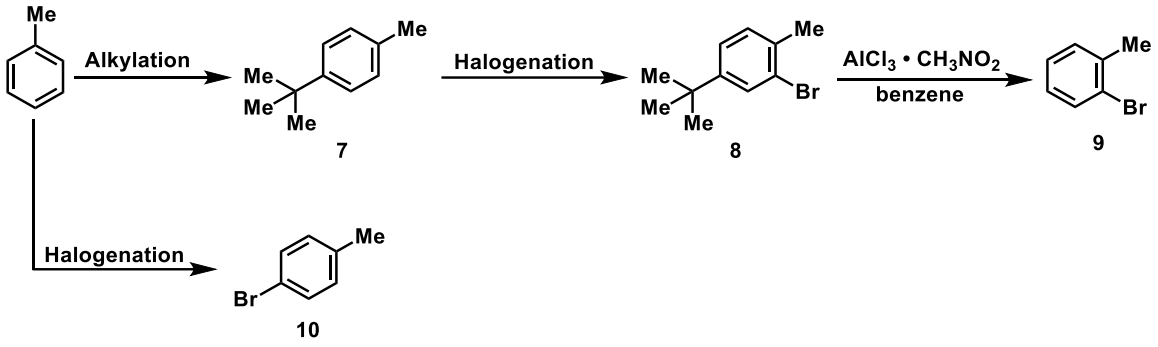

Figure 1.5 A method for the synthesis of 2–bromotoluene
Through the utilization of a positional protecting groups the standard selectivity of EAS reactions can be circumvented.

This method is limited, only allowing for the formation of functionalized benzenes whose functional groups will not react in the deprotection step. The remainder of this section will focus on the variety of electrophiles that work for this reaction, with a primary focus on the ones that will be relevant in later chapters.

1.2.1 *Arene halogenation via electrophilic aromatic substitution*

Aryl halides are attractive synthesis targets for their applications in a wide array of drug target molecules.[19] As such, the ability to utilize EAS reactions to directly install a halogen is of great interest. The earliest example involved the treatment of phenol with bromine in carbon disulfide, yielding the *para*-substituted product.[20] However, the danger of working with elemental bromine made other alternatives desirable. Also, when this method is utilized in the presence of any benzylic C–H bonds, the benzylic halogenation pathway dominates, giving the benzyl bromide product.[21] This problem can be circumvented through the utilization of an iron(III) Lewis acid, which allows for arene halogenation in the presence of a benzylic C–H.[22] To avoid the need for molecular bromine, NBS can be utilized allowing for direct halogenation of rings in the presence of benzylic C–H bonds provided the temperature is controlled.[23] This reaction also alleviates the need for molecular chlorine to perform chlorinations, as NCS is also reactive in this transformation.[24] This change is an important one as the gaseous nature of chlorine makes it a challenge to work with. Over the years, to facilitate these key transformations a number of chlorinating[25], brominating[26], and iodinating[27] agents have been developed (**Figure 1.6**).

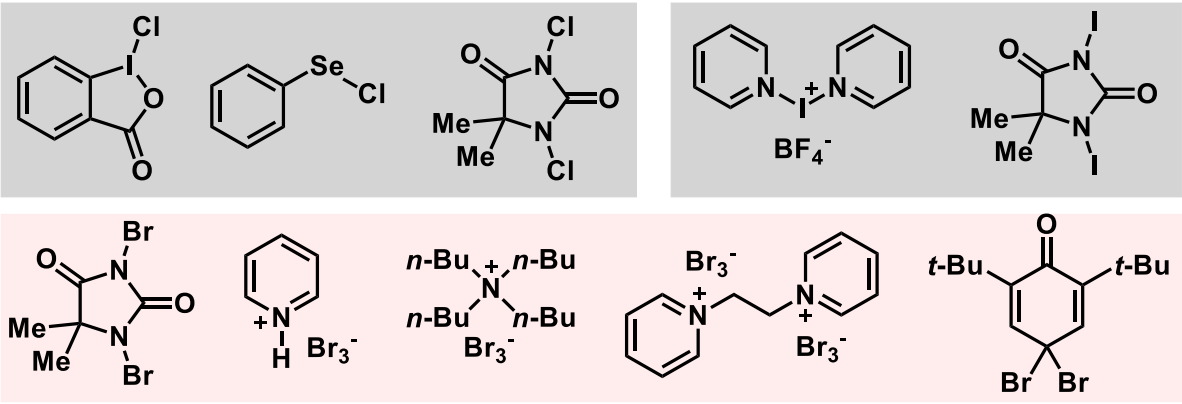

Figure 1.6 A selection of common halogenation agents
The structures of commonly used chlorinating (top left), brominating (bottom), and iodinating (top right) agents used in arene halogenation.

1.2.2 *The Friedel-Crafts alkylation*

In the pharmaceutical industry, the ability to form C–C bonds on arene rings is a key transformation. In particular, the installation of sp^3 hybridized carbons has been of interest as a link has been found between higher degrees of saturation and clinical success.[28] This success is explained by improved binding affinity, aqueous solubility, and decreased crystallinity, key traits for the development of a drug molecule.[29] For this reason, the ability to use EAS to achieve this transformation has been heavily explored.

In 1877, the first example of an EAS reaction being used to alkylate aromatic rings was reported.[30] This reaction was named after Charles Friedel and James Mason Crafts who discovered it. The original report (**Figure 1.7**) utilized amyl chloride (**11**) and a strong Lewis acid, primarily $AlCl_3$ and $FeCl_3$, to perform direct alkylation of benzene.

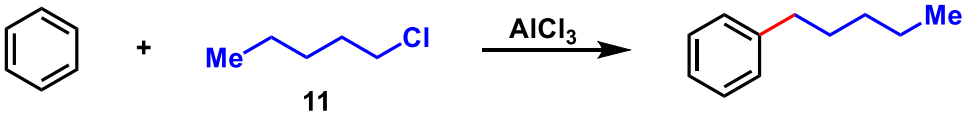

11

Figure 1.7 The first reported Fridel-Crafts alkylation utilizing $AlCl_3$ as a Lewis acid

In the time since its initial discovery, this reaction has been demonstrated to work with a variety of different Lewis acids, catalyzed by various strong Brønsted acids or super acid promoters.[31] One of the biggest problems that needed to be tackled with this reaction is the utilization of toxic alkyl halides, leading to the generation of stoichiometric quantities of inorganic salts as byproducts of the reaction. To address this issue, a variety of electrophiles have been tested. Substrate classes that have seen thorough exploration are activated allylic, benzylic, and propargylic alcohols; however, those discoveries will be essential to the project discussed in the third chapter of this document and as such will be discussed in the introduction of that chapter.

Another class of feedstock chemical that has been targeted for the Friedel-Crafts alkylation are alkenes. Due to the availability of propene as a feedstock chemical, its usage in this reaction has been the subject of great interest. Through the usage of BF_3•H_3PO_4[32] and $AlCl_3$•$MeNO_2$[33] catalyst systems, this reaction was achieved with limited regioselectivity (**Figure 1.8**).

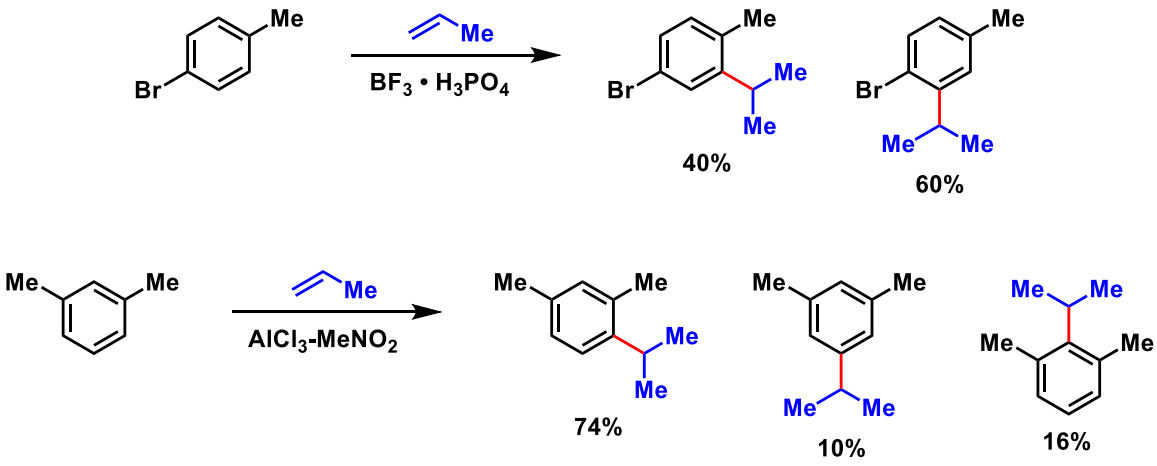

Figure 1.8 Early examples of Friedel-Crafts alkylations on propylene

The product distribution in these reactions is largely driven by electronic effects on the ring, preferring to alkylate *ortho-para* to the strongest EDG, and sterics when the electronics are similar.

α,β-Unsaturated ketones (**Figure 1.9**) work similarly well when utilizing the same catalytic system that was originally reported by Friedel and Crafts.[34] Mechanistically this reaction resembles a Lewis acid catalyzed Michael addition to achieve alkylation.

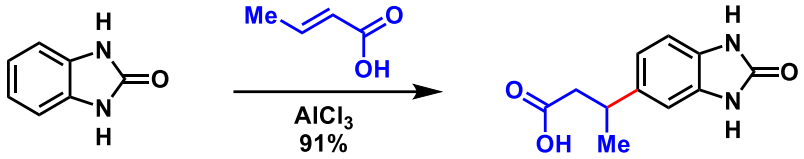

Figure 1.9 Friedel-Crafts reaction on electron-deficient alkenes

The utility of this transformation has led to a large body of research on methods to render this reaction asymmetric. The first success was discovered by the Jørgensen group utilizing Cu(II)-BOX Lewis acids (**Figure 1.10**).[35] The enantioselectivity is heavily tied to the presence of two Lewis basic sites in the vicinity of the alkene being attacked. This is demonstrated by the success of β,γ-unsaturated-α-ketoesters **12** and α'-hydroxyenones **13** while alkylidine malonates **14** only showed moderate enantioselectivity.[36,37] The need for an additional coordinating group can be circumvented when Sc(III)-PYBOX[38], Pd(II)-BINAP[39], Al(III)-salen[40], Zr(IV)-BINOL[41], or Zn(II)-BOX[42] complexes are employed.

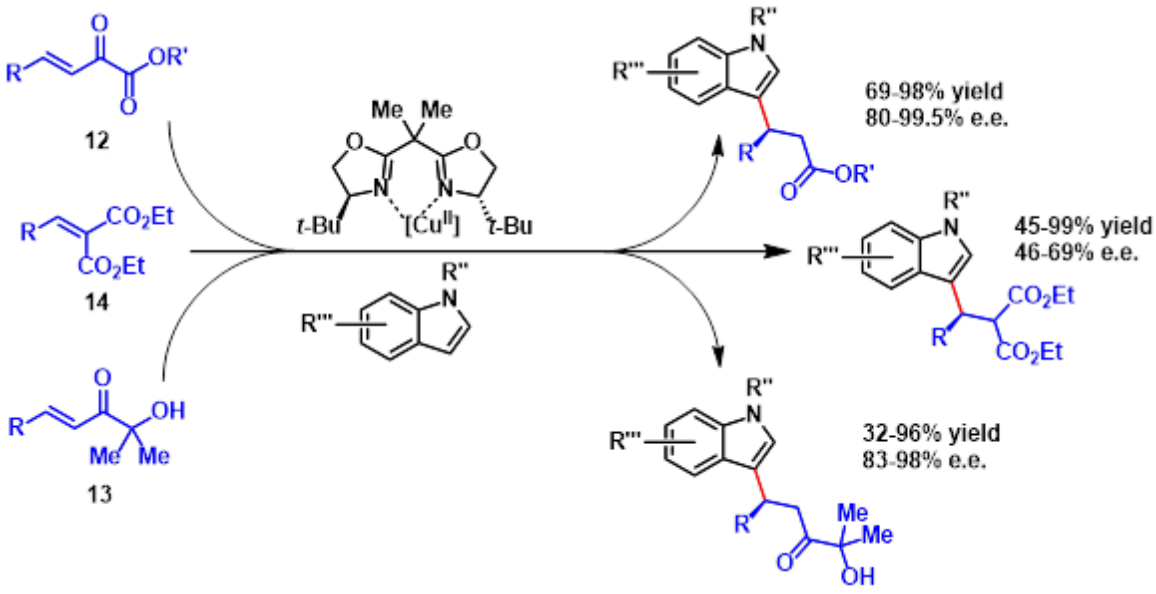

Figure 1.10 Asymmetric Friedel-Crafts alkylations of enones
Enantioselective Friedel-Crafts reaction with indoles chosen for the sake of comparison. Furans and anisoles (top) and indoles (bottom) were also effective substrates for this chemistry.

This chemistry also carries over well to direct addition into carbonyl carbons. In these cases, the attack occurs to yield a benzylic alcohol; however, this adjacency to the benzene ring allows for additional reactivity to occur (**Figure 1.11**), generating a new product. In the first reported reaction of this type, benzaldehyde reacts with benzene to generate diphenylmethanol (**15**), which then forms diphenylmethane cation (**16**) en route to triphenylmethane (**17**) as the final product.[43]

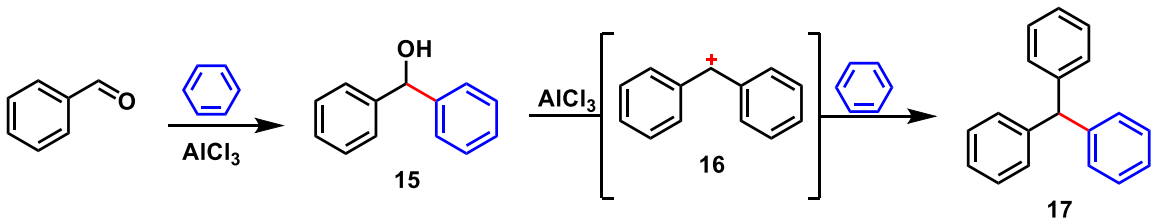

Figure 1.11 Friedel-Crafts alkylations on aldehydes

1.3 Aryl cross-coupling reactions

While EAS provides an incredibly useful method for the functionalization of arene rings, limitations exist. Since the reaction relies on the nucleophilicity of the arene, electron-deficient arenes tend not to be viable substrates. Furthermore, while the scope of electrophiles is broad, certain substrates, like electron-rich arenes, perform poorly in this role due to their electronics and inability to form a complex with the Lewis acid, which is essential for the reaction to proceed. For this reason, other methods have been explored to access C(aryl)–C(aryl) bonds, while targeting electron-deficient arenes, which normally present a challenge for EAS reactions.

1.3.1 *C(sp^2)–C(sp^2) Cross-coupling reactions*

In 2010, the Nobel Prize in Chemistry was awarded to Richard Heck, Ei-ichi Negishi, and Akira Suzuki for their development of palladium-catalyzed methods for C–C bond formations. These new methods represented the pioneering steps for a field of research that has exploded in the years since. The first of these methods was developed by Heck (**Figure 1.12**) and involved the coupling of an organomercury to various electron-deficient alkenes utilizing a palladium and copper catalytic system.[44] Owing to a desire to move away from the utilization of toxic mercury reagents, Heck[45] and Mizoroki[46] independently developed alternatives using aryl iodides as substitutes.

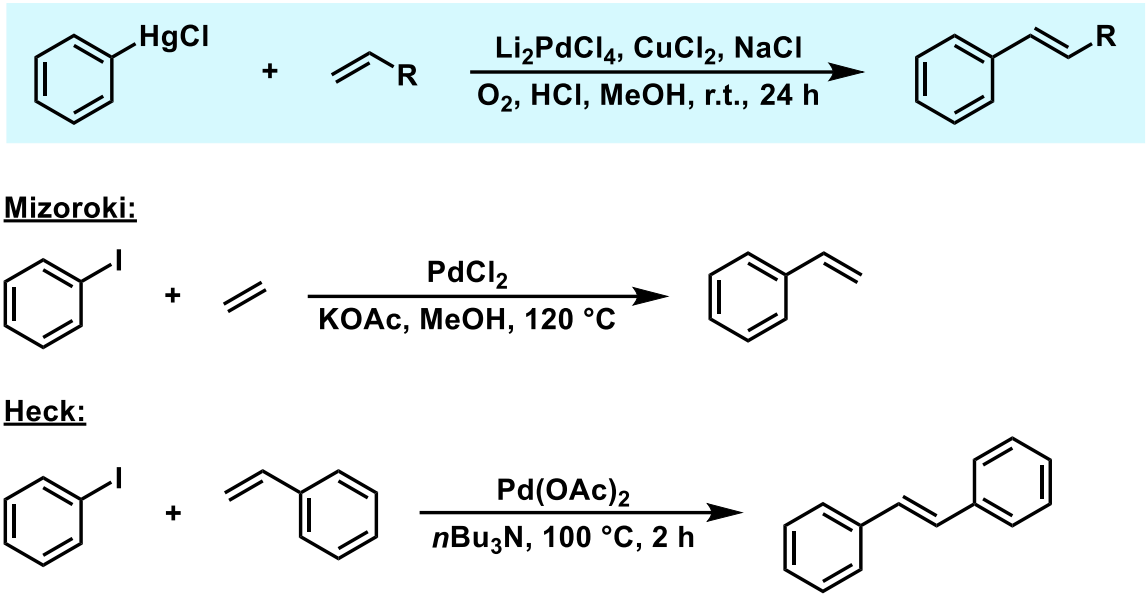

Figure 1.12 The first discovered Palladium catalyzed cross-couplings
The similarity and time proximity of these publications led to this class of reactions being referred to as the Mizoroki-Heck reaction.

Negishi's seminal contribution utilized organoaluminium reagents[47]; however, the synthesis of the organoaluminium reagents presented a challenge that shifted his focus to organozinc reagents[48] (**Figure 1.13**), which did not suffer from the same problems.

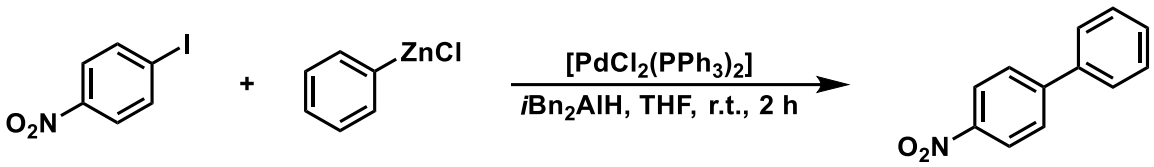

Figure 1.13 Conditions for the Negishi cross-coupling

Suzuki studied an element that shares a group with the aluminum that made up the start of Negishi's work, namely boron. While Heck had shown that boronic acids could be utilized when stoichiometric palladium was employed[49], Suzuki and his co-worker Miyaura rendered the reaction catalytic.[50] This reaction presented several advantages over

the reactions that preceded it. The first and most important is that the boronic acid starting materials are typically air stable, making them significantly easier to handle than other organometallic reagents. Furthermore, the reaction conditions were milder and the inorganic byproducts of the reaction are easier to remove and much less toxic than the metal salts generated by other methods.

These three reaction classes can be sorted into two mechanistic paradigms, with the Heck reaction separating itself from the other two (**Figure 1.14**). Both cases begin with an oxidative addition of the palladium catalyst into the aryl halide, generating intermediate **18**. For the Heck reaction, the mechanism proceeds with the formation of a π-complex **19** between palladium and the alkene. Migratory insertion of the alkene into the palladium-carbon bond generates palladium alkyl **20**, which undergoes β-hydride elimination to generate a new π-complex **21**, followed by ejection of the product **22**. Reaction of the metal hydride with base regenerates the catalyst. The Suzuki and Negishi reactions involve **18** undergoing transmetalation with the organoboron and organozinc coupling partners **23** to generate dialkylpalladium **24**, which then reductively eliminates to yield product **25**, while regenerating the catalyst.

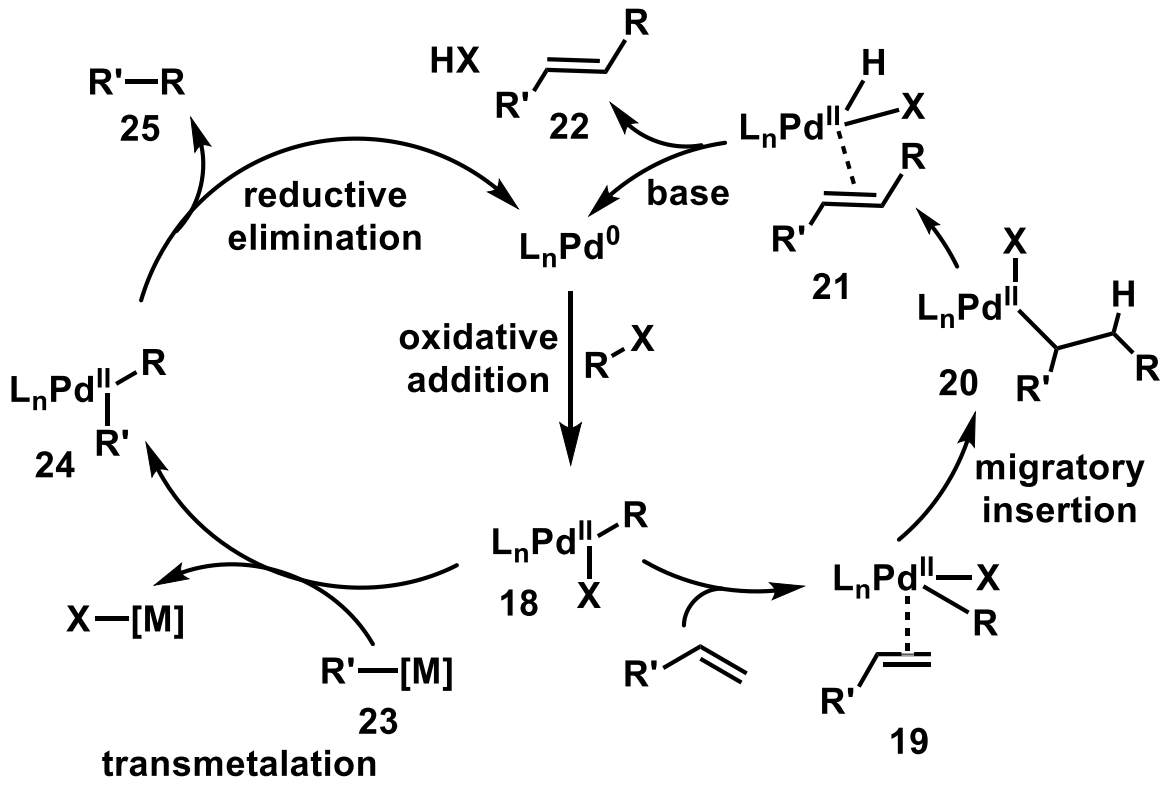

Figure 1.14 Catalytic cycles for cross-coupling reactions
The Heck (right) and Negishi/Suzuki (left) reaction mechanisms start similarly but differ with how the palladium catalyst engages the non-halogen coupling partner.

Beyond the three Nobel prize winners, there is an extensive collection of named reactions (**Figure 1.15**) that varies the organometallic nucleophiles to give access to other groups of substrates. These include Grignard reagents, organolithiums[51], organostannanes[52], and organosilanes[53]. Three substrate classes that do not technically fit in this section but bear mentioning due to their utility are acetylide cuprates, which perform $C(sp^2)$–C(sp) couplings[54,55], amines which can be used to form new C–N bonds[56,57], and alcohols which make C–O bonds.[58]

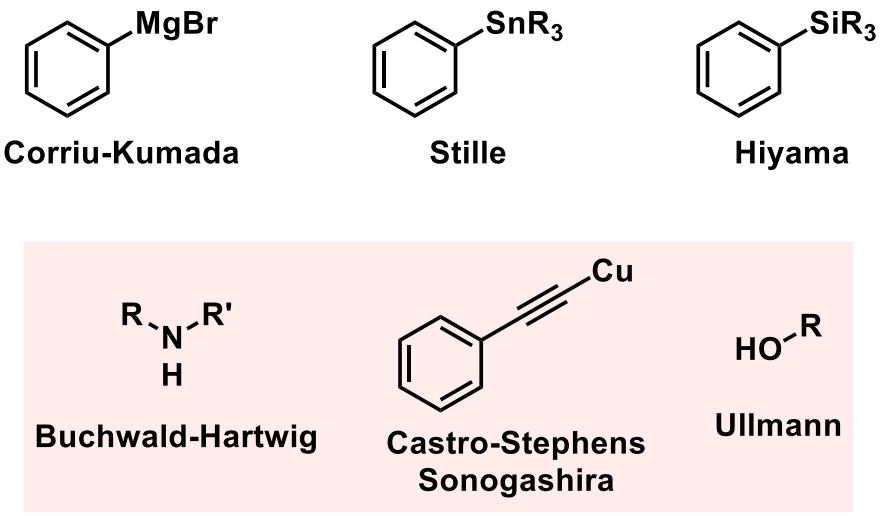

Figure 1.15 Collection of cross-coupling partners and their named reactions

One final, less commonly utilized cross-coupling advancement is the swapping of one of the coupling partners for a benzoic acid. This decarboxylative method has been utilized to replace the aryl halide of the Heck reaction[59] or the transmetalation components (*i.e.*, organostannane, organozinc, etc.) of the other cross-coupling methods.[60] The simplicity of these reactions has led to their heavy adoption in industrial synthesis processes. This ease of carrying out the chemistry, coupled with the biological activity, are the main reasons for modern pharmaceutical compounds containing multiple aromatic rings, a trend that has only recently been reevaluated due to discoveries about drug efficacy.

1.3.2 *C(sp^2)–C(sp^3) Cross-couplings*

Concurrent to the development of arene–arene C(sp^2)–C(sp^2) cross-coupling reactions was the development of C(sp^2)–C(sp^3) coupling methodologies. The Corriu-Kumada[61], Negishi[62], Stille[63], and Suzuki[64] coupling reactions all have early examples with

alkyl coupling partners, with only the Negishi coupling having significantly lowered yields relative to the arene-arene coupling. When more complicated Grignard reagents are utilized in these reactions (**Figure 1.16**), the original conditions can present a challenge when using standard catalysts like $PdCl_2(PPh_3)_2$.[65] In this case, the utilization of the dppf ligand improves the reactivity to produce synthetically useful yields.

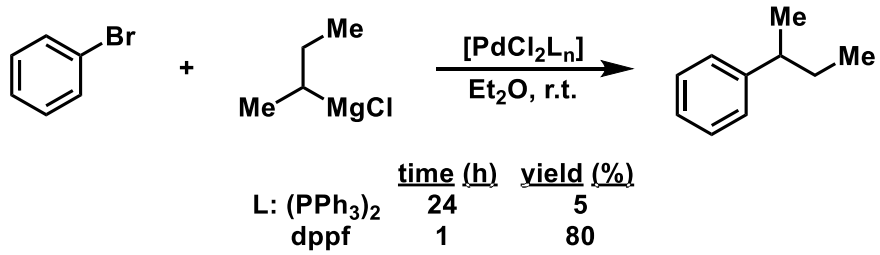

Figure 1.16 Ligand effects in the Corriu-Kumada coupling

Additionally, the utilization of 2-alkyl and 2-arylaziridines (**Figure 1.17**) can yield cross–coupling products when paired with arylboronic acids. This chemistry demonstrates a high degree of regioselectivity, and when the right ligand is utilized, these reactions can also be rendered enantioselective, generating chirality found in pharmaceutical development.[66,67]

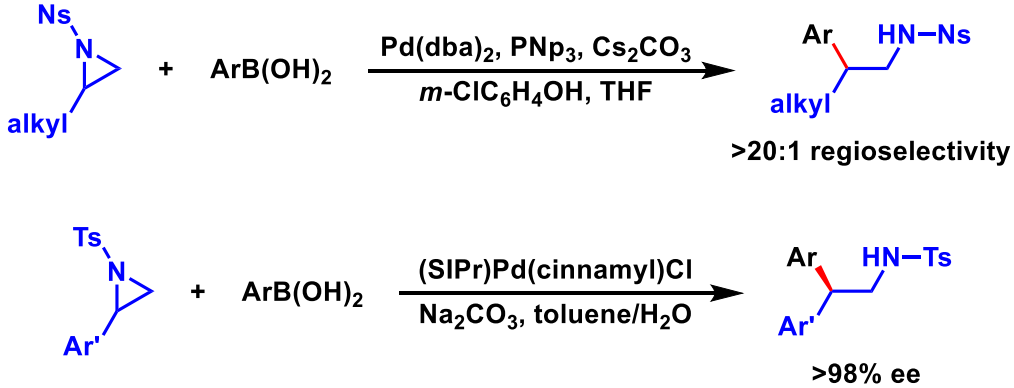

Figure 1.17 Cross-coupling reactions utilizing aziridine coupling partners

In a manner like the one above, the utilization of new palladium/ligand systems can allow access to other enantioenriched compounds. For example, when MandyPhos was employed (**Figure 1.18**) by the Morken group, an enantioselective conjunctive cross-coupling took place to form an alkylborane, which can then be oxidized to give chiral alcohols, installing the alcohol and benzene ring in a single step.[68]

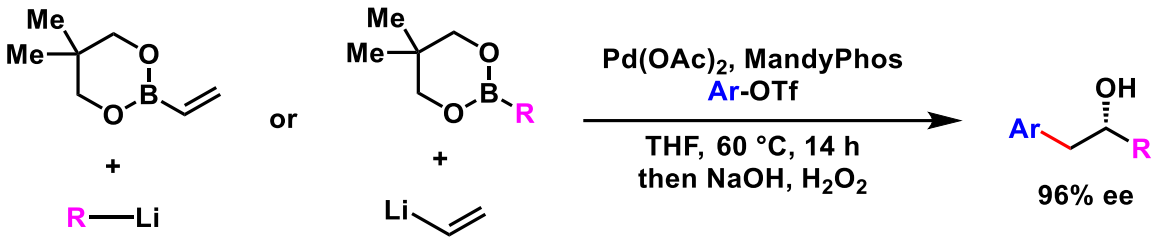

Figure 1.18 Enantioselective Suzuki-type conjunctive cross-coupling

The more recent developments in this area have primarily focused on the movement away from the palladium catalytic systems to other metals; however, this transition will be more relevant to the discussions that will occur in **Section 1.5**, and as such those reactions will be discussed in-depth in that section.

1.4 C–H activations

While the discovery of cross-coupling reactions added greatly to the toolbox of chemists looking to functionalize arene rings, it suffers from one major drawback, namely the need for both coupling partners to be functionalized, with one being a halide and the other having a carbon-metal bond. An early example of a reaction that avoids this requirement involved a metal inserting into an arene C–H bond when the auration of

benzene by a Au(I) catalyst was reported.[69] One of the defining characteristics of this chemistry is the utilization of directing groups to guide the site of metal insertion. The nature of this direction was shown when the isolation of the complex (**Figure I.19**) derived from the azo-directed insertion of nickel into an arene C–H bond was accomplished.[70]

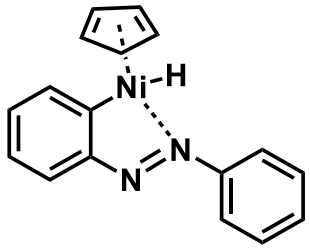

Figure 1.19 Isolated nickel C–H activation complex

With the metal integrated into the arene, the next step is for it to engage another reactant. The Fujiwara reaction (**Figure 1.20**) represents one of the pioneering examples of this chemistry that complements the Heck reaction by removing the need for the arene component to be prefunctionalized.[71] This reaction involves an initial C–H activation by concerted-metalation-deprotonation (CMD) to form organopalladium **26**, followed by migratory insertion of the alkene into the carbon–palladium bond. The remainder of reaction pathway resembles the traditional Heck reaction (**Figure 1.12**) to yield the alkenylated product.

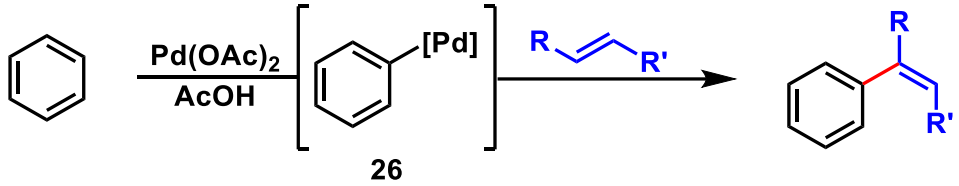

Figure 1.20 General scheme for the Fujiwara reaction

The Suzuki reaction can also be improved in a similar manner. Through the utilization of amide, oxime, and pyridine directing groups, or even in the absence of directing groups, the coupling of alkyl and aryl boronic acids to arenes can be accomplished.[72] The main limitation of the non-directed version of this reaction is the reliance on a high degree of substitution to block off reactive sites and minimize over-alkylation. Electron-rich heterocycles (*e.g.* indoles) are also capable of reacting without directing group assistance, preferring to react at the 2-position of the ring. The reactivity can also extend to alkyl C–H bonds, performing β-arylation (**Figure 1.21**), albeit in low yields.[73]

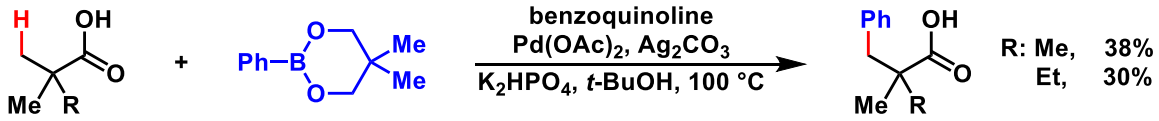

Figure 1.21 C–H activation of alkyl C–H bonds

This reactivity can also be extended to Hiyama- and Stille-type couplings, commonly requiring a copper co-catalyst to act as a sacrificial oxidant to keep the reaction catalytic in terms of the much more expensive palladium component. The major undesirable feature of this chemistry is the need for a directing group to facilitate the C–H activation step, guiding the metal to a specific location. One solution (**Figure 1.22**) that gets around this problem utilizes indole, a motif commonly seen in pharmaceutical molecules, as the directing group for a Heck-type reaction, though this method is only effective when the desired product contains the indole moiety.[74]

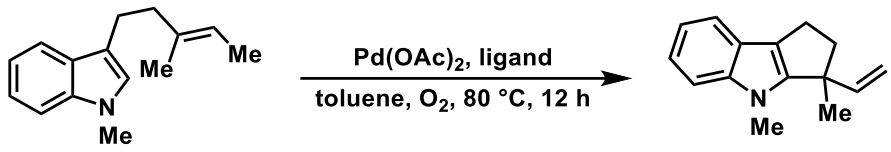

Figure 1.22 The utilization of indole as a self-directing C–H activation target

Beyond their functionalization, the synthesis of indoles is important due to the wide array of pharmacological properties associated with them.[75] The Glorius lab developed a two-step method (**Figure 1.23**) to synthesize indoles from anilines, starting with an enamine condensation to arrive at **27**, then a subsequent C–H activation step to yield indole-3-carboxylic acid esters **28**.[76]

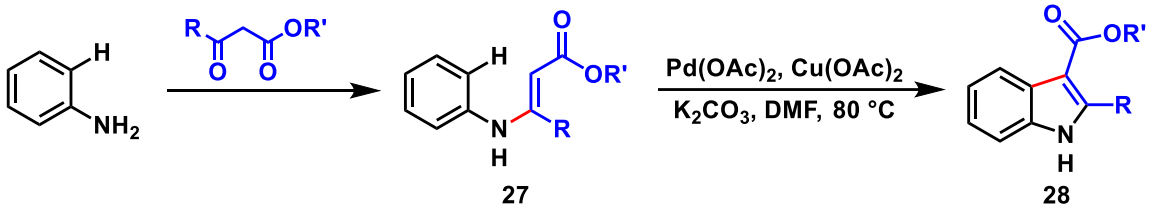

Figure 1.23 C–H activation as a method for indole synthesis

Similar to cross-coupling chemistry, the use of chiral ligands imparts enantiocontrol for C–H activation. One of the early successes involved a desymmetrization of triarylmethanes (**Figure 1.24**) by enantioselectively functionalizing one of the two tolyl rings.[77]

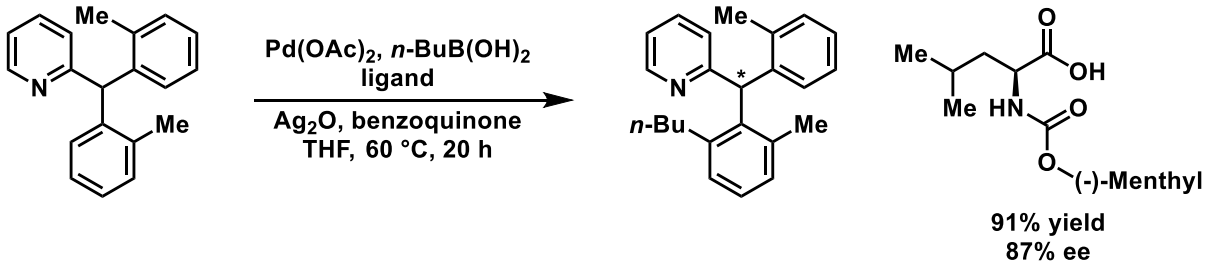

Figure 1.24 Early example of C–H activation driven enantioselectivity

In recent years, several sophisticated ligands have been developed to expand this reactivity, allowing for arylations, alkylations, and other transformations that greatly expand the range of substrates to be made asymmetrically.[78]

While the utilization of palladium in C–H activation chemistry has been heavily studied, rhodium and its utilization has been dragged into the forefront due to its improved reactivity and high functional group tolerance. The pioneering example followed a similar pathway to that of palladium, performing a Heck-type reaction, this time utilizing a pyridine directing group.[79] The difference, however, comes in the oxidation state of the final product which can be explained by the mechanism (**Figure 1.25**). The reaction begins similarly with C–H cleavage directed by the pyridine ring. From there, migratory insertion of the alkene into the resultant rhodium hydride **29** forms alkylrhodium species **30**, which then reductively eliminates to generate the alkylation product. The observed migratory insertion into the Rh–H bond is unsurprising as the catalyst being used for this chemistry is Wilkinson's catalyst, a modestly air- and moisture-stable catalyst that is commonly used for hydrogenation reactions.

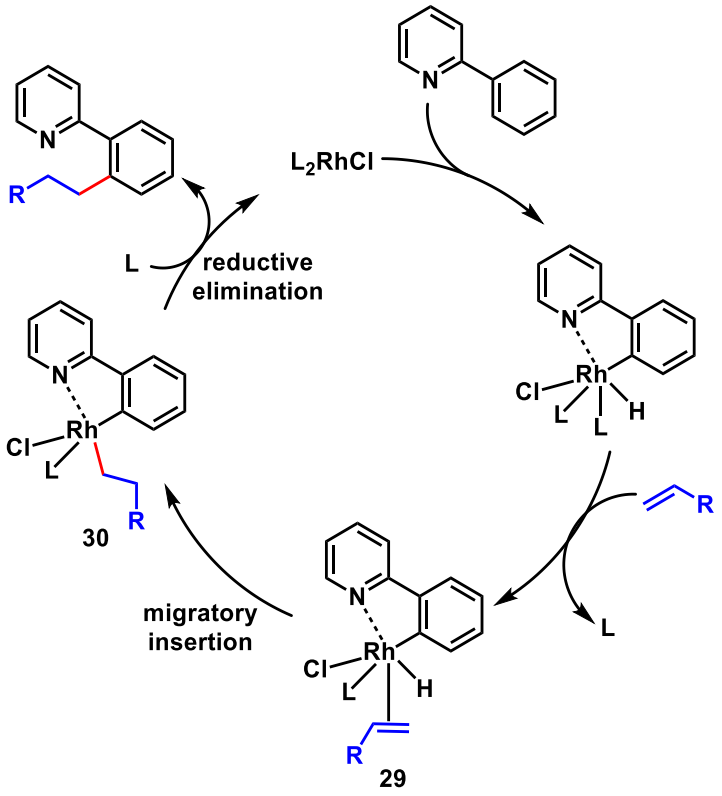

Figure 1.25 Proposed catalytic cycle for the alkylation of 2-phenylpyridines

When benzylic amines are utilized, for example (**Figure 1.26**), transfer hydrogenation sacrifices one equivalent of the alkene to generate imine **31**. Hydroiminoacylation leads to intermediate **32**, which can then direct a C–H insertion alkylation to give the final imine, which can then be hydrolyzed to give the ketone product **33** which has been alkylated in two places.[80]

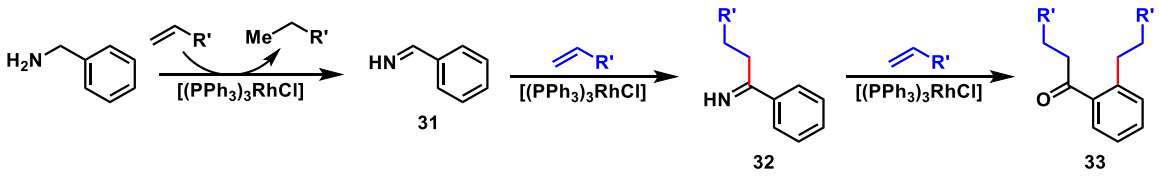

Figure 1.26 Sequence for the generation of phenyl ketones from benzylic amines

This chemistry can also be applied to intramolecular ring formation reactions by appending an alkene on to the arene undergoing functionalization. This method can be used in the formation of five- and six-membered rings and works regardless of the identity or hybridization of the atom used to attach the alkene to the ring.[81] Through the utilization of chiral phosphine ligands, this cyclization can be rendered asymmetric (**Figure 1.27**) with both saturated positions of the dihydrofuran targetable.[82]

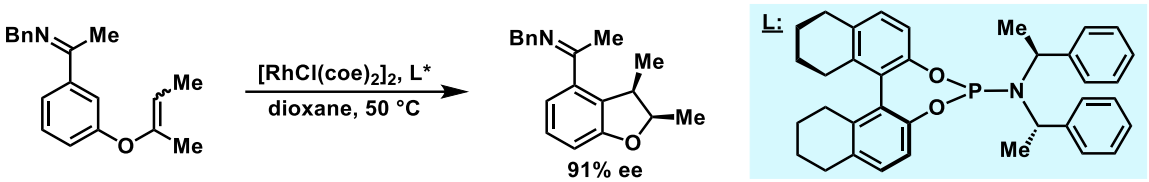

Figure 1.27 Enantioselective ring closing via C–H activation

C–H activation has another advantage in its ability to mimic the Friedel-Crafts acylation. This reaction is referred to as a carbonylation and utilizes carbon monoxide and an alkene as coupling partners. When carbon monoxide and ethylene are utilized (**Figure 1.28**), the installation of a propyl group can be accomplished *ortho* to the directing group.[83]

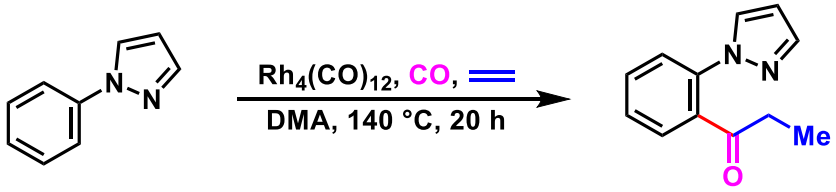

Figure 1.28 Rhodium-catalyzed carbonylation

Pyridines have been the subject of a great deal of interest due to their inclusion in many drug scaffolds.[84] Rhodium-catalyzed C–H activation provides a unique method through the coupling of an α, β-unsaturated imine and an alkyne (**Figure 1.29**), generating

benzyl-protected dihydropyridine **34**, which can undergo hydrogenative deprotection to generate di- to penta-substituted pyridine derivatives.[85]

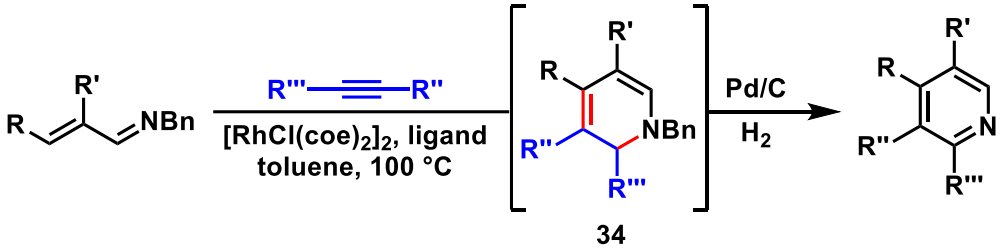

Figure 1.29 C–H activation as a method for pyridine synthesis

The final advancement in rhodium C–H activation chemistry that will be discussed in this section is the utilization of aryl halides as coupling partners once the rhodium-carbon bond has been formed. This coupling reaction can form new bonds with any arene that can undergo C–H activation; however, it is important to utilize an electron-rich coupling partners to prevent undesired homocoupling of the haloarenes. The bulk of the examples (**Figure 1.30**) utilize heterocycles as the coupling partners; however, anisoles are suitable reactants in selectively yielding the alkylation products.[86]

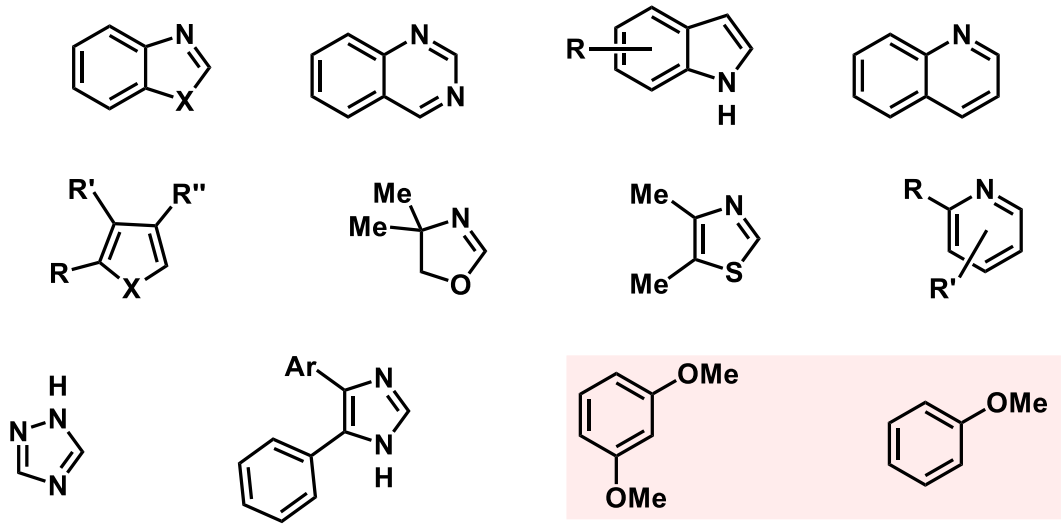

Figure 1.30 Scope of heterocycles arylated with aryl halides

In this way, the range of reactions that can be accomplished by C–H activation comes full circle, accomplishing the aryl-aryl couplings that were the hallmark of the original palladium cross-coupling reactions, improving on this methodology by circumventing the need for one of the arenes to be functionalized, but requiring an electron-rich coupling partner, excess oxidant, and superstoicheometric quantities of the coupling partner to aid the reactivity.

1.5 Sustainability in arene functionalization

One of the main driving forces in modern chemical synthesis in recent years stems from the environmental footprint brought about by mass chemical synthesis and processing. This movement has drawn attention to a set of tenets that were developed in the 1980's known as the 12 principles of green chemistry.[87] They are as follows: prevent waste, improve atom economy, lower synthesis hazards synthesis, use safer chemicals, select safer solvents and auxiliaries, consider energy efficiency, find renewable feedstocks, reduce derivatives, prioritize catalysis, design for degradation, employ real-time analysis for pollution prevention, and find inherently safer chemistry for accident prevention. The work described in the rest of this thesis will be closely tied to these principles, with primary focuses on renewability, catalysis, and atom economy areas.

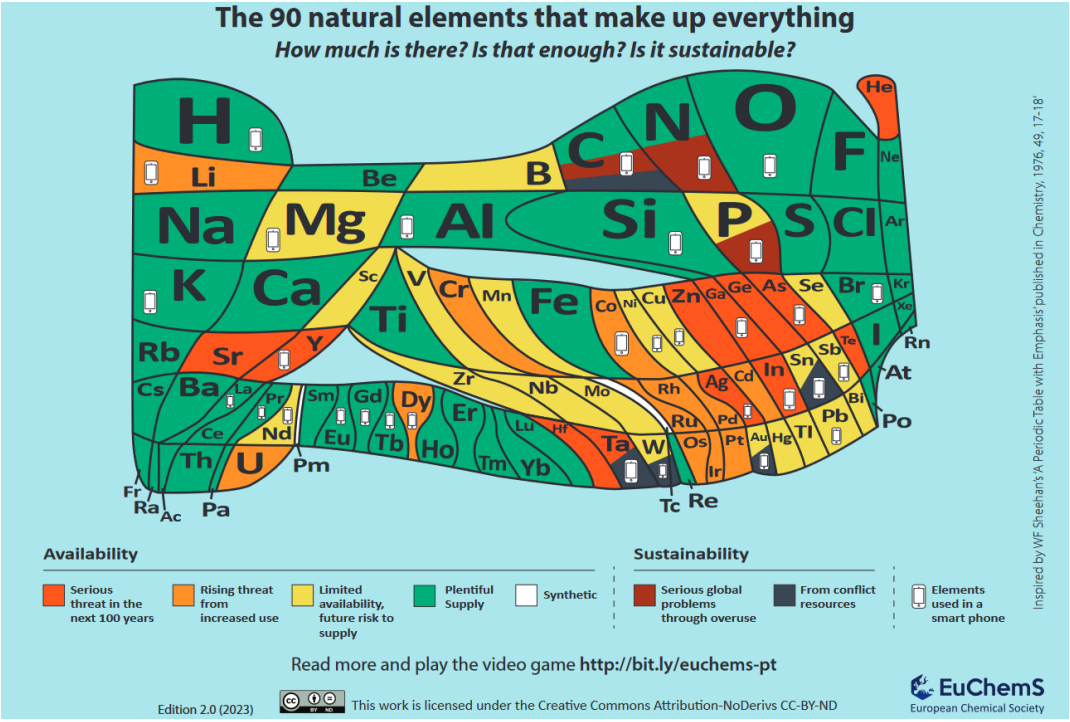

Figure 1.31 Periodic table scaled based on abundance

A consideration for those who seek to develop new catalytic methods is the relative abundance of the metal reagents. It is often the case that the most effective catalysts traditionally, namely palladium, platinum, rhodium, and ruthenium, are also the rarest (**Figure 1.31**), thus presenting a serious challenge when ton-scale synthesis is the goal. One of the most prevalent ways of tackling this problem is the way that nickel has been utilized to catalyze cross-coupling reactions. The precedent for doing so dates back to the early development of the Corriu-Kumada coupling, allowing for aryl[88] and vinyl[89] halides to be coupled to Grignard reagents without the need for a palladium catalyst. Similarly, Negishi's seminal work also utilized a nickel catalyst, which allowed for a lower reaction time and temperature than was required for palladium with a similar yield.[50] While the

reactivity is successful for highly reactive coupling partners, problems begin to arise when attempting to apply this catalysis to Suzuki-Miyaura couplings. These reactions require a much higher catalyst loading[90] and have a slower reaction rate,[91] which make them less desirable. To address this problem, a hemi-labile catalyst, ProPhos, that can activate the boronic acid has been developed (**Figure 1.32**), which greatly improves the yield and versatility of the reaction.

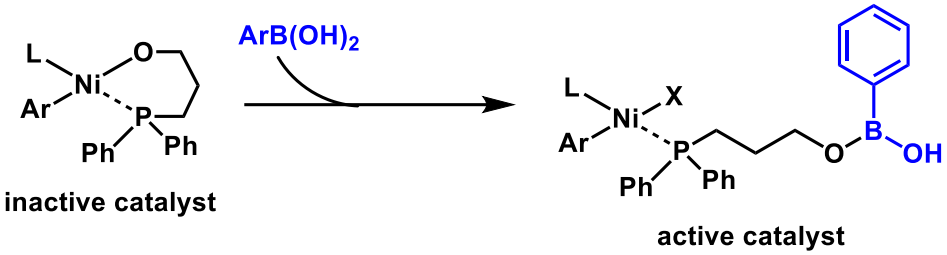

Figure 1.32 ProPhos, a ligand to improve the nickel-catalyzed Suzuki reaction

Most relevant to this thesis is the utilization of nickel to catalyze bond formation between unactivated tertiary alkyl bromides and aryl boronic esters (**Figure 1.33**).[92] Though 2.5 equivalents of the aryl coupling partner are required, this catalytic system allows the synthesis of all carbon quaternary centers. The scope of the reactivity that is possible through the utilization of nickel catalysis is very wide; however, it lies outside of the scope of this thesis and as such any further discussion will be left for other reviews.[93-94]

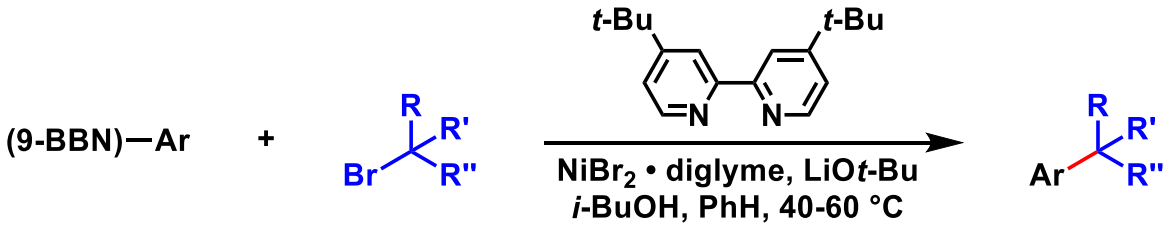

Figure 1.33 Nickel reaction with unactivated tertiary halides

One of the green chemistry problems with cross-coupling chemistry that is not addressed by the nickel catalysis above is the need for prefunctionalization of both reactants, which presents an atom economy issue. The alkyl halide and metal coupling partners that are lost in the process of the oxidative addition and transmetalation steps are not recoverable in a way that would allow for them to be repurposed, and presents a serious disposal problem when the reactions are run on production scale. Furthermore, the need for complex ligands to promote the reactivity of these metal catalysts add to the problem, as the metal complexes are not easily isolated for reuse and thus add to the waste generated by a reaction. For this reason, the focus of this thesis will be on ways that accomplish the formation of $C(sp^2)$–$C(sp^3)$ bonds via the functionalization of arenes with the primary goal of targeting highly abundant metals as catalysts, minimizing the need to prefunctionalize either of the starting materials, and cutting down on the number of steps required to synthesize a target molecule. In so doing, we hope to present methods that can cut down on the waste and the cost associated with the development of a new pharmaceutical target.

1.6 References

1. Lipinski, C. A.; Lombardo, F.; Dominy, B. W.; Feeney, P. J., Experimental and computational approaches to estimate solubility and permeability in drug discovery and development settings. *Advanced Drug Delivery Reviews* **1997**, *23*(1–3), 3–25.

2. Leeson, P. D.; Springthorpe, B., The influence of drug-like concepts on decision-making in medicinal chemistry. *Nature Reviews Drug Discovery* **2007**, *6*(11) 881–890.

3. Ritchie, T. J.; Macdonald, S. J. F., The impact of aromatic ring count on compound developability-are too many aromatic rings a liability in drug design? *Drug Discovery Today* **2009**, *14*(21-22) 1011–1020.

4. Roughley, S. D.; Jordan, A. M., The medicinal chemist's toolbox: an analysis of reactions used in the pursuit of drug candidates. *Journal of Medicinal Chemistry* **2011**, *54*, 3451–3479.

5. Cernak, T.; Dykstra, K. D.; Tyagarajan, S.; Vachal, P.; Krska, S. W., The medicinal chemist's toolbox for late stage functionalization of drug-like molecules. *Chemical Society Reviews* **2016**, *45*, 546–576.

6. Guillemard, L.; Kaplaneris, N.; Ackermann, L.; Johansson, M. J., Late-stage C–H functionalization offers new opportunities in drug discovery. *Nature Reviews Chemistry* **2021**, *5*, 522–545.

7. Rueda-Zubiaurre, A.; Yahiya, S.; Fischer, O. J.; Hu, X.; Saunders, C. N.; Sharma, S.; Straschil, U.; Shen, J.; Tate, E. W.; Delves, M. J.; Baum, J.; Barnard, A.; Fuchter, M. J., Structure-activity relationship studies of a novel class of transmission blocking antimalarials targeting male gametes. *Journal of Medicinal Chemistry* **2019**, *63*(5), 2240–2262.

8. Delves, M. J.; Miguel–Blanco, C.; Matthews, H.; Molina, I.; Ruecker, A.; Yahiya, S.; Straschil, U.; Abraham, M.; León, M. L.; Fischer, O. J.; Rueda–Zubiaurre, A.; Brandt, J. R.; Cortés, Á.; Barnard, A.; Fuchter, M. J.; Calderón, F.; Winzeler, E. A.; Sinden, R. E.; Herreros, E.; Gamo, F. J.; Baum, J., A high throughput screen for next-generation leads targeting malaria parasite transmission. *Nature Communications* **2018**, *9*(3805), 1–13.

9. Scott, D. E.; Coyne, A. G.; Hudson, S. A.; Abell, C., Fragment-based approaches in drug discovery and chemical biology. *Biochemistry* **2012**, *51*, 4990–5003.

10. Zheng, H.; Hou, J.; Zimmerman, M. D.; Wlodawer, A.; Minor, W., The future of crystallography in drug discovery. *Expert Opinion on Drug Discovery* **2013**, *9*(2), 125–137.

11. Tahtouh, T.; Elkins, J. M.; Filippakopoulos, P.; Soundararajan, M.; Burgy, G.; Durieu, E.; Cochet, C.; Schmid, R. S.; Lo, D. C.; Delhommel, F.; Oberholzer, A. E.; Pearl, L. H.; Carreaux, F.; Bazureau, J.; Knapp, S.; Meijer, L., Selectivity, cocrystal structures, and neuroprotective properties of leucettines, a family of protein kinase inhibitors derived from the marine sponge alkaloid leucettamine B. *Journal of Medicinal Chemistry* **2012**, *55*(21), 9312–9330.

12. Göckler, N.; Jofre, G.; Papadopoulos, C.; Soppa, U.; Tejedor, F. J.; Becker, W., Harmine specifically inhibits protein kinase DYRK1A and interferes with neurite formation. *FEBS Journal* **2009**, *276*, 6324–6337.

13. Becker, W.; Soppa, U.; Tejedor, F. J., DYRK1A: A potential drug target for multiple Down syndrome neuropathologies. *CNS and Neurological Disorders-Drug Targets* **2014**, *13*(1), 26–33.

14. Wurzlbauer, A.; Rüben, K.; Gürdal, E.; Chaikuad, A.; Knapp, S.; Sippl, W.; Becker, W.; Bracher, F., How to separate kinase inhibition from undesired monoamine oxidase A inhibition-the development of the DYRK1A inhibitor AnnH75 from the alkaloid harmine. *Molecules* **2020**, *25*(24), 5962–5996.

15. Kumar, K.; Wang, P.; Sanchez, R.; Swartz, E. A.; Stewart, A. F.; DeVita, R. J., Development of kinase-selective, harmine-based DYRK1A inhibitors that induce pancreatic human β-cell proliferation. *Journal of Medicinal Chemistry* **2018**, *61*(17), 7687–7699.

16. Ressel, W. J., *Proceedings of the Chemical Society, London* **1890**, *6*(85), 95–106.

17. Stamenković, N.; Ulrih, N. P.; Cerkovnik, J., An analysis of electrophilic aromatic substitution: a "complex approach." *Physical Chemistry Chemical Physics* **2021**, *23*(9), 5051–5068.

18. Tashiro, M.; Fukata, G., Selective electrophilic aromatic substitutions via positional protective groups: a review. *Organic Preparations and Procedures International* **1976**, *8*(2), 51–74.

19. Hernandes, M. Z.; Cavalcanti, S. M.; Moreira, D. R.; de Azevedo Junior, W. F.; Leite, A. C., Halogen atoms in the modern medicinal chemistry: hints for the drug design. *Current Drug Targets* **2010**, *11*(3), 303−314.

20. Adams, R.; Marvel, C. S., *p*-bromophenol. *Organic Syntheses* **1921**, *1*, 39.

21. Tanko, J. M.; Blackert, J. F., Free-radical side-chain bromination of alkylaromatics in supercritical carbon dioxide. *Science* **1994**, *263*, 203−205.

22. Venkatachalapathy, C.; Pitchumani, K., Selectivity in bromination of alkylbenzenes in the presence of montmorillonite clay. *Tetrahedron* **1997**, *53*(7), 2581−2584.

23. Ma, H. M.; Liu, Z. Z.; Chen, S. Z., Regioselective bromination of 3,4-dimethoxytoluene with *N*-bromosuccinimide. *Chinese Chemical Letters* **2003**, *14*(4), 371−374.

24. Zanka, A.; Kubota, A., Practical and efficient chlorination of deactivated anilines and anilides with NCS in 2-propanol. *Synlett* **1999**, *12*, 1984–1986.

25. Wang, M.; Zhang, Y.; Wang, T.; Wang, C.; Xue, D.; Xiao, J., Story of an age-old reagent: an electrophilic chlorination of arenes and heterocycles by 1-chloro-1,2-benziodoxol-3-one. *Organic Letters* **2016**, *18*(9), 1976–1979.

26. Streuff, J.; Riedel, S.; Beck, T.; Haller, H., Brominations with Pr4NBr9 as a solid reagent with high reactivity and selectivity. *Synthesis* **2014**, *46*(6), 740–747.

27. Orazi, O. O.; Corral, R. A.; Bertorello, H. E., *N*-Iodohydantoins. II. Iodonations with 1,3-diiodo-5,5-dimethylhydantoin. *The Journal of Organic Chemistry* **1965**, *30*(4), 1101–1104.

28. Lovering, F.; Bikker, J.; Humblet, C., Escape from flatland: increasing saturation as an approach to improving clinical success. *Journal of Medicinal Chemistry* **2009**, *52*(21), 6752–6756.

29. Méndez–Lucio, O.; Medina–Franco, J. L., The many roles of molecular complexity in drug discovery. *Drug Discovery Today* **2017**, *22*(1), 120–126.

30. Friedel, C.; Crafts, J. M., A new general method for producing hydrocarbons. *Journal of Chemical Society* **1877**, *32*, 725.

31. Rueping, M.; Nachtsheim, B. J., A review of new developments in the Friedel–Crafts alkylation–from green chemistry to asymmetric catalysis. *Beilstein Journal of Organic Chemistry* **2010**, *6*, 6.

32. Zavgorodnii, S. V.; Bereznitskii, G. K.; Pisanenko, D. A., Synthesis of 2- and 3-alkyl-4-bromotoluenes. *Russian Journal of Organic Chemistry* **1972**, *8*(7), 1484–1486.

33. Olah, G. A.; Flood, S. H.; Kuhn, S. J.; Moffatt, M. E.; Overchuck, N. A., Aromatic substitution. XVI. Friedel-Crafts isopropylation of benzene and methylbenzenes with isopropyl bromide and propylene. *Journal of the American Chemical Society* **1964**, *86*, 1046.

34. Kadyrov, C. S.; Khalikov, S. S., Carboxyalkylation of benzimidazolin-2-ones by crotonic acid in the presence of anhydrous aluminum chloride. *Proceedings of the USSR Academy of Sciences* **1983**, *2*, 31–32.

35. Jensen K. B.; Thorhauge, J.; Hazell R. G.; Jørgensen, K. A., Catalytic asymmetric Friedel-Crafts alkylation of β,γ-unsaturated α-ketoesters: enantioselective addition of aromatic C–H bonds to alkenes. *Angewandte Chemie International Edition* **2001**, *40*(1), 160–163.

36. Zhuang, W.; Hansen T.; Jørgensen, K. A., Catalytic enantioselective alkylation of heteroaromatic compounds using alkylidene malonates. *Chemical Communications* **2001**, 347–348.

37. Palomo, C.; Oiarbride, M.; Kardak, B. G.; Garcia, J. M.; Linden, A., Highly enantioselective Friedel-Crafts alkylations of pyrroles and indoles with α'-hydroxy enones under Cu(II)-simple bis(oxazoline) catalysis. *Journal of the American Chemical Society* **2005**, *127*(12), 4154–4155.

38. Evans, D. A.; Fandrick, K. R.; Song, H., Enantioselective Friedel–Crafts alkylations of α,β–unsaturated 2–acyl amidazoles catalyzed by bis(oxazolinyl)pyridine-scandium(III) triflate complexes. *Journal of the American Chemical Society* **2005**, *127*(5), 8942–8943.

39. Bandini, M. Melloni, A.; Piccinelli, F.; Sinisi, R.; Tommasi, S.; Umani–Rochi, A., Highly enantioselective synthesis of tetrahydro-β-carbolines and tetrahydro-γ-carbolines vi Pd-catalyzed intramolecular allylic alkylation. *Journal of the American Chemical Society* **2006**, *128*(5), 1424–1425.

40. Bandini, M.; Garelli, A.; Rovinetti, M.; Tommasi, S.; Umani–Ronchi, A., Catalytic enantioselective addition of indoles to arylniroalkenes: an effective route to enantiomerically enriched tryptamine precursors. *Chirality* **2005**, *17*, 522–529.

41. Blay, G.; Fernández, I.; Pedro, J. R.; Vila, C., Highly enantioselective Friedel-Crafts alkylations of indoles with simple enones catalyzed by Zirconium(IV)-BINOL complexes. *Organic Letters* **2007**, *9*(13), 2601–2604.

42. Lu, S.; Du, D.; Xu, Z., Enantioselective Friedel-Crafts alkylation of indoles with nitroalkenes catalyzed by bifunctional tridentate bis(oxazoline)-Zn(II) complex. *Organic Letters* **2006**, *8*(10), 2115–2118.

43. Calloway, N. O., The Friedel-Crafts syntheses. *Chemical Reviews* **1935**, *17*(3), 293–442.

44. Heck R. F., Acylation, methylation, and carboxyalkylation of olefins by group VIII metal derivatives. *Journal of the American Chemical Society* **1968**, *90*(20), 5518–5526.

45. Mizoroki, T. Mori, K.; Ozaki, A., Alkylation of aryl iodide catalyzed by palladium. *Bulletin of the Chemical Society of Japan* **1971**, *44*(2), 581.

46. Heck R. F.; Nolley Jr., J. P., Palladium-catalyzed vinylic hydrogen substitution reactions with aryl, benzyl, and styryl halides. *The Journal of Organic Chemistry* **1972**, *37*(14), 2320–2322.

47. Baba, S.; Negishi, E., A novel stereospecific alkenyl-alkenyl cross-coupling by a palladium- or nickel-catalyzed reaction of alkenylalanes with alkenyl halides. *Journal of the American Chemical Society* **1976**, *98*(21), 6729–6731.

48. Negishi, E.; King A. O.; Okukado, N., Selective carbon-carbon bond formation via transition metal catalysis. 3. A highly selective synthesis of unsymmetrical biaryls and diarylmethanes by the nickel- or palladium-catalyzed reaction of aryl- and benzylzinc derivatives with aryl halides. *The Journal of Organic Chemistry* **1977**, *42*(10), 1821–1823.

49. Dieck, H. A.; Heck, R. F., Palladium-catalyzed conjugated diene synthesis from vinylic halides and olefinic compounds. *The Journal of Organic Chemistry* **1975**, *40*(8), 1083–1090.

50. Miyaura, N.; Suzuki, A., Stereoselective synthesis of arylated I-alkenes by the reaction of alk-1-enylboranes with aryl halides in the presence of palladium catalyst. *Journal of the Chemical Society, Chemical Communications* **1979**, *19*, 866–867.

51. Yamamura, M.; Moritani, I.; Murahashi, S., The reaction of σ-vinylpalladium complexes with alkyllithiums. Stereospecific syntheses of olefins from vinyl halides and alkyllithiums. *Journal of Organometallic Chemistry* **1975**, *91*(2), C39–C42.

52. Azarian, D.; Dua, S. S.; Eaborn, C.; Walton, D. R. M., Reaction of organic halides with R_3MMR_3 compounds (M = Si, Ge, Sn) in the presence of tetrakis(triarylphosphine) palladium. *Journal of Organometallic Chemistry* **1976**, *117*(3), C55–C57.

53. Hatanaka, Y.; Hiyama, T., Cross–coupling of organoslinaes with organic halides mediated by a palladium catalyst and tris(diethylamino)sulfonium difluorotrimethyl silicate. *The Journal of Organic Chemistry* **1988**, *53*(4), 918–920.

54. Sonogashira, K.; Tohda, Y.; Hagihara, N., A convenient synthesis of acetylenes: catalytic substitutions of acetylenic hydrogen with bromoalkenes, iodoarenes and bromopyridines. *Tetrahedron Letters* **1975**, *16*(50), 4467–4470.

55. Stephens, R. D.; Castro, C. E., The substitution of aryl iodides with cuprous acetylides. A synthesis of tolanes and heterocyclics. *The Journal of Organic Chemistry* **1963**, *28*(12), 3313–3315.

56. Guram, A. S.; Rennels, R. A.; Buchwald, S. L., A simple catalytic method for the conversion of the aryl bromides to arylamines. *Angewandte Chemie International Edition* **1995**, *34*(12), 1348–1350.

57. Louie, J.; Hartwig, J. F., Palladium-catalyzed synthesis of arylamines from aryl halides. Mechanistic studies lead to coupling in the absence of tin reagents. *Tetrahedron Letters* **1995**, *36*(21), 3609–3612.

58. Sambiagio, C.; Mardsen, S. P.; Blacker, A. J.; McGowan, P. C., Copper catalyzed Ullmann type chemistry: from mechanistic aspects to modern development. *Chemical Society Reviews* **2014**, *43*, 3525–3550.

59. Myers, A. G.; Tanaka, D.; Mannison, M. R., Development of a decarboxylative palladation reaction and its use in Heck-type olefination of arene carboxylates. *Journal of the American Chemical Society* **2002**, *124*(38), 11205–11251.

60. Goossen, L. J.; Rodríguez, N.; Melzer, B.; Linder, C.; Deng, G.; Levy, L. M., Biaryl synthesis via Pd-catalyzed decarboxylative coupling of aromatic carboxylates with aryl halides. *Journal of the American Chemical Society* **2007**, *129*(15), 4824–4833.

61. Fauvarque, J. F.; Jutand, A., Reaction of various nucleophiles with organopalladium compounds. *Bulletin of the French Chemical Society* **1976**, *5*(6), 765–770.

62. Fauvarque, J. F.; Jutand, A., Arylation of the Reformatsky reagent catalyzed by zerovalent complexes of palladium and nickel. *Journal of Organometallic Chemistry* **1977**, *132*(2), C17–C19.

63. Kosugi, M.; Sasazawa, K.; Shimizu, Y.; Migita, T., Reactions of allyltin compounds III. Allylation of aromatic halides with allyltributyltin in the presence of tetrakis(triphenylphosphine) palladium(0). *Chemistry Letters* **1977**, *6*(3), 301–302.

64. Diederich, F.; Stang, P.J., in *Metal-Catalyzed Cross-Coupling Reactions* **1998**, Wiley-VCH: New York.

65. Hayashi, T.; Konishi, M.; Kumada, M., Dichloro[1,1'-bis(diphenylphosphino) ferrocene]palladium(II): an effective catalyst for cross-coupling reaction of a secondary alkyl Grignard reagent with organic halides. *Tetrahedron Letters* **1979**, *21*, 1871–1874.

66. Duda, M. L.; Michael, F. E., Palladium-catalyzed cross-coupling of *N*-sulfonylaziridines with boronic acids. *Journal of the American Chemical Society* **2013**, *135*(49), 18347–18349.

67. Takeda, Y.; Ikeda, Y.; Kuroda, A.; Tanaka, S.; Minakata, S., Pd/NHC-catalyzed enantiospecific and regioselective Suzuki-Miyaura arylation of 2-arylaziridines: synthesis

of enantioenriched 2-arylphenethylamine derivatives. *Journal of the American Chemical Society* **2014**, *136*(24), 8544–8547.

68. Zhang, L.; Livinger, G. J.; Edelstein, E. K.; Szymaniak, A. A.; Chierchia, M. P.; Morken, J. P., Catalytic conjunctive cross-coupling enabled by metal-induced metallate rearrangement. *Science* **2016**, *351*(6268), 70–74.

69. Karash, M. S.; Isbell, H. S., The chemistry of organic gold compounds. III. Direct introduction of gold into the aromatic nucleus. *Journal of the American Chemical Society* **1931**, *53*(8), 3053–3059.

70. Kleinman, J. P.; Dubeck, M., The preparation of cyclopentadienyl [*o*-(phenylazo)phenyl] nickel. *Journal of the American Chemical Society* **1963**, *85*(10), 1544–1545.

71. Fujiwara, Y.; Moritani, I.; Danno, S.; Asano, R.; Teranishi, S., Aromatic substitution of olefins. VI. Arylation of olefins with palladium(II) acetate. *Journal of the American Chemical Society* **1969**, *91*(25), 7166–7169.

72. Sun, C.; Li, B.; Shi, Z., Pd-catalyzed oxidative coupling with organometallic reagents via C–H activation. *Chemical Communications* **2010**, *46*, 677–685.

73. Giri, R.; Maugel, N.; Li, J.; Wang, D.; Breazzano, S. P.; Saunders, L. B.; Yu, J., Palladium-catalyzed methylation and arylation of sp^2 and sp^3 C–H bonds in simple carboxylic acids. *Journal of the American Chemical Society* **2007**, *129*(12), 3510–3511.

74. Ferreira, E. M.; Stoltz, B. M., Catalytic C–H bond functionalization with palladium(II): aerobic oxidative annulations of indoles. *Journal of the American Chemical Society* **2003**, *125*(32), 9578–9579.

75. Sravanthi, T. V.; Manju, S. L., Indoles-a promising scaffold for drug development. *European Journal of Pharmaceutical Sciences* **2016**, *91*, 1–10.

76. Würtz, S.; Rakshit, S.; Neumann, J. J.; Dröge, T.; Glorius, F., Palladium-catalyzed oxidative cyclization of *N*-aryl enamines: from anilines to indoles. *Angewandte Chemie International Edition* **2008**, *47*(38), 7230–7233.

77. Shi, B.; Maugel, N.; Zhang, Y.; Yu, J., Pd^{II}-catalyzed enantioselective activation of C(sp^3)–H bonds using monoprotected amino acids as chiral ligands. *Angewandte Chemie International Edition* **2008**, *47*(26), 4882–4886.

78. Yang, K.; Song, M.; Liu, H.; Ge, H., Palladium-catalyzed direct asymmetric C–H bond functionalization enabled by the directing group strategy. *Chemical Sciences* **2020**, *11*, 12616–12632.

79. Lim, Y.; Kim, Y. H.; Kang, J., Rhodium-catalyzed regioselective alkylation of the phenyl ring of 2-phenylpyridines with olefines. *Journal of the Chemical Society, Chemical Communications* **1994**, *19*, 2267–2268.

80. Jun, C.; Chung, K.; Hong, J., C–H and C–C bond activation of primary amines through dehydrogenation and transmission. *Organic Letters* **2001**, *3*(5), 785–787.

81. Thalji, R. K.; Ahrendt, K., A.; Bergman, R.; G.; Ellman, J. A., Annulation of aromatic imines via directed C–H bond activation. *The Journal of Organic Chemistry* **2005**, *70*(17), 6775–6781.

82. Harada, H.; Thalji, R. K.; Bergman, R. G.; Ellman, J. A., Enantioselective intramolecular hydroarylation of alkenes via directed C–H bond activation. *The Journal of Organic Chemistry* **2008**, *73*(17), 6772–6779.

83. Asaumi, T.; Matsuo, T.; Fukuyamna, T.; Ie, Y.; Kakiuchi, F.; Chatani, N., Ruthenium and rhodium-catalyzed direct carbonylation of the ortho C–H bond in the benzene ring of *N*-arylpyrazoles. *The Journal of Organic Chemistry* **2004**, *69*(13), 4433–4440.

84. Ling, Y.; Hao, Z. Y.; Liang, D.; Zhang, C. L.; Liu, Y. F.; Wang, Y., The expanding role of pyridine and dihydropyridine scaffolds in drug design. *Drug Design, Development and Therapy* **2021**, *15*, 4289–4338.

85. Parthasarathy, K.; Jeganmohan, M.; Cheng, C., Rhodium-catalyzed one-pot synthesis of substituted pyridine derivatives from α, β-unsaturated ketoximes and alkynes. *Organic Letters* **2007**, *10*(2), 325–328.

86. Colby, D. A.; Bergman, R. G.; Ellman, J. A., Rhodium-catalyzed C–C bond formation via heteroatom-directed C–H bond activation. *Chemical Reviews* **2010**, *110*(2), 624–655.

87. Warner, J. C.; Cannon, A. S.; Dye, K. M., Green chemistry. *Environmental Impact Assessment Review* **2004**, *24*(7–8), 775–779.

88. Tamao, K.; Kiso, Y.; Sumitani, K.; Kumada, M., Alkyl group isomerization in the cross–coupling reaction of secondary alkyl Grignard reagents with organic halides in the presence of nickel-phosphine complexes as catalysts. *Journal of the American Chemical Society* **1972**, *94*(26), 9268–9269.

89. Corriu, R. J. P.; Masse, J. P., Activation of Grignard reagents by transition-metal complexes. A new and simple synthesis of *trans*-stilbenes and polyphenyls. *Journal of the Chemical Society, Chemical Communications* **1972**, *3*, 144a–144a.

90. Chirik, P. J.; Engle, K. M.; Simmons, E. M.; Wisniewski, S. R., Collaboration as a key to advance capabilities for Earth-abundant metal catalysis. *Organic Process Research & Development* **2023**, *27*(7), 1160–1184.

91. Cooper, A. K.; Burton, P. M.; Nelson, D. J., Nickel versus palladium in cross-coupling catalysis: on the role of substrate coordination to zerovalent metal complexes. *Synthesis* **2020**, *52*(4), 565–573.

92. Zultanski, S. L.; Fu, G. C., Nickel-catalyzed carbon–carbon bond-forming reactions of unactivated tertiary alkyl halides: Suzuki arylations. *Journal of the American Chemical Society* **2013**, *135*(2), 624–627.

93. Gu, J.; Wang, X.; Xue, W.; Gong, H., Nickel-catalyzed reductive coupling of alkyl halides with other electrophiles: concept and mechanistic considerations. *Organic Chemistry Frontiers* **2015**, *2*, 1411–1421.

94. Poremba, K. E.; Dibrell S. E.; Riesman, S. E., Nickel-catalyzed reductive cross-coupling reactions. *ACS Catalysis* **2020**, *10*(15), 8237–8246.

Chapter 2 Synthesis of diarylmethanes via a Fenton's reagent aromatic radical cation pathway

2.1 Introduction

The Scholl reaction (**Figure 2.1**), developed in the early 1900's, involves the synthesis of a new C(aryl)–C(aryl) bond, occurring through the intermediacy of arene radical cation **35**, which then engages a second arene reactant to form the new bond.[1]

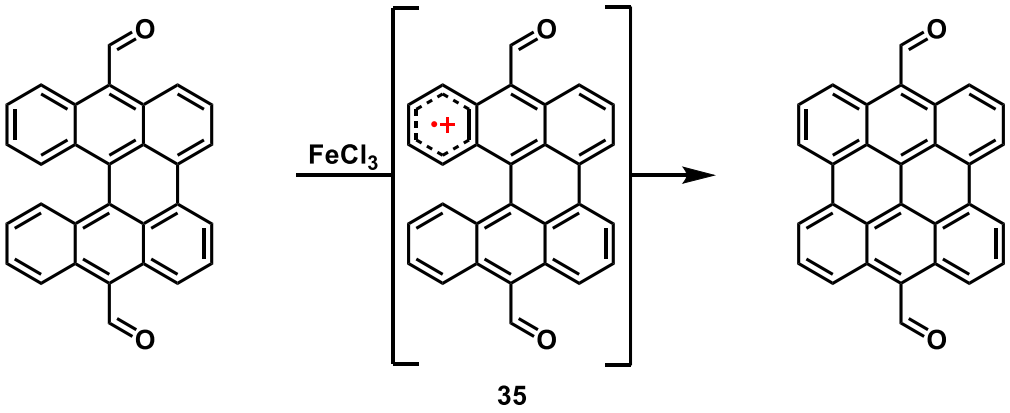

Figure 2.1 The original Scholl reaction scheme

This chemistry is not confined to intramolecular reactivity, but also effective in intermolecular settings.[2] The main limitation lies in the cross-coupling of two different arenes. One successful example involves a biphasic system where two solid reactants are suspended in water, requiring a preformed, stable hydrogen–bonding complex of the two starting materials to ensure selectivity.[3] Despite this limitation, the Scholl reaction is commonly employed in materials applications to synthesize large arene networks and graphite mimics.[4]. In particular, the nature of the radical cation intermediate (**Figure 2.2**)

was probed by integrating bulky alkyl groups at every position of the arene not bearing an electron–donating group, which stabilized the intermediate long enough for it to be crystallized.[5]

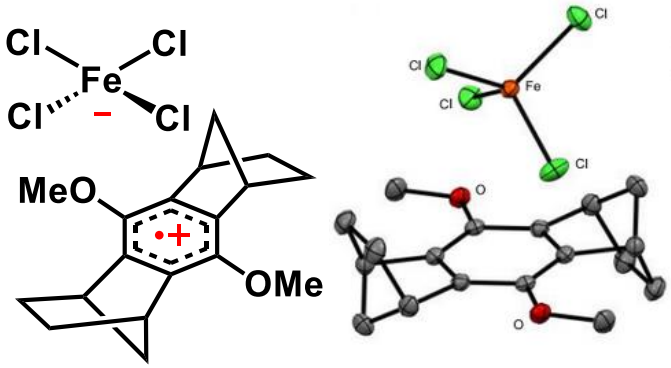

Figure 2.2 Evidence for the radical cation intermediate
The radical cation generated from electron-rich arenes using iron (left) was able to be crystallized (right) through the usage of bulky alkyl groups.

While the ability for this reactivity to catalyze the formation of $C(sp^2)$–$C(sp^2)$ bonds is well understood, we set our sights on a reaction type that has been much more difficult to accomplish without the need of expensive and rare transition metal catalysts, namely $C(sp^2)$–$C(sp^3)$ cross–couplings. To accomplish this transformation, we began searching for reactions that can generate alkyl radicals, with the hopes of being able to pair them together to accomplish alkylations of electron-rich arene rings.

The Minisci reaction is one such reaction, developed in the 1960s, allowing for the alkylation of basic heterocycles with carboxylic acids.[6] Silver catalyzes an oxidative decarboxylation to generate alkyl radical **37**, which adds into protonated heterocycle **36** to arrive at the product after loss of a hydrogen atom (**Figure 2.3**).

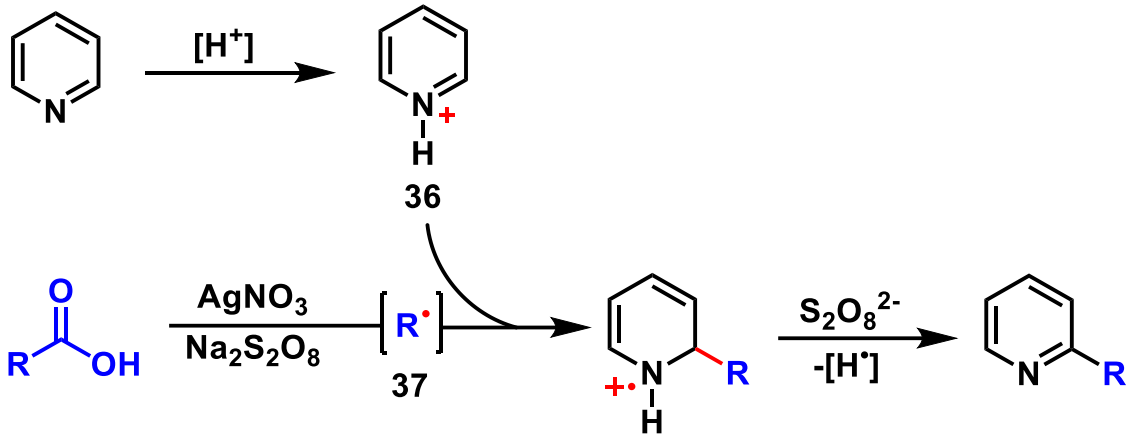

Figure 2.3 The general reaction scheme for the Minisci reaction

The accessibility of carboxylic acids as coupling partners and mild reaction conditions have led to the Minisci reaction being utilized in late-stage alkylations to synthesize pharmaceutically relevant molecules.[7] Its two major limitations are selectivity and scope. When multiple reaction sites are possible, the reaction tends to be unselective, forming a mixture of mono, di, and tri substituted products. In terms of scope, most examples involve electron-deficient heterocycles, with isolated examples of electron-rich heterocycles reacting with alkyl radicals.[8] This reaction is also pertinent to the methodology that we are seeking to develop, as described in this chapter, because even in the early days of its development, the utilization of iron to catalyze this chemistry was reported (**Figure 2.4**).[9]

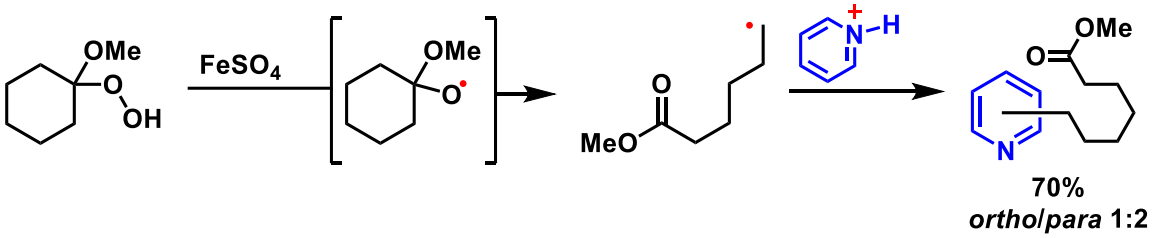

Figure 2.4 Iron-catalyzed Minisci type reaction

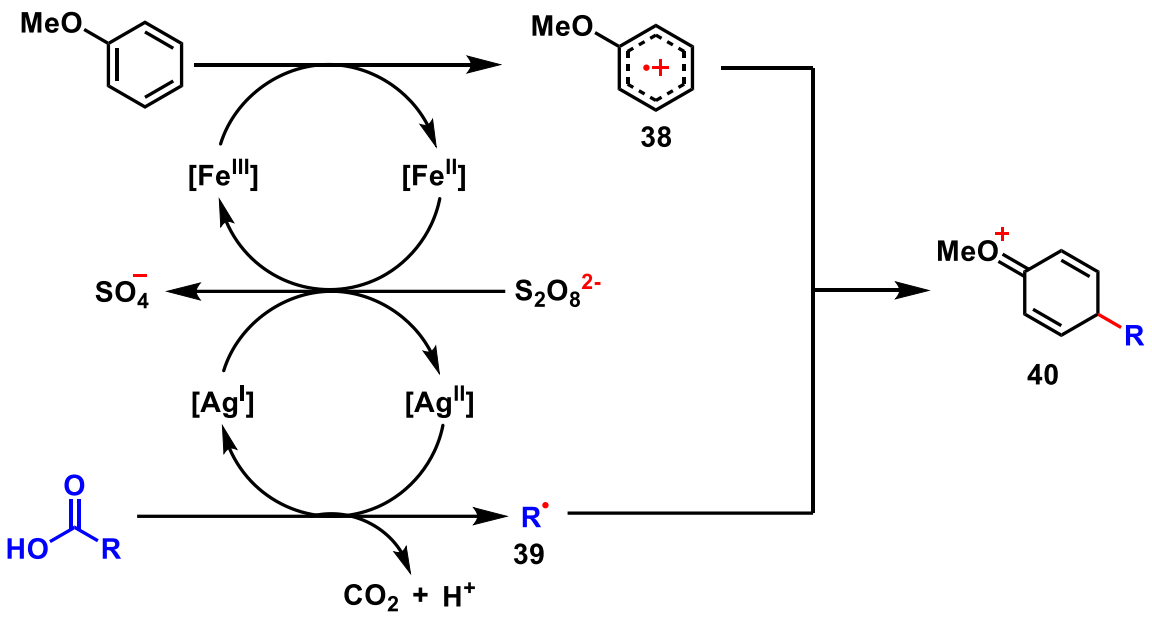

Figure 2.5 Imagined reaction pathway for the expanding of the Minisci reaction

We rationalize that iron(III) can generate radical cation **38** from an electron-rich arene, such as anisole (**Figure 2.5**). The stabilized radical cation **38** will react with alkyl radical **39** arising from the silver-promoted decarboxylation to forge aryl cation **40**, which aromatizes to the alkylated product. The addition of persulfate as an oxidant is anticipated to regenerate the catalyst. It is with this proposed catalytic cycle in mind that we began our investigation.

2.2 Results

2.2.1 *Catalytic system development*

Initial studies began with a catalytic quantities of iron and silver (**Figure 2.6**) with the inclusion of an oxidant and TFA, which are commonly used to promote Minisci-type reactions. We utilized 2-methylanisole as it proved successful in the Friedel–Crafts

inspired reaction developed in our lab, which will be discussed in **Chapter 3**. With some optimization we found that in 1:1 DCE/water as the solvent, the mono chlorinated product **41** was formed in 54% yield rather than the expected *tert*-butylation.

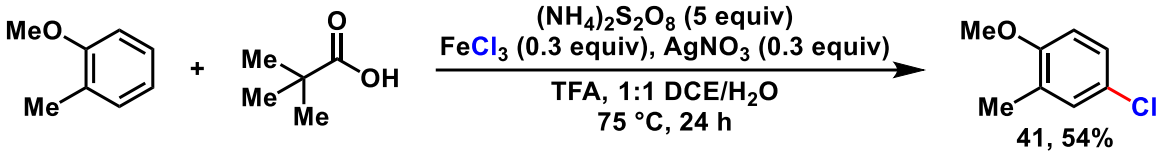

Figure 2.6 Unexpected halogenation in initial catalysis studies

We suspect this unintended reactivity comes about from the salting out of silver (I) chloride, making it unavailable to perform the decarboxylation. From there the chlorides remaining on the iron catalyst are oxidized to hypochlorous acid which then engages the arene in an EAS manner, a reaction that has been known since the late nineteenth century.[10] While this method proved ineffective, Fenton's reagent, an iron and peroxide catalyzed method, offers a desirable alternative.

When we began our investigation into this reaction, we made another unexpected discovery. When attempting to alkylate 2-methylanisole with acetic acid, diarylmethane **42** was formed as the product in 30% yield instead of the expected 2,4-dimethylanisole. Upon further investigation, the carboxylic acid was found to not be an active reactant as its exclusion resulted in the same product formation in 31% yield. Upon optimization, the ideal conditions were found (**Figure 2.7**), giving the product in 84% yield. The solvent methanol was discerned to be the actual coupling partner in this reaction.

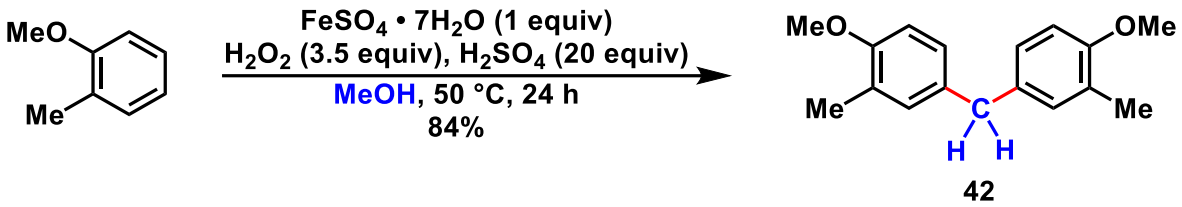

Figure 2.7 Optimized conditions for diarylmethane synthesis

The development of this reaction incurred several challenges. The first being the need for stoichiometric amounts of the metal, meaning this reaction is not truly catalytic. That being said, $FeSO_4$ costs ~$0.20/g, so the downside of its excess use is the generation of waste. The second, which took the longest time to resolve, was the degradation of the starting material by the reaction conditions. Through a series of optimizations, we were able to circumvent this problem by including a 15-minute latency period before the addition of anisole. **Table 2.1** summarizes selected parameters that were examined. When the iron source was swapped for ones with organic ligands (entry 2–3), or when an iron(III) source was used (entry 4) the reaction yields were drastically lower. When the iron loading is reduced to 0.5 equivalent (entry 5), the yield declines to be in line with the amount of metal added. Reducing the amount of peroxide (entry 7) or acid (entry 9) similarly decreased the yields, and their removal (entries 8 and 10) halted the reactivity entirely. Attempts to use methanol in reagent quantities (3 equiv) dissolved in other solvents (entry 11–14) with the hopes of improving the versatility of the reaction were not fruitful. The use of water as the solvent provided some promise (entry 14, 36%); however, the yields could not be improved to synthetically useful levels.

Table 2.1 Optimization of reaction conditions for diarylmethane synthesis

Entry	Conditions	% Yield
1	Standard	84
2	$Fe(acac)_3$ instead of $FeSO_4 \cdot 7\ H_2O$	8
3	FeTPPCl instead of $FeSO_4 \cdot 7\ H_2O$	10
4	$Fe_2(SO_4)_3$ instead of $FeSO_4 \cdot 7\ H_2O$	13
5	0.5 equiv $FeSO_4 \cdot 7\ H_2O$ instead of 1.0 eq.	48
6	No $FeSO_4 \cdot 7\ H_2O$	0
7	1.75 equiv H_2O_2 instead of 3.5	59
8	No H_2O_2	0
9	10 equiv of H_2SO_4 instead of 20 eq.	11
10	No H_2SO_4	0
11	3 equiv CH_3OH in DCE solvent	7
12	3 equiv CH_3OH in 1,4-dioxane solvent	9
13	3 equiv CH_3OH in HFIP solvent	6
14	3 equiv CH_3OH in H_2O solvent	36

2.2.2 *Substrate Scope*

This reaction represents a new method for the direct synthesis of diarylmethane products without the need to prefunctionalize either of the aryl components or the alcohol. The scope of this reaction (**Figure 2.8**) was explored. The substrates that will be discussed in this thesis will be the ones synthesized by the author. For the full substrate scope, please refer to the published study.[11] For the *ortho*-substituted anisoles, 2-methyl- and 2-ethyl-anisole **43-44** were both transformed in 84% and 68% yield respectively. When the electron-donating alkyl groups were swapped for halogens, namely 2-fluoro- and 2-bromo-anisole **45-46**, the yields declined significantly to 29% and 45%, while requiring longer reaction times and higher temperatures. When the *para*–position is blocked, alkylation proceeds at the expected *ortho*-site, though the reaction slows greatly as an extended reaction time of 48 hours is necessary for 4-methyl-, 4-ethyl-, and 4-*tert*-butyl- anisole

substrates **47-49** to achieve good yields (73-65%). Elevated reaction temperature gives a comparatively lower yield due to starting material degradation. Halogenated 4-chloro-, 4-bromo-, 4-iodoanisole **50-52** saw a similar decline in yields, requiring elevated temperatures. When ester- and carboxylic acid-functionalized anisole derivatives are used as starting materials, the reactions proceed as expected, but also undergoes esterification or transesterification to give the methyl ester products. This transformation occurs if the ester group in question is attached by an alkyl chain **53** or it is bound directly to the anisole ring **54**, though the benzoic acid derivative required elevated reaction temperature. When *meta*-substituted starting materials were utilized, alkylation at the less hindered *ortho*-position is favored. Similar to the *para*-substituted substrates, 3-*iso*propyl anisole **55** required an extended reaction time to achieve synthetically relevant yields. When 3-chloro-**56** and 3-bromoanisole **57** were used, extended time and elevated temperature parameters gave yields in line with the *para*-substituted halides. This reaction also works well when the methyl group of the anisole is swapped for ethyl **58** or bromopropyl **59** substituents. In the latter case, decomposition relating to the alkyl bromide chain did not occur. Complications arose when multiple strong electron–donating groups were added to the ring. 1,3,5-Trimethoxybenzene **60**, while it required a slightly longer reaction time to overcome the steric hinderance at all possible reaction sites, worked without complications, but 1,3-dimethoxybenzene led to a mixture of dimer **61** and trimer **62** in roughly a 1:1 ratio (32% yield). Dihydroxynapthalene is transformed to the corresponding diarylether **63** in 36% yield.

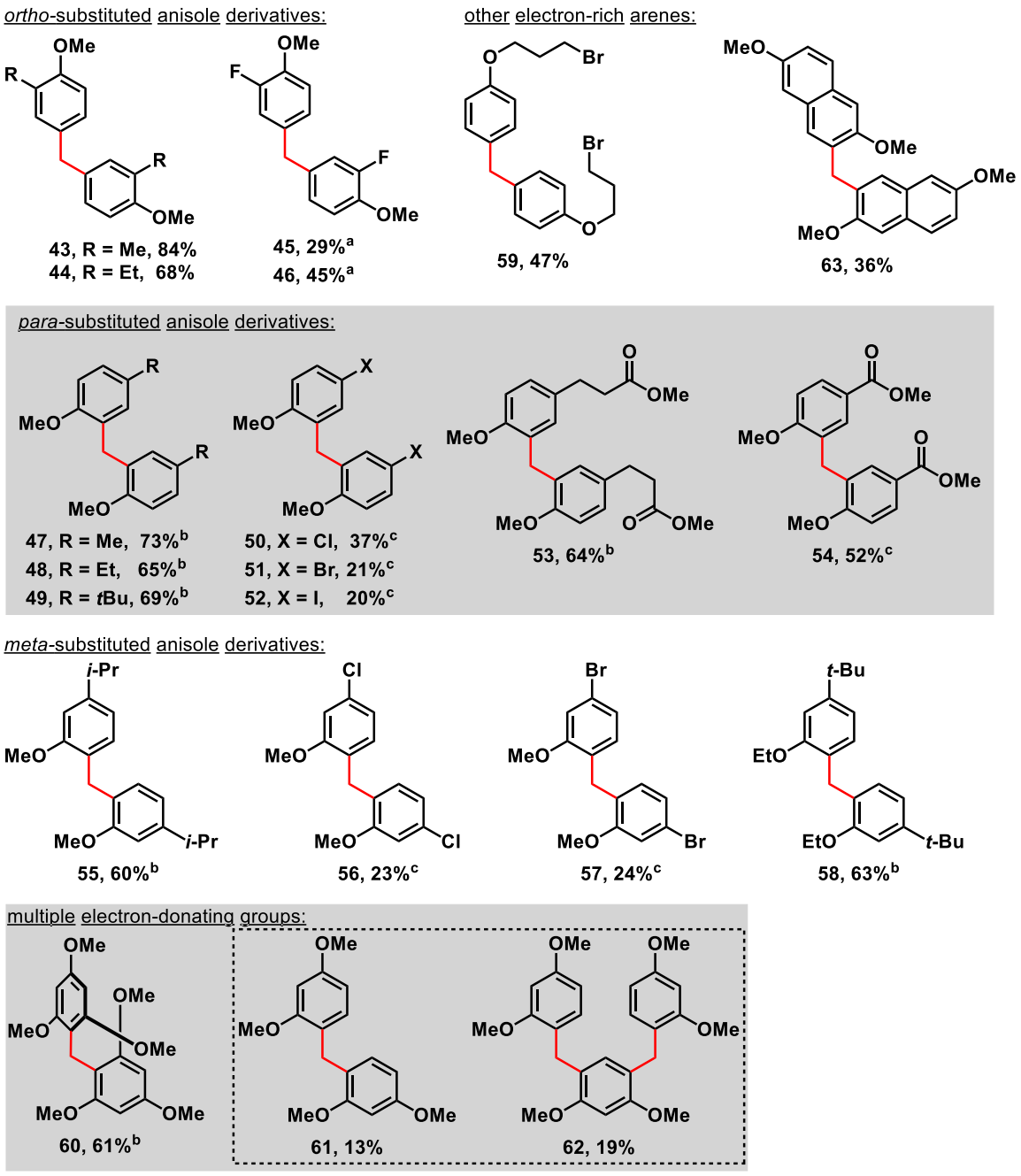

Figure 2.8 Scope of the substrates targeted by this reaction

Conditions: anisole (0.2 mmol), Fe_2SO_4 •7 H_2O (0.2 mmol), $H_2O_{2(aq)}$ (0.7 mmol), H_2SO_4 (4 mmol), MeOH (0.4 mL, 0.5 M), 50 °C, 24 h . a) Run at 75 °C for 24 h, b) run at 50 °C for 48 h, c) run at 75 °C for 48 h.

This reaction also can be scaled up, giving 86% yield on a 2 mmol scale. Two minor problems needed to be addressed, the first being that the larger scale reaction was more sluggish, requiring an additional day of reaction time to reach the observed yield. Attempts to increase concentration with the goal of reducing reaction time instead resulted in reduced yield. The other issue is related to the reaction setup, specifically at the moment the peroxide is added, which generated a strong exotherm, and that additional care would be needed to prevent a thermal runaway. This was remedied by ensuring the reaction is cooled to 0 °C before the peroxide is added dropwise, and warming the reaction mixtures to room temperature slowly.

To explore if other simple alcohols would be viable substrates, ethanol was utilized (**Figure 2.9**), giving the diarylethane **64** product in only 30% yield, despite requiring a three-day reaction time and elevated reaction temperature (75 °C). The lowered reactivity can be attributed to the decreased solubility of iron sulfate in ethanol. With the scope of the reaction in hand we began our investigation into the mechanism of this reaction.

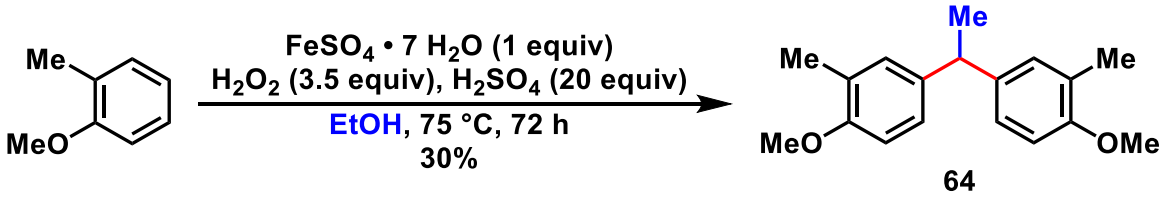

Figure 2.9 Reaction result for ethanol as a solvent

2.2.3 *Mechanistic Studies*

To test for the involvement of radical intermediates in this reaction, one equivalent of TEMPO was added, which led to a reduction in the yield to 24%, though the TEMPO trapped adduct was not observed. The reaction proceeds well when CD_3OD is utilized as

the solvent (**Figure 2.10**), generating the deuterated diarylmethane **65** in good yield. When a 1:1 mixture of CH_3OH/CD_3OD was used, partial deuteration was observed, giving KIE ≈ 7, which implies the C–H bond breakage is the rate–determining step of the reaction.

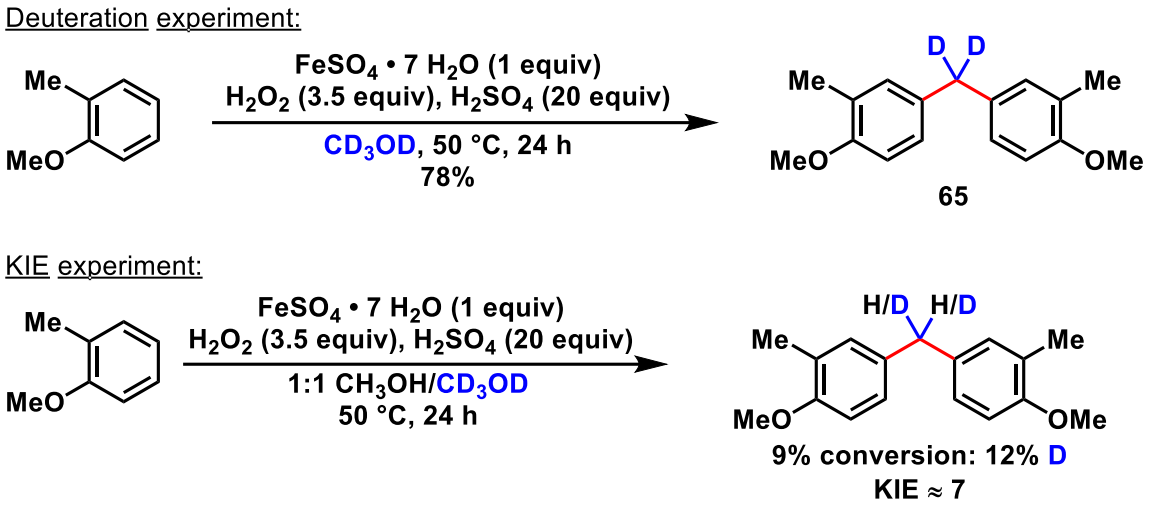

Figure 2.10 Deuterium labelling studies

When 1,3,5-trimethoxybenzene was used as a substrate (**Figure 2.12**), reacting for 3.5 h allowed us to observe the radical cation intermediate by UV-vis spectroscopy. The λ_{max} values 515 nm and 417 nm, are consistent with the values previous reported for a similar designer complex, 519 nm and 483 nm, indicating a similarity in structure between the two (**Figure 2.11**).[5]

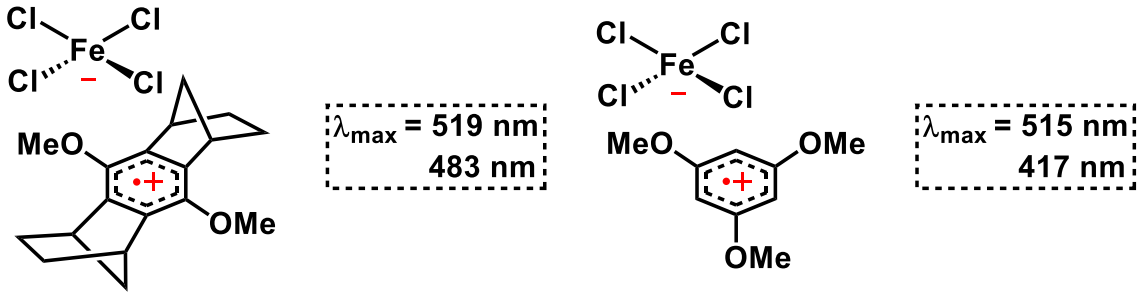

Figure 2.11 UV-vis data for aryl radical cations

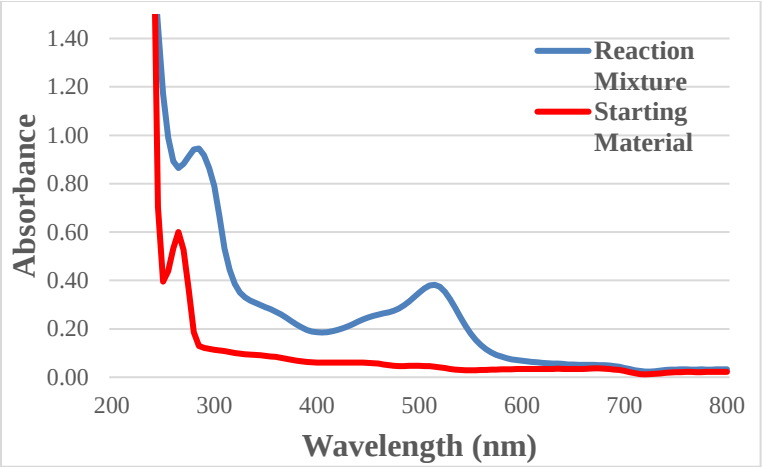

Figure 2.12 UV-vis absorbance spectra

Using cyclic voltammetry, the oxidative potential of five anisolic reactants, as well as a select product **43** were measured (**Table 2.2** work by Justin DeBow). We learned that the substrates that require elevated reaction temperatures (*e.g.*, anisole and 4-fluoro-anisole, entries 3–4) have oxidative potentials between 0.919–1.07 V that exceed the reductive potential of the iron sulfate (0.323V), indicating that their oxidations by iron sulfate are unlikely and that an alternative mechanistic pathway may be operative in those reactions. Similarly, the near doubling of the reduction potential of the product **43** of this reaction may help to explain why multiple alkylation events only occur when multiple electron-donating groups are present on the molecule, as in **61** and **62**.

Table 2.2 Reductive potentials of selected substrates

Enty	Substrate	Oxidative potential (V)
1	2-methyl anisole	0.378
2	3-*tert*-butyl anisole	0.302
3	anisole	0.919
4	4-fluoroanisole	1.07
5	4-bromoanisole	0.976
6	diarylmethane (**50**)	0.668

2.3 Discussion

Based on the experiments described above, we propose the following mechanism. The reaction begins with the iron-mediated peroxide cleavage that Fenton's reagent is known for, generating a hydroxyl radical in the process. That radical then abstracts a hydrogen atom from methanol, generating a methanol radical and water. It is at this point that the mechanisms diverge (**Figure 2.13**), depending on the oxidative potential of the anisole derivative. For those with low oxidative potentials that can be oxidized by iron(III), the radical cation is formed and then reacts with the hydroxymethyl radical to form cationic intermediate **66**, which aromatizes to form benzylic alcohol **67**. This intermediate, which we were unable to observe, presumably undergoes a rapid S_N1-type ejection of water, generating a benzylic cation that reacts in an EAS fashion to form the final product.

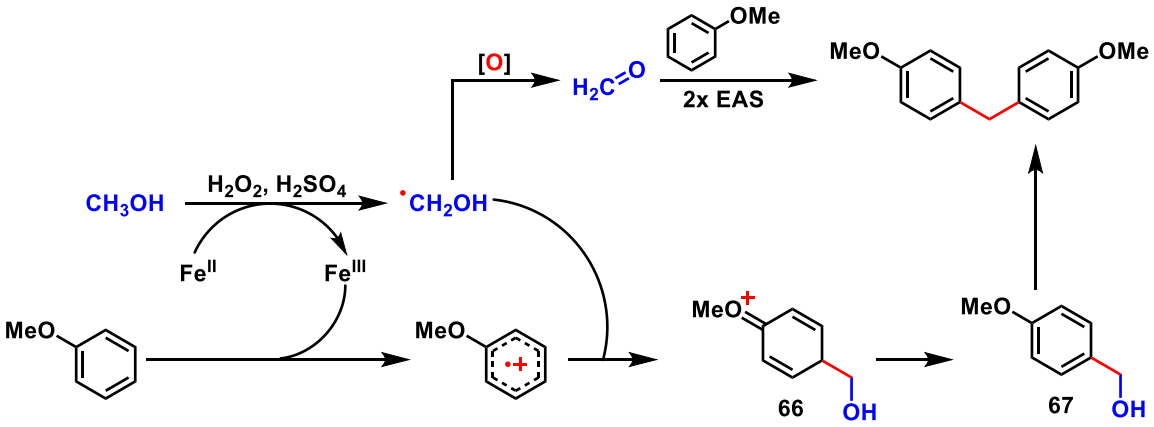

Figure 2.13 Proposed reaction mechanisms
Two potential mechanism paths are proposed for this reaction. When the oxidative potential is sufficiently low, radical combination pathway (bottom) is more likely. When the oxidative potential is higher, the double EAS pathway (top) is most reasonable.

When the oxidative potential of the anisole is high enough, its reaction with iron is slow. In such cases, the hydroxymethyl radical can be further oxidized to formaldehyde, which

under acidic conditions undergo a Friedel–Crafts alkylation. Methodologies that utilize formaldehyde or paraformaldehyde to synthesize diarylmethanes are known, though they require excess amounts of the arene with respect to formaldehyde and elevated reaction temperatures that exceed those required in our methodolgy.[12] We hypothesize that the requirement for stoichiometric quantities of the iron is caused by a significant quantity of the iron being utilized as a counter ion for the aryl radical cation.

While the chemistry reported above provides easy access to symmetric diarylmethane products, the coupling of two different arenes would massively improve the utility of this reaction. When this was attempted utilizing 2-methylanisole and 4-methyl-anisole as the coupling partners, we observed only homocoupling of 2-methylanisole leading to its diarylmethane product, with minimal to no reaction with 4-methylanisole. The preference for homocoupling withstood any attempt to alter the conditions, so we turned to other potential methods to achieve cross-coupling. To that end, we hoped to be able to resubject the diarylmethane product of this reaction with an equivalent of a different anisole to generate triarylmethane **68**. We imagined that this transformation (**Figure 2.14**) would occur via abstraction of a hydrogen atom from the doubly benzylic methylene group to generate stabilized radical **69**, which would then engage the radical cation derived from anisole to give the triarylmethane product.

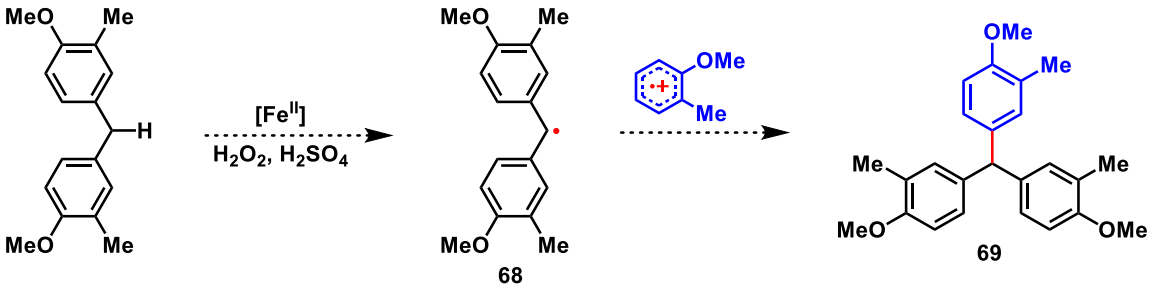

Figure 2.14 Proposed reaction pathway for triarylmethane synthesis

Unfortunately, the proposed pathway was elusive. Even when we waited for 1 h before additional anisole was added to the reaction, with the hopes of giving the benzylic radical enough time to form, the observed result was the homocoupling of the excess 2-methylanisole to generate more of the diarylmethane product without any triarylmethane generation. Despite our inability to accomplish these transformations, this method still presents a unique concept for the formation of diarylmethanes without the need to prefunctionalize the aryl coupling partners, while using the more expensive arene component as the limiting reagent. The utilization of iron(II) sulfate to promote this reaction ensures that, while stoichiometric quantities are required, the reaction is sustainable as it utilizes an abundant metal and does not require the added steps that would be needed to prepare the arenes.

2.4 Materials and Methods

2.4.1 *Solvents and Reagents*

Commercial reagents were purchased from MilliporeSigma, Acros Organics, Chem–Impex, TCI, Oakwood, and Alfa Aeser and used without purification. Solvents were purchased from Fischer Scientific, Acros Organics, Alfa Aeser, and MilliporeSigma.

Dichloroethane was purchased in a Sure/Seal bottle and dispensed under N_2. Deuterated solvents were obtained from Cambridge Isotope Laboratories, Inc. or MilliporeSigma. Non-anisolic aryl ethers (**Figure 2.15**) were prepared using our previously published procedure.[13]

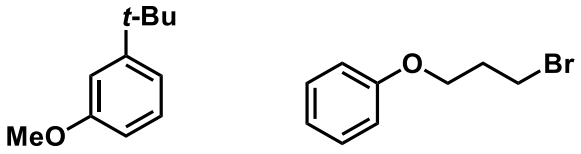

Figure 2.15 Aryl ethers synthesized to be substrates

2.4.2 *Analytical instrumentation*

Melting points were taken using the BÜCHI B-545 melting point apparatus.

Proton, carbon, fluorine, and deuterium NMR spectra were recorded on Bruker Avance NEO 400 MHz or Bruker Avance 600 MHz spectrometers. Chemical shifts (δ) are reported in ppm relative to the residual solvent signal (δ 7.26 for ^{1}H NMR, δ 77.16 for ^{13}C{^{1}H} NMR in $CDCl_3$). Data for ^{1}H NMR spectroscopy are reported as follows: chemical shift (δ ppm), multiplicity (s = singlet, d = doublet, t = triplet, q = quartet, m = multiplet, br = broad, dd = doublet of doublets, dt = doublet of triplets), coupling constant (Hz), integration. Data for ^{13}C and ^{19}F NMR spectroscopy are reported in terms of chemical shift (δ ppm).

IR spectroscopic data was recorded on a NICOLET 6700 FT-IR spectrophotometer using a diamond attenuated total reflectance accessory. Samples are loaded onto the diamond

surface either neat or as a solution in organic solvent and the data acquired after the solvent had evaporated.

High resolution accurate mass (ESI) spectral data were obtained from the Analytical Chemistry Instrumentation Facility at the University of California, Riverside, on an Agilent 6545 Q–TOF LC/MS instrument (supported by NSF grant CHE–1828782). High resolution accurate mass (EI) spectral data were obtained from the Mass Spectrometry Facility at the University of California, Irvine, on a ThermoFinnegan TraceMS+ GC EI/CI instrument.

UV-vis spectra were recorded on an Agilent Cary 60 UV-vis spectrophotometer (190–1100 nm wavelength range with 1.5 nm resolution).

Cyclic voltammograms were recorded on an IKA Electrasyn 2.0 at room temperature.

2.4.3 *Reaction setup, monitoring, and purification*

All reagents, including the solvent, were added under ambient conditions open to air. The reactions were heated on a heating block that rests directly over top of a heating plate (0.2 mmol scale) or by submerging in an oil bath (>0.2 mmol scale). Reaction progresses were monitored using thin-layer chromatography (TLC) on EMD Silica Gel 60 F254 of Macherey–Nagel SIL HD (60 Å mean pore size, 0.75 mL/g specific pore volume, 5–17 μm particle size, with fluorescent indicator) silica gel plated. Visualization of the developed plated was performed under UV light (254 nm). Purification and isolation of products were performed via silica gel chromatography (both column and preparative thin-layer chromatography). Organic solutions were concentrated under reduced pressure on IKA®

temperature-controlled rotary evaporator equipped with a condenser flowing ethylene glycol/water coolant.

2.4.4 *General procedure*

In a 1-dram vial, iron sulfate heptahydrate (55.6 mg, 0.2 mmol, 1 equiv) was suspended in methanol (0.4 mL, 0.5 M). The solution was chilled to 0 °C in an ice-water bath before addition of H_2SO_4 (217 μL, 4.0 mmol, 20 equiv) and 30% H_2O_2 (75 μL, 0.7 mmol, 3.5 equiv). The resultant solution was warmed to room temperature and stirred for 15 min before arene addition (0.2 mmol, 1 equiv). The reaction mixture was heated at 50–75 °C for 18–72 h on a heating block, at which time the solution was diluted with 15% aqueous NaOH solution (0.5 mL) and water (3 mL), then extracted with CH_2Cl_2 (3 x 5 mL). The combined organic extract was wasted with brine (5 mL) and dried over Na_2SO_4. The solution was concentrated *in vacuo* and purified via silica gel chromatography to obtain the alkylation product.

Safety Note: The mixture of sulfuric acid and hydrogen peroxide is strongly oxidizing. An exothermic reaction occurs when the two are mixed neat. It is important to sufficiently cool the solution in an ice-water bath and ensure rapid stirring before the dropwise addition of the hydrogen peroxide solution. The exotherm/effervescence may be hard to notice on small scale. The aqueous waste obtained after liquid-liquid extraction should be neutralized with a saturated solution of sodium bisulfite before disposal.

2.4.5 *Kinetic isotope effect study*

This experiment was carried out using the general procedure detailed for 2-methylanisole (25 μL, 0.20 mmol, 1 equiv) in a 1:1 mixture of CH_3OH/CD_3OD as solvent (0.4 mL total), reacting at 50 °C on a heating block for 24 h or 4 h to obtain 9% conversion. NMR analysis of the crude reaction mixture and HRMS analysis revealed 17% deuterium incorporation at full conversion. At 9% conversion the deuterium incorporation was 12%. The NMR analysis was performed in CD_3OD to separate the methylene C–H peak from the methoxy C–H peak to be used for analysis. This was needed as these two peaks overlap in $CDCl_3$.

2.4.6 *TEMPO trapping experiment*

In a 1-dram vial, iron sulfate heptahydrate (55.6 mg, 0.2 mmol, 1 equiv) was suspended in methanol (0.4 mL, 0.5 M). The solution was chilled to 0 ºC before addition of H_2SO_4 (217 μL, 4.0 mmol, 20 equiv) and 30% H_2O_2 (75 μL, 0.7 mmol, 3.5 equiv). The resultant solution was warmed to rt and stirred for 15 min before arene (0.2 mmol, 1 equiv) and TEMPO (0.2 mmol, 1 equiv) addition. The reaction mixture was heated at 50 °C for 18 h, at which time the solution was diluted with 15% aqueous NaOH solution (0.5 mL) and water (3 mL), then extracted with CH_2Cl_2 (3 x 5 mL). The combined organic extract was washed with brine (5 mL) and dried over Na_2SO_4. The crude mixture was analyzed via ^1H NMR to determine the extent of conversion to product.

2.4.7 *Cyclic voltammetry studies*

Cyclic voltammogram of iron sulfate was recorded on an IKA Electrasyn 2.0 at room temperature in 1 M HCl. A Pt foil electrode was used as the working electrode and the counter electrode was a Pt plated copper electrode. A silver electrode in 3 M KCl was used as the reference electrode and all potentials are expressed versus this reference system.

All other cyclic voltammograms were recorded on an IKA Electrasyn 2.0 at room temperature in MeCN. *n*-Bu_4BF_4 was used as the supporting electrolyte. A Pt foil electrode was used as the working electrode and the counter electrode was a Pt plated copper electrode. A silver electrode in 3 M KCl was used as the reference electrode and all potentials are expressed versus this reference system.

Cyclic voltammogram recorded on Pt foil working electrode and Pt plated copper counter electrode with Ag/AgCl reference electrode. The scan rate was 200 mV s^{-1}. Iron sulfate (30 μM) in 1 M HCl; 2-methyl anisole (30 μM) in 0.1 M *n*-Bu_4BF_4 MeCN solution; 4-fluoroanisole (30 μM) in 0.1 M *n*-Bu_4BF_4 MeCN solution; 4-bromoanisole (30 μM) in 0.1 M *n*-Bu_4BF_4 MeCN solution; anisole (30 μM) in 0.1 M *n*-Bu_4BF_4 MeCN solution; diarylmethane (30 μM) in 0.1 M *n*-Bu_4BF_4 MeCN solution; 3-*tert*-butyl anisole (30 μM) in 0.1 M *n*-Bu_4BF_4 MeCN solution.

2.4.8 *UV-vis spectroscopy studies*

Samples used for UV-vis spectroscopy were prepared via the general procedure with 1,3,5-trimethoxybenzene (34 mg, 0.2 mmol, 1 equiv), using a cap with a septa, reacting at 50 °C

for 3.5 h. The reaction is removed from the heat and 0.5 μL of the solution is dissolved in methanol (3 mL) in a quartz cuvette.

The analogous experiments with 2-methylanisole and 1,3-dimethoxybenzene did not yield signals that are indicative of radical cation species. The UV-vis absorbance spectra of the reaction mixture bear close resemblance to their respective arene reactants.

2.4.9 *Characterization of reported compounds*

3, 3'-Dimethyl-4, 4'-dimethoxydiphenylmethane (43)

Prepared via the general procedure with 2-methylanisole (25 μL, 0.20 mmol), reacting at 50 °C for 18 h. Purification by flash chromatography (eluting with 19:1 hexanes/EtOAc) afforded **43** (0.0215 g, 84%) as a clear oil. R_f: 0.38 (19:1 hexanes/EtOAc). ^{1}H NMR ($CDCl_3$, 600 MHz): δ 6.96 (m, 4H), 6.74 (d, J = 8.0 Hz, 2H), 3.80 (s, 8H), 2.18 (s, 6H); ^{13}C NMR ($CDCl_3$, 126 MHz): δ 156.2, 133.6, 131.3, 126.9, 126.6, 110.0, 55.5, 40.3, 16.4. IR (ATR): 3030, 2905, 2833, 1610, 1500, 1463, 1440, 1377, 1294, 1219, 1182, 1060, 917, 888, 750, 581, 564 cm^{-1}. HRMS (ESI+): *m/z* $[M+H]^+$ calculated for $[C_{17}H_{21}O_2]^+$: 257.1536; found: 257.1535. The spectral data are consistent with those previously reported in the literature.[14]

3, 3'-Diethyl-4, 4'-dimethoxydiphenylmethane (44)

Prepared via the general procedure with 2-ethylanisole (30 μL, 0.20 mmol), reacting at 50 °C for 18 h. Purification by flash chromatography (eluting with 9:1 hexanes/EtOAc) afforded **44** (0.0194 g, 68%) as a yellow oil. R_f: 0.48 (9:1 hexanes/EtOAc). ^{1}H NMR ($CDCl_3$, 600 MHz): δ 7.01 (s, 2H), 6.99 (d, J = 7.8 Hz, 2H), 6.80 (d, J = 8.4 Hz, 2H), 3.87

(s, 2H), 3.83 (s, 6H), 2.63 (q, J = 7.2 Hz, 4H), 1.20 (t, J = 7.8 Hz, 6H); ^{13}C NMR ($CDCl_3$, 126 MHz): δ 156.0, 133.9, 132.8, 129.9, 127.1, 110.5, 55.7, 40.7, 23.7, 14.6. IR (ATR): 3072, 2961, 2931, 2833, 1609, 1498, 1462, 1288, 1242, 1181, 1134, 1033, 928, 884, 804, 746, 635, 576, 539, 528 cm^{-1}. HRMS (ESI+): *m/z* $[M+H]^+$ calculated for $[C_{19}H_{25}O_2]^+$: 285.1849; found: 285.1842.

bis(3-Fluoro-4-methoxyphenyl)methane (45)

Prepared via the general procedure with 2-fluoroanisole (22 μL, 0.20 mmol), reacting at 75 °C for 48 h. Purification by flash chromatography (eluting with 19:1 hexanes/EtOAc) afforded **45** (0.0077 g, 29%) as a colorless oil. R_f: 0.48 (19:1 hexanes/EtOAc). ^{1}H NMR ($CDCl_3$, 600 MHz): δ 6.87 (m, 6H), 3.86 (s, 6H), 3.82 (s, 2H); ^{13}C NMR ($CDCl_3$, 126 MHz): δ 152.3 (d, J = 201.6 Hz), 146.0 (d, J = 8.8 Hz), 133.9 (d, J = 4.7 Hz), 124.3, 116.5 (d, J = 15.2 Hz), 113.5, 56.4, 40.0; ^{19}F NMR ($CDCl_3$, 564 MHz): δ 135.2 (dd, J = 10.8, 7.8 Hz). IR (ATR): 3025, 3005, 2917, 2839, 1509, 1464, 1141, 1269, 1219, 1124, 1028, 966, 806, 761, 750, 669, 575, 536 cm^{-1}. HRMS (ESI+): *m/z* $[M+H]^+$ calculated for $[C_{15}H_{15}F_2O_2]^+$: 265.1035; found: 265.1019.

bis(3-Bromo-4-methoxyphenyl)methane (46)

Prepared via the general procedure with 2-bromoanisole (25 μL, 0.20 mmol), reacting at 75 °C for 48 h. Purification by flash chromatography (eluting with 19:1 hexanes/EtOAc) afforded **46** (0.0173 g, 45%) as a white solid. R_f: 0.33 (19:1 hexanes/EtOAc). M.p. 100–101 °C (lit. 102–103 °C). ^{1}H NMR ($CDCl_3$, 600 MHz): δ 7.37 (d, J = 1.8 Hz, 2H), 7.09 (dd, J = 8.4, 2.4 Hz, 2H), 6.85 (d, J = 8.4 Hz, 2H), 3.90 (s, 6H), 3.84 (s, 2H); ^{13}C NMR ($CDCl_3$, 126 MHz): δ 154.5, 134.6, 133.7, 128.8, 112.1, 111.8, 56.4, 39.5. IR (ATR): 3011,

2914, 2838, 2359, 1726, 1600, 1569, 1489, 1464, 1454, 1437, 1400, 1287, 1248, 1205, 1180, 1151, 1050, 1016, 898, 877, 812, 799, 754, 704, 674, 666, 621, 554 cm^{-1}. HRMS (ESI+): *m/z* $[M+Na]^+$ calculated for $[C_{15}H_{14}Br_2O_2Na]^+$: 408.9232; found: 408.9236. The spectral data are consistent with those previously reported in the literature.[15]

bis(2-methoxy-5-methylphenyl)methane (47)

Prepared via the general procedure with 4-methylanisole (25 μL, 0.20 mmol), reacting at 50 °C for 48 h. Purification by flash chromatography (eluting with 19:1 hexanes/EtOAc) afforded **47** (0.0188 g, 73%) as a colorless oil. R_f: 0.46 (19:1 hexanes/EtOAc). ^{1}H NMR (CDCl3, 600 MHz): δ 6.98 (d, J = 9.6 Hz, 2H), 6.83 (s, 2H), 6.77 (d, J =8.4 Hz, 2H), 3.91 (s, 2H), 3.80 (s, 6 H), 2.23 (s, 6H); ^{13}C NMR ($CDCl_3$, 126 MHz): δ 155.7, 131.2, 129.6, 129.2, 127.4, 110.4, 55.8, 29.5, 20.7. IR (ATR): 3079, 2997, 2922, 2832, 1498, 1463, 1288, 1240, 1182, 1128, 1110, 1034, 910, 803, 766, 733, 564, 536, 460 cm^{-1}. HRMS (ESI+): m/z $[M+H]^+$ calculated for $[C_{17}H_{21}O_2]^+$: 257.1536; found: 257.1533.

bis(5-Ethyl-2-methoxyphenyl)methane (48)

Prepared via the general procedure with 4-ethylanisole (28 μL, 0.20 mmol), reacting at 50 °C for 48 h. Purification by flash chromatography (eluting with 19:1 hexanes/EtOAc) afforded **48** (0.0184 g, 65%) as a white solid. R_f: 0.67 (19:1 hexanes/EtOAc). M.p. 41.6–42.0 °C. ^{1}H NMR ($CDCl_3$, 600 MHz): δ 7.00 (dd, *J* = 8.4, 1.8 Hz, 2H), 6.88 (s, 2H), 6.79 (d, *J* = 7.8 Hz, 2H), 3.92 (s, 2H), 3.80 (s, 6H), 2.52 (q, *J* = 7.8 Hz, 4H), 1.15 (t, *J* = 7.2 Hz, 6H); ^{13}C NMR ($CDCl_3$, 126 MHz): δ 155.8, 136.1, 130.2, 129.1, 126.1, 110.4, 55.7, 29.9, 28.1, 16.1. IR (ATR): 3012, 2992, 2960, 2928, 2868, 2834, 1607, 1499, 1455, 1371, 1302,

1255, 1183, 1131, 1030, 924, 883, 814, 761, 739, 697, 656, 592, 526 cm^{-1}. HRMS (ESI+): *m/z* $[M+H]^+$ calculated for $[C_{19}H_{25}O_2]^+$: 285.1849; found: 285.1840.

bis(5-(*tert*-Butyl)-2-methoxyphenyl)methane (49)

Prepared using General Procedure with 4-*tert*-butylanisole (35 µL, 0.200 mmol), reacting at 75 °C for 18 h. Purification by flash chromatography (eluting with 19:1 hexanes/EtOAc) afforded **49** (0.0235 g, 69%) as a white solid. R_f: 0.63 (19:1 hexanes/EtOAc). M.p. 86.0–86.8 °C (lit. 83–84 °C). ^{1}H NMR ($CDCl_3$, 600 MHz): δ 7.16 (m, 4H), 6.77 (d, *J* = 8.4 Hz, 2H), 3.94 (s, 2H), 3.80 (s, 6H), 1.24 (s, 18H); ^{13}C NMR ($CDCl_3$, 126 MHz): δ 155.5, 142.7, 128.4, 128.1, 123.3, 109.6, 55.3, 34.0, 31.5, 30.6. IR (ATR): 3025, 2949, 2901, 2899, 1606, 1497, 1462, 1438, 1389, 1360, 1303, 1268, 1255, 1175, 1142, 1111, 1082, 941, 819, 764, 633, 532 cm^{-1}. HRMS (ESI+): *m/z* $[M+H]^+$ calculated for $[C_{23}H_{33}O_2]^+$: 341.2475; found: 341.2480. The spectral data are consistent with those previously reported in the literature.[16]

bis(5-Chloro-2-methoxyphenyl)methane (50)

Prepared via the general procedure with 4-chloroanisole (25 µL, 0.20 mmol), reacting at 75 °C for 48 h. Purification by flash chromatography (eluting with 19:1 hexanes/EtOAc) afforded **50** (0.0089 g, 30%) as a white solid. R_f: 0.58 (19:1 hexanes/EtOAc). M.p. 92.8–93.5 °C. ^{1}H NMR ($CDCl_3$, 600 MHz): δ 7.18 (dd, *J* = 9.0, 2.4 Hz, 2H), 7.02 (d, *J* = 1.8 Hz, 2H), 6.81 (d, *J* = 9.0 Hz, 2H), 3.90 (s, 2H), 3.84 (s, 6H); ^{13}C NMR ($CDCl_3$, 126 MHz): δ 156.1, 130.2, 130.1, 127.0, 125.2, 111.5, 55.7, 29.6. IR (ATR): 3006, 2962, 2912, 2834, 2359, 1592, 1485, 1454, 1404, 1297, 1253, 1179, 1130, 1025, 920, 860, 807, 762, 643, 563, 530 cm^{-1}. GCMS (EI+): *m/z* $[M]^+$ calculated for $C_{15}H_{14}Cl_2O_2$: 296.0; found: 296.0. HRMS (ESI+): *m/z* $[M+H]^+$ calculated for $[C_{15}H_{15}Cl_2O_2]^+$: 297.0444; found: 297.0449.

bis(5-Bromo-2-methoxyphenyl)methane (51)

Prepared via the general procedure with 4-bromoanisole (25 μL, 0.20 mmol), reacting at 75 °C for 48 h. Purification by flash chromatography (eluting with 19:1 hexanes/EtOAc) afforded **51** (0.0081 g, 21%) as a white solid. R_f: 0.50 (19:1 hexanes/EtOAc). M.p. 106.1–107.2 °C (lit. 107–109 °C)[17]. ^{1}H NMR ($CDCl_3$, 600 MHz): δ 7.29 (dd, J = 8.4, 2.4 Hz, 2H), 7.13 (d, J = 2.4 Hz, 2H), 6.73 (d, J = 8.4 Hz, 2H), 3.85 (s, 2H), 3.80 (s, 6H); ^{13}C NMR ($CDCl_3$, 126 MHz): δ 156.7, 133.1, 130.8, 130.2, 112.8, 112.1, 55.8, 29.7. IR (ATR): 3073, 2996, 2955, 2925, 2831, 2360, 2342, 1587, 1483, 1454, 1436, 1400, 1295, 1252, 1176, 1191, 1132, 1118, 1030, 896, 873, 850, 805, 797, 625, 563, 554, 538 cm^{-1}. HRMS (ESI+): *m/z* $[M+H]^+$ calculated for $[C_{15}H_{15}Br_2O_2]^+$: 384.9433; found: 384.9449. Spectral data consistent with literature.[15]

bis(5-Iodo-2-methoxyphenyl)methane (52)

Prepared via the general procedure with 4-iodoanisole (47 mg, 0.20 mmol), reacting at 75 °C for 48 h. Purification by flash chromatography (eluting with 5:1 hexanes/CH_2Cl_2) afforded **52** (0.0096 g, 20%) as a white solid. R_f: 0.84 (5:1 hexanes/DCM). M.p. 134.6–135.2 °C. ^{1}H NMR ($CDCl_3$, 600 MHz): δ 7.50 (dd, J = 8.4, 1.2 Hz, 2H), 7.34 (s, 2H), 6.66 (d, J = 9.0 Hz, 2H), 3.84 (s, 2H), 3.83 (s, 6H); ^{13}C NMR ($CDCl_3$, 126 MHz): δ 157.6, 138.9, 136.3, 131.3, 112.8, 83.0, 55.6, 29.5. IR (ATR): 3064, 2931, 2835, 1584, 1511, 1484, 1439, 1394, 1271, 1243, 1221, 1174, 1126, 1027, 866, 802, 761, 635, 616, 560, 529 cm^{-1}. HRMS (ESI+): *m/z* $[M+Na]^+$ calculated for $[C_{15}H_{14}I_2O_2Na]^+$: 502.8975; found: 502.8971.

Dimethyl 3,3'-(methylenebis(4-methoxy-3,1-phenylene))dipropionate (53)

Prepared via the general procedure with methyl 3-(4-methoxyphenyl)propanoate (35 μL, 0.20 mmol), reacting at 50 °C for 48 h. Purification by flash chromatography (eluting with 9:1 hexanes/EtOAc) afforded **53** (0.0250 g, 64%) as a clear oil. R_f: 0.10 (9:1 hexanes/EtOAc). ^{1}H NMR ($CDCl_3$, 600 MHz): δ 7.00 (d, J = 8.4, 2H), 6.84 (s, 2H), 6.78 (d, J = 8.4 Hz, 2H), 3.89 (s, 2H), 3.80 (s, 6H), 3.63 (s, 6H), 2.82 (t, J = 7.8Hz, 4H), 2.54 (t, J = 7.8 Hz, 4H); ^{13}C NMR ($CDCl_3$, 126 MHz): δ 173.7, 156.2, 132.3, 130.4, 129.2, 126.8, 110.4, 55.6, 51.7, 36.2, 30.4, 29.9. IR (ATR): 3008, 2959, 2928, 2834, 2359, 2341, 1735, 1608, 1499, 1456, 1437, 1251, 1177, 1130, 1030, 882, 813, 761, 738, 697, 587, 541, 533, 526 cm^{-1}. HRMS (ESI+): *m/z* $[M+H]^+$ calculated for $[C_{23}H_{29}O_6]^+$: 401.1959; found: 401.1973.

Dimethyl 3,3'-methylenebis(4-methoxybenzoate) (54)

Prepared via the general procedure with 4-methoxy-methylbenzoate (33 mg, 0.20 mmol), [or 4-methoxybenzoic acid, (30 mg. 0.20 mmol, 1 equiv)] reacting at 75 °C for 18 h. Purification by flash chromatography (eluting with 19:1 hexanes/EtOAc) afforded **54** (0.0170 g, 52%), as a white solid. R_f: 0.31 (19:1 hexanes/EtOAc). M.p. 143.7–144.9 °C. ^{1}H NMR ($CDCl_3$, 600 MHz): δ 7.91 (d, J = 10.2 Hz, 2H), 7.75 (s, 2H), 6.87 (d, J = 8.4 Hz, 2H), 3.96 (s, 2H), 3.88 (s, 6H), 3.84 (s, 6H); ^{13}C NMR ($CDCl_3$, 126 MHz): δ 167.3, 161.5, 132.0, 130.0, 128.6, 122.3, 109.9, 55.7, 51.9, 30.1. IR (ATR): 3005, 2953, 2842, 2359, 1708, 1604, 1500, 1438, 1289, 1262, 1241, 1190, 1138, 1102, 1022, 995, 900, 825, 763, 637, 560 cm^{-1}. HRMS (ESI+): *m/z* $[M+H]^+$ calculated for $[C_{19}H_{21}O_6]^+$: 345.1333; found: 345.1339.

bis(4-(Isopropyl)-2-methoxyphenyl)methane (55)

Prepared via the general procedure with 1-(isopropyl)-3-methoxybenzene (32 µL, 0.20 mmol), reacting at 75 °C for 18 h. Purification by flash chromatography (eluting with 5:1 hexanes/CH_2Cl_2) afforded **55** (0.0188 g, 60%) as a colorless oil. R_f: 0.70 (5:1 hexanes/DCM). ^{1}H NMR ($CDCl_3$, 600 MHz): δ 6.87 (d, *J* = 2.4 Hz, 2H), 6.77 (d, *J* = 8.4 Hz, 2H), 6.63 (dd, *J* =8.4, 2.4 Hz, 2H), 3.93 (s, 2H), 3.80 (s, 6H), 3.09 (m, 2H), 1.20 (d, *J* = 6.6 Hz, 12H); ^{13}C NMR ($CDCl_3$, 126 MHz): δ 158.5, 148.5, 130.7, 130.1, 111.7, 110.3, 55.3, 33.9, 29.2, 23.7. IR (ATR): 3012, 2959, 2868, 2833, 1609, 1576, 1490, 1463, 1383, 1363, 1285, 1235, 1205, 1069, 1036, 930, 871, 802, 668 cm^{-1}. HRMS (ESI+): *m/z* $[M+H]^+$ calculated for $[C_{21}H_{29}O_2]^+$: 313.2162; found: 313.2153.

bis(2-(Chloro)-4-methoxyphenyl)methane (56)

Prepared via the general procedure with 3-chloroanisole (24 µL, 0.20 mmol), reacting at 75 °C for 48 h. Purification by flash chromatography (eluting with hexanes, 5 elutions) afforded **56** (0.0077 g, 26%) as a colorless oil. R_f: 0.11 (95:5 hexanes/EtOAc). ^{1}H NMR ($CDCl_3$, 600 MHz): δ 6.92 (d, *J* = 2.4 Hz, 2H), 6.93 (d, *J* = 8.4 Hz, 2H), 6.74 (dd, *J* = 8.4, 2.4 Hz, 2H), 4.05 (s, 2H), 3.78 (s, 6H); ^{13}C NMR ($CDCl_3$, 126 MHz): δ 158.8, 134.8, 131.2, 129.6, 114.9, 113.1, 55.6, 35.2. IR (ATR): 2939, 2835, 1575, 1491, 1462, 1436, 1283, 1236, 1201, 1181, 1034, 912, 839, 801, 762, 691, 605, 551, 528 cm^{-1}. HRMS (ESI+): *m/z* $[M+Na]^+$ calculated for $[C_{15}H_{14}Cl_2O_2Na]^+$: 319.0263; found: 319.0255.

bis(2-(Bromo)-4-methoxyphenyl)methane (57)

Prepared via the general procedure with 3-bromoanisole (25 µL, 0.200 mmol), reacting at 75 °C for 48 h. Purification by flash chromatography (eluting with hexanes, 5 elutions)

afforded **57** (0.0092 g, 24%) as a clear oil. R_f: 0.42 (95:5 hexanes/EtOAc). ^{1}H NMR ($CDCl_3$, 600 MHz): δ 7.15 (d, *J* = 2.4 Hz, 2H), 6.89 (d, *J* = 8.4 Hz, 2H), 6.78 (dd, *J* = 8.4, 2.4 Hz, 2H), 4.06 (s, 2H), 3.79 (s, 6H); ^{13}C NMR ($CDCl_3$, 126 MHz): δ 158.8, 131.4, 131.1, 125.1, 118.1, 113.7, 55.7, 40.4. IR (ATR): 3011, 2914, 2838, 2359, 1569, 1489, 1464, 1454, 1437, 1400, 1287, 1248, 1205, 1180, 1151, 1050, 1016, 898, 877, 812, 799, 754, 704, 674, 666, 621, 554 cm^{-1}. The spectroscopic data is consistent with those previously reported in the literature.[18]

bis(4-(*tert*-Butyl)-2-ethoxyphenyl)methane (58)

Prepared via the general procedure with 1-(*tert*-butyl)-3-ethoxybenzene (35 mg, 0.20 mmol), reacting at 75 °C for 18 h. Purification by flash chromatography (eluting with 19:1 hexanes/EtOAc) afforded **58** (0.0232 g, 63%) as a colorless oil. R_f: 0.85 (19:1 hexanes/EtOAc). ^{1}H NMR ($CDCl_3$, 600 MHz): δ 7.08 (d, *J* = 8.4 Hz, 2H), 6.87–6.86 (m, 4H), 4.06 (q, *J* = 7.2 Hz, 4H), 3.91 (s, 2H), 1.42 (t, *J* = 7.2 Hz, 6H), 1.30 (s, 18H); ^{13}C NMR ($CDCl_3$, 126 MHz): δ 156.7, 150.1, 130.3, 127.1, 117.1, 109.1, 63.8, 34.8, 31.6, 29.2, 15.2. IR (ATR): 3086, 2962, 2870, 1609, 1574, 1500, 1408, 1391, 1266, 1230, 1136, 1105, 1047, 962, 909, 855, 813, 732, 674, 648 cm^{-1}. HRMS (ESI+): *m/z* $[M+H]^+$ calculated for $[C_{25}H_{37}O_2]^+$: 369.2788; found: 369.2778.

bis(4-(3-Bromopropoxy)phenyl)methane (59)

Prepared via the general procedure with 3-bromophenoxypropane (32 μL, 0.20 mmol), reacting at 50 °C for 18 h. Purification by flash chromatography (eluting with 9:1 hexanes/Et_2O) afforded **59** (0.0096 g, 47%) as a yellow oil. R_f: 0.36 (9:1 hexanes/Et_2O). ^{1}H NMR ($CDCl_3$, 600 MHz): δ 7.08 (d, *J* = 8.4 Hz, 4H), 6.82 (d, *J* = 8.4 Hz, 4H), 4.07 (t,

J = 5.4 Hz, 4H), 2.05 (s, 2H), 3.60 (t, *J* = 6.6 Hz, 4H), 2.30 (qt, *J* = 6.0 Hz, 4H); ^{13}C NMR ($CDCl_3$, 126 MHz): δ 157.2, 134.1, 129.9, 114.6, 65.4, 40.3, 32.6, 31.1. IR (ATR): 3068, 2923, 1609, 1583, 1506, 1468, 1435, 1387, 1299, 1235, 1172, 1109, 1029, 929, 851, 818, 778, 737, 668, 655, 598, 552, 529 cm^{-1}. HRMS (ESI+): *m/z* $[M+NH_4]^+$ calculated for $[C_{19}H_{26}Br_2NO_2]^+$: 458.0325; found: 458.0319.

bis(2,4,6-Trimethoxyphenyl)methane (60)

Prepared via the general procedure with 1,3,5-trimethoxybenzene (33.6 mg, 0.20 mmol), reacting at 50 °C for 48 h. Purification by flash chromatography (eluting with 3:1 hexanes/EtOAc) afforded **60** (0.0214 g, 61%) as a clear oil. R_f: 0.51 (3:1 hexanes/EtOAc). ^{1}H NMR ($CDCl_3$, 600 MHz): δ 6.09 (s, 4H), 3.83 (s, 2H), 3.77(s, 6H), 3.70 (s, 12H); ^{13}C NMR ($CDCl_3$,126 MHz): δ 159.4, 158.8, 112.1, 91.3, 56.2, 56.3, 16.8. IR (ATR): 3002, 2956, 2925, 2849, 1593, 1496, 1454, 1411, 1327, 1224, 1197, 1146, 1106, 1057, 1033, 946, 877, 812, 793, 720, 631, 530, 499 cm^{-1}. HRMS (ESI+): *m/z* $[M+H]^+$ calculated for $[C_{19}H_{25}O_6]^+$: 349.1646; found 349.1642.

Bis(2,4-Dimethoxyphenyl)methane (61)

Prepared via the general procedure with 1,3-dimethoxybenzene (26 μL, 0.20 mmol), reacting at 50 °C for 18 h. Purification by flash chromatography (eluting with 4:1 hexanes/CH_2Cl_2) afforded **61** (0.0037 g, 12%) as a colorless oil. R_f: 0.67 (4:1 hexanes/CH_2Cl_2). ^{1}H NMR ($CDCl_3$, 600 MHz): δ 6.91 (d, *J* = 8.3 Hz, 2H), 6.46 (d, *J* = 2.4 Hz, 2H), 6.39 (dd, *J* = 8.3, 2.4 Hz, 2H), 3.79 (d, *J* = 8.0 Hz, 12H), 3.75 (s, 2H); ^{13}C NMR ($CDCl_3$,126 MHz): δ 159.1, 158.4, 130.4, 122.0, 103.8, 98.4, 55.5, 55.4, 28.5. IR (ATR):

3048, 2934, 2834, 2360, 1611, 1586, 1463, 1437, 1418, 1290, 1257, 1206, 1154 cm^{-1}. HRMS (ESI+): *m/z* $[M+H]^+$ calculated for $[C_{17}H_{21}O_4]^+$: 289.1434; found 289.1435.

4,4'-((4,6-dimethoxy-1,3-phenylene)bis(methylene))bis(1,3-dimethoxybenzene) (62)

Prepared via the general procedure with 1,3-dimethoxybenzene (26 µL, 0.20 mmol), reacting at 50 °C for 18 h. Purification by flash chromatography (eluting with 9:1 CH_2Cl_2/hexanes) afforded **62** (0.00554g, 19%) as a colorless oil. R_f: 0.85 (9:1 CH_2Cl_2/hexanes). ^1H NMR ($CDCl_3$, 400 MHz): δ 6.88 (d, *J* = 8.2 Hz, 2H), 6.70 (s, 1H), 6.46 (s, 1H), 6.40 (s, 2H), 6.35 (d, *J* = 8.1 Hz, 2H), 3.81 (s, 6H), 3.77 (s, 7H), 3.74 (s, 4H), 3.70 (s, 6H), 3.67 (s, 1H), 3.65 (s, 1H); ^{13}C NMR ($CDCl_3$,176 MHz): δ 159.0, 158.3, 156.5, 132.1, 130.3, 122.2, 120.7, 103.8, 98.3, 95.5, 55.8, 55.3, 55.3, 28.5; IR (ATR): 2996, 2880, 2440, 2287, 2050, 1855, 1463, 1416, 1207, 1178, 1109 cm^{-1}. HRMS (ESI+): *m/z* $[M+NH_4]^+$ calculated for $[C_{26}H_{30}O_6]^+$: 456.238; found 456.2367.

bis(3,7-Dimethoxynaphthalen-2-yl)methane (63)

Prepared via the general procedure with 2,6-dimethoxynapthalene (38 mg, 0.20 mmol), reacting at 50 °C for 18 h. Purification by flash chromatography (eluting with 19:1 hexanes/EtOAc), followed by trituration with ethanol afforded **63** (0.0140 g, 36%) as a tan solid. R_f: 0.10 (19:1 hexanes/EtOAc). M.p. 209.5–210.4 °C. ^1H NMR ($CDCl_3$, 600 MHz): δ 8.12 (d, *J* = 9.6 Hz, 2H), 7.62 (d, *J* = 9.0 Hz, 2H), 7.27 (m, 2H), 7.04 (s, 2H), 7.01 (dd, *J* = 9.6, 2.4 Hz, 2H), 4.87 (s, 2H), 3.88 (s, 6H), 3.87 (s, 6H); ^{13}C NMR ($CDCl_3$, 126 MHz): δ 156.7, 153.3, 130.7, 129.3, 126.7, 126.2, 124.5, 118.5, 114.9, 106.3, 57.2, 55.3, 21.9. IR (ATR): 3062, 2931, 2837, 2360, 2342, 1626, 1595, 1506, 1453, 1374, 1341, 1253, 1091,

1022, 943, 854, 730, 663 cm^{-1}. HRMS (ESI+): *m/z* $[M+Na]^+$ calculated for $[C_{25}H_{24}O_4Na]^+$: 411.1567; found: 411.1561.

4,4'-(Ethane-1,1-diyl)bis(1-methoxy-2-methylbenzene) (64)

Prepared via the general procedure with 2-methylanisole (25 µL, 0.20 mmol) using EtOH as a solvent, reacting at 75 °C for 72 h. Purification by flash chromatography (eluting with 19:1 hexanes/EtOAc) afforded **64** (0.0089 g, 33%) as a clear oil. R_f: 0.38 (19:1 hexanes/EtOAc). ^1H NMR ($CDCl_3$, 600 MHz): δ 7.01-6.95 (m, 4H), 6.74 (d, *J* = 8.4 Hz, 2H), 3.99 (q, *J* = 7.2 Hz, 1H), 3.79 (s, 6H), 2.18 (s, 6H), 1.57 (d, *J* = 7.2 Hz, 3H); ^{13}C NMR ($CDCl_3$, 126 MHz): δ 156.1, 138.8, 130.1, 126.4, 125.5, 110.0, 55.5, 43.3, 22.5, 16.4. IR (ATR): 3006, 2959, 2926, 2833, 1609, 1503, 1464, 1414, 1373, 1293, 1245, 1219, 1134, 1035, 994, 926, 886, 810, 754, 606, 494, 423, 409 cm^{-1}. HRMS (ESI+): *m/z* $[M+H]^+$ calculated for $[C_{18}H_{22}O_2]^+$: 271.1693; found: 271.1689.

bis(4-Methoxy-3-methylphenyl)methane-*d2* (65)

Prepared via the general procedure with 2-methylanisole (25 µL, 0.20 mmol) using CD_3OD as solvent, reacting at 50 °C for 18 h. Purification by flash chromatography (eluting with 19:1 hexanes/EtOAc) afforded **65** (0.0201 g, 78%) as a colorless oil. R_f: 0.38 (19:1 hexanes/EtOAc). ^1H NMR ($CDCl_3$, 600 MHz): δ 6.96-6.97 (m, 4H), 6.74 (d, *J* = 7.8 Hz, 2H), 3.80 (s, 6H), 2.18 (s, 6H); ^2H NMR ($CDCl_3$, 93 MHz): δ 3.78; ^{13}C NMR ($CDCl_3$, 126 MHz): δ 156.2, 133.5, 131.2, 126.9, 126.6, 110.0, 55.5, 16.4. IR (ATR): 3004, 2947, 2832, 1609, 1501, 1482, 1463, 1440, 1377, 1300, 1235, 1183, 1132, 1032, 884, 811, 779, 748, 622, 576, 540 cm^{-1}. HRMS (ESI+): *m/z* $[M+H]^+$ calculated for $[C_{17}H_{19}D_2O_2]^+$: 259.1662; found: 259.1668.

2.5 References

1. Scholl R.; Mansfeld, J., *meso*-Benzodianthro, *meso*-napthdianthro, and a new way to flavanthern. *Berichte der Deutschen Chemischen Gesellschaft* **1910**, *43*(2), 1734–1736.

2. Jempty, T. C.; Miller, L. L.; Mazur, Y., Oxidative coupling reactions using silica-bound ferric chloride. *The Journal of Organic Chemistry* **1980**, *45*(4), 749–751.

3. Ding, K.; Xu, Q.; Wang, Y.; Liu, J.; Yu, Z.; Du, B.; Wu, Y.; Koshima, H.; Matsuura., Novel two-phase oxidative cross-coupling of the two-component molecular crystal of 2-napthol and 2-napthylamine. *Chemical Communications* **1997**, *7*, 693–694.

4. Sarhan, A. A. O.; Bolm, C., Iron (III) chloride in oxidative C–C coupling reactions. *Chemical Society Reviews* **2009**, *38*(9), 2730–2744.

5. Horibe, T.; Ohmura, S.; Ishihara, K., Structure and reactivity of aromatic radical cations generated by $FeCl_3$. *Journal of the American Chemical Society* **2019**, *141*(5), 1877–1881.

6. Minisci, F.; Bernardi, R.; Bertini, F.; Perchinummo, M., Nucleophilic character of alkyl radical VI: a new and convenient selective alkylation of heteroaromatic bases. *Tetrahedron* **1971**, *27*(15), 3575–3579.

7. Duncton M. A. J., Minisci reactions: versatile C–H functionalizations for medicinal chemists. *Medical Chemical Communications* **2011**, *12*(2), 1135–1161.

8. Baciocchi, E., Muraglia, E., Synthesis of perfluoroalkylpyrroles by homolytic substitution with perfluoroalkyl radicals. *Tetrahedron Letters* **1993**, *34*(23), 3799–3800.

9. Minisci, F.; Galli, R.; Cecere, M.; Malatesta, V.; Caronna, T., Nucleophilic character of alkyl radical: new syntheses by alkyl radicals generated in redox processes. *Tetrahedron Letters* **1968**, *9*(54), 5609–5612.

10. Voudrias, E. A.; Reinhard, M., Reactivities of hypochlorous acid and hypobromous acid, chlorine monoxide, hypobromous acidium iron, chlorine, bromine, and bromine chloride in electrophilic aromatic substitution reactions with *p*-xylene in water. *Environmental Science & Technology* **1988**, *22*(9), 985–1112.

11. Crowley, R. III; Lujan, B.; Martinez, A.; Manasi, R.; DeBow, J. D.; Kou, K. G. M., A Fenton approach to aromatic radical cations and diarylmethane synthesis. *Journal of Organic Chemistry* **2023**, *88*, 15060-15066.

12. Li, Z. X.; Duan, Z.; Wu, Y. J., $FeCl_3$ catalyzed diarylmethanes formations. *Chinese Chemical Letters* **2009**, *20*(5), 511–513.

13. Pan, A.; Chojnacka, M.; Crowley III, R.; Göttemann, L.; Haines, B. E.; Kou, K. G. M., Synergistic Brønstead/Lewis acid catalyzed aromatic alkylation with unactivated tertiary alcohols or di-tert-butylperoxide to synthesize quaternary carbon centers. *Chemical Science* **2022**, *13*, 3539–3548.

14. Tashiro, M.; Fukata, G., Studies on Friedel-Crafts chemistry. 2. The aluminum trichloride-nitromethane catalyzed novel transbenzylation of 4,4'-dihydroxy diphenylmethanes in toluene. *The Journal of Organic Chemistry* **1977**, *8*(70), 1208–1213.

15. Tummatorn, J.; Thonsornkleeb, C.; Ruchirawat, S., Acid-promoted rearrangement of arylmethyl azides: application toward the synthesis of *N*-arylmethyl arenes and polycyclic heteroaromatic compounds. *Tetrahedron* **2012**, *68*(24), 4732–4739.

16. Tashiro, M.; Tsuge, A.; Sawada, T.; Makishima, T.; Horie, S.; Arimura, T.; Mataka, S.; Yamato, T., Metacyclophanes and related compounds. 26. Tetrahydroxy[2.n.2.n.] metacyclophanes. Preparation, reactions, and spectra. *The Journal of Organic Chemistry* **1990**, *55*(8), 2404–2409.

17. Shiomi, Y.; Saisho, M.; Tsukagoshi, K.; Shinkai, S., Specific complexation of glucose with a diphenylmethane-3,3'-diboronic acid derivative: correlation between the absolute configuration of mono- and di-saccharides and the circular dichroic activity of the complex. *Journal of the Chemical Society. Perkin Transactions I* **1993**, *17*, 2111–2118.

18. Doan, T.; Chardon, A.; Osi, A.; Mahaut, D.; Tumanov, N.; Wouters, J.; Champagne, B.; Berionni, G., Methylene bridging effect on the structures, Lewis acidities and optical properties of semi-planar triarylboranes. *Chemistry a European Journal* **2021**, *27*(5), 1736–1743.

Chapter 3: Iron "super-acid" catalyzed arene alkylation with unactivated tertiary alcohols and di-*tert*-butylperoxide

3.1 Introduction

The Friedel-Crafts reaction is a powerful, yet simple method for the alkylation of arenes. A limitation with the traditional procedures is their reliance on the usage of alkyl halides as reactive electrophiles, which are much less available as reagents than alcohols, and are often more toxic and hazardous to handle. Their use also results in the generation of a stoichiometric amount of inorganic salt waste. Activated benzylic alcohols have risen as a valuable alternative electrophile as they address hazard and waste concerns, generating water as a side-product, addressing multiple of the green chemistry principles.[1] The first example of this transformation was discovered accidentally in 1986 when the halogenation of 1-phenylethanol with tellurium chloride was attempted in toluene solvent (**Figure 3.1**).[2] Instead of the expected halogenation product, the authors observed the formation of diarylethane **70**.

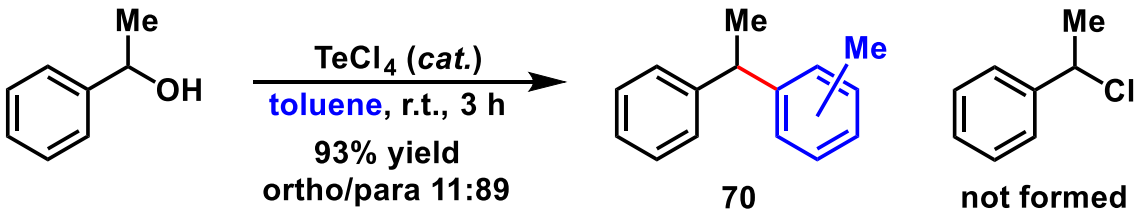

Figure 3.1 First reported benzylic alcohol Friedel-Crafts reaction

The need for solvent quantities of the arene was unnecessary with scandium triflate as the Lewis acid, in which case both benzylic and allylic alcohols reacted effectively in DCE solvent.[3] The use of a non-halogenated Lewis acid catalyst suggested that *in situ*

halogenation is likely not occurring in the reaction, though the formation of an alkyl triflate was not ruled out. This chemistry can also be catalyzed by strong Brønsted acids, and can accommodate alkyl chloride substrates.[4,5] A free hydroxy group is not necessary for reactivity. The same catalyst promotes alkylation with methyl, phenyl, and benzyl ethers, yielding the same products as the corresponding alcohols.[6] A gold complex catalyzes Friedel–Crafts alkylation with benzylic acylates, an attractive reaction as acetate is used as a protecting group for alcohols.[7] This method was highlighted in the synthesis (**Figure 3.2**) of the cholesterol regulator beclobrate (**71**).

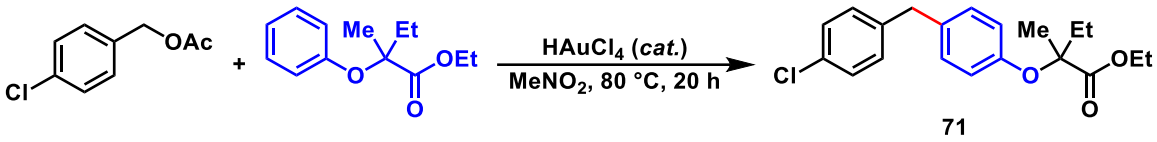

Figure 3.2 Synthesis of beclobrate via Friedel-Crafts alkylation

When strongly reactive heteroarenes, such as indoles and pyrroles, are used, the reaction can proceed without Brønsted or Lewis acid catalysts, occurring at 80 °C in water.[8] This reaction is limited to doubly benzylic alcohols, which generates stabilized carbocation intermediates.

While these reports address many of the challenges associated with Friedel-Crafts alkylations, there is a large substrate class of alcohols beyond activated allylic and benzylic alcohols that can potentially act as suitable electrophiles. To this end, methods have been developed to expand on this limitation. Through the utilization of a silver salt in conjunction with $FeCl_3$[9] or triflic acid in HFIP solvent,[10] the Friedel-Crafts reaction of primary and secondary alcohols as substrates is possible (**Figure 3.3**). Ironically,

unactivated tertiary alcohols, which mimic substrates commonly used in the original Friedel-Crafts reaction, are underexplored electrophiles. This chapter discusses advancing Friedel-Crafts reactions with tertiary alcohols for the formation of all-carbon quaternary centers.

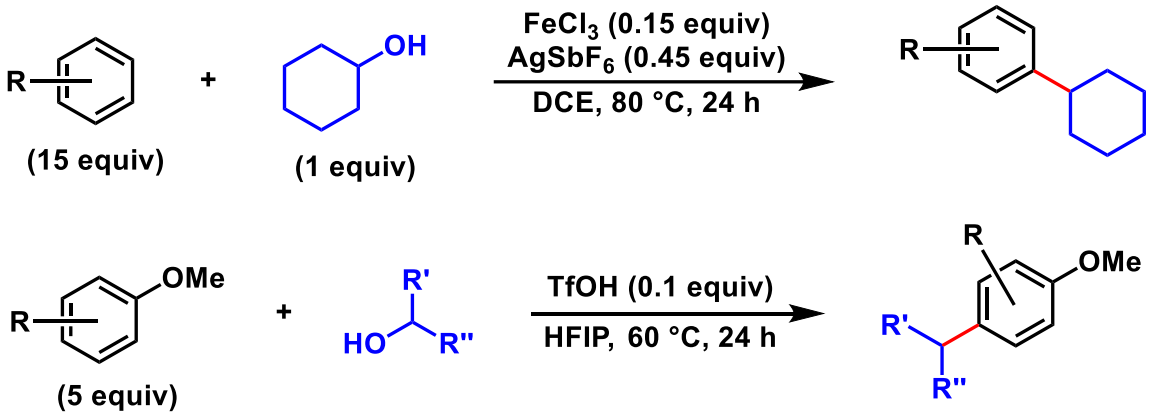

Figure 3.3 Examples of unactivated alcohol Friedel-Crafts

3.2 Results

3.2.1 *Initial studies*

Our investigations into this reaction were serendipitous and began with an entirely different reaction design. We envisioned coupling the anisole radical cation (**Chapter 2**) to the radical formed from the Fenton-mediated decomposition of di-*tert*-butylperoxide. This proposal (**Figure 3.4**) would allow for the direct formation of aryl ether bonds, a challenging transformation in organic synthesis. Instead, the combination of 2-methylanisole and di-*tert*-butylperoxide with $FeCl_3$ and HCl as catalysts, resulted in *tert*-butylation of the aromatic ring.

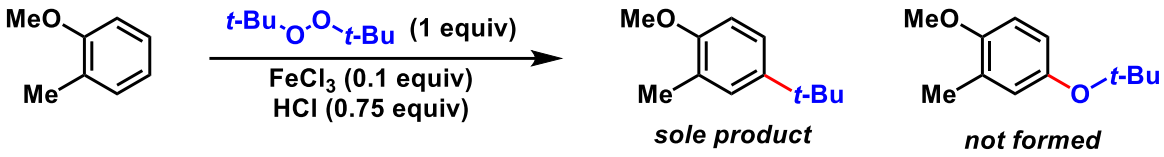

Figure 3.4 Anticipated and observed reactivity of initial studies

We hypothesized that this unexpected reactivity was caused by the *tert*-butanol generated when Fenton's reagent cleaves the peroxide bond in the presence of acid. To test this theory, the peroxide was substituted for the *tert*-butanol, which resulted in the same product formation. This represented a major improvement over the peroxide procedure as the number of commercially available tertiary alcohols far exceeds the number of peroxides. 3-*tert*-Butylphenol and *tert*-amyl alcohol **72** were employed as the model system for optimizing the reaction conditions (**Table 3.1**). When the organic acid TFA was utilized (entry 2), the reaction did not yield any product. Interestingly, the absence of acid still shows some reactivity (10%, entry 4), while swapping HCl for HBr (entry 3) decreased the yield slightly to 66%. Exchanging the iron(III) catalyst for its iron(II) counterpart (entry 5) decreased the yield significantly to 15%. This trend was not observed with $FeBr_3$ and $FeBr_2$, both resulting in 70% yields (entries 6–7). Decreasing and increasing the amount of acid used (entries 8–9), as well as changing the solvent (entries 10–14) led to decreased reactivity, with DCE being the most successful.

The conditions were also operable when anisoles were used as substrates, and was moderately successful with arenes bearing weakly electron-donating groups as well. For more challenging substrates, increased catalyst loading was required, which will be noted in the substrate scope to come.

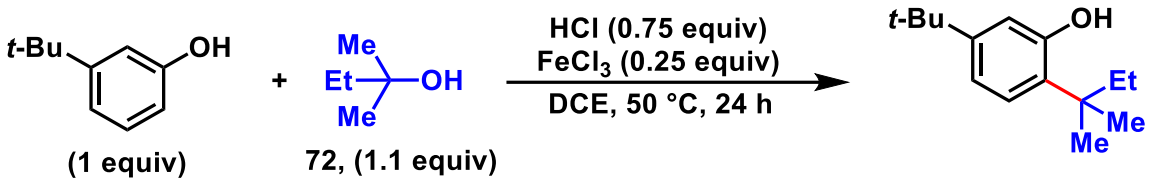

Table 3.1 Optimizing conditions for Friedel-Crafts alkylation

Entry	[Fe]	Acid	Acid Eq.	Solvent	% yield
1	$FeCl_3$	HCl	75	DCE	72
2	$FeCl_3$	TFA	75	DCE	0
3	$FeCl_3$	HBr	75	DCE	66
4	$FeCl_3$	HCl	0	DCE	10
5	$FeCl_2$	HCl	75	DCE	15
6	$FeBr_3$	HCl	75	DCE	70
7	$FeBr_2$	HCl	75	DCE	70
8	$FeCl_3$	HCl	50	DCE	63
9	$FeCl_3$	HCl	100	DCE	60
10	$FeCl_3$	HCl	75	HFIP	13
11	$FeCl_3$	HCl	75	PhCl	75
12	$FeCl_3$	HCl	75	PhMe	43
13	$FeCl_3$	HCl	75	IPA	0
14	$FeCl_3$	HCl	75	THF	0

3.2.2 *Substrate scope*

While the reaction works well for a variety of phenolic substrates, this dissertation focuses on the non-phenolic substrates that the author studied (**Figure 3.5**). In addition to 2-methyl- anisole **81**, ethyl phenyl ether **74**, benzodioxole **75**, and bromopropyl phenyl ether **76** are alkylated in 34–94% yields. Bulkier alcohols like cumyl alcohol, methyl cyclohexanol, methyl cyclopentanol, and adamantanol combine with 2-methylanisole to produce **77-80** in 59–99% yields. 2-Ethylanisole was transformed to alkylated **83** in 99% yield, while 2-bromoanisole is converted to alkylated **84** in decreased yield (37%). Most of the *meta*- substituted anisole derivatives exhibited lower reactivity, with the exception of 3-*tert*-butylanisole **73** reacting with good yield (75%). Anisole derivatives containing

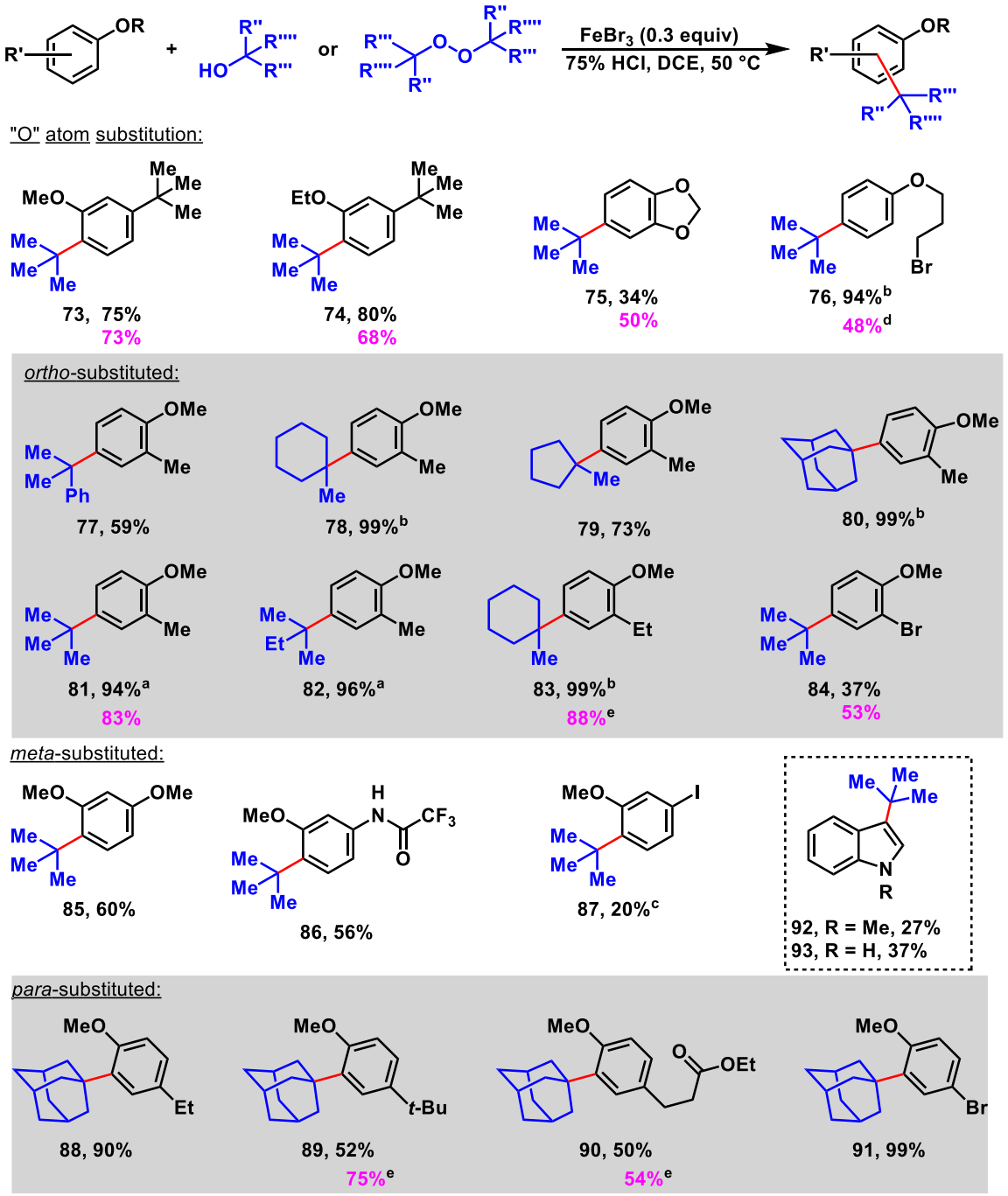

Figure 3.5 Scope of tertiary alcohol/peroxide Friedel-Crafts reaction

Conditions: anisole (0.2 mmol), tertiary alcohol (0.22 mmol), $FeCl_3$ (0.3 mmol), $HCl_{(aq)}$ (0.15 mmol), DCE (0.8 mL, 0.25 M), 50 °C, 24 h. Purple yields used DTBP (0.22 mmol). a) 0.01 equiv $FeBr_3$ b) 0.1 equiv $FeBr_3$ c)1 equiv $FeBr_3$ d) Isolated as the di-*tert*-butyl product e) Isolated as the *tert*-butylation product

multiple electron-donating groups **85-86** showed a lower yield (56–60%). Similar to the 2-bromo-anisole, when 3-iodoanisole **87** was used, the yield declined to 20% even when stoichiometric iron was used. 4-Ethyl- and 4-*tert*-butylanisole **88-89** worked well, giving 90% and 52% yields, respectively. Appending an ester group on a tether attached to the *para*–position **90** had a similarly decent yield (50%), with the ester being untouched in the reaction. Interestingly, 4-bromoanisole **91** had a surprisingly high yield of 99%, which far exceeded the other halogenated anisoles used. This reactivity is not limited to arenes with strong electron-donating groups, (**Figure 3.6**) with successful reactions occurring for *ortho*-xylene (**94-96**, 35-97% yields) and tetralin (**97**, 88% yield). Indoles were also workable substrates for this reaction, with both *N*-methyl indole **92** and indole **93** giving 27% and 37% yields, respectively, largely due to issues in isolation. This range of substrates also work well when employing the reactive conditions with *tert*-butyl peroxide, giving exclusively the *tert*-butylation product.

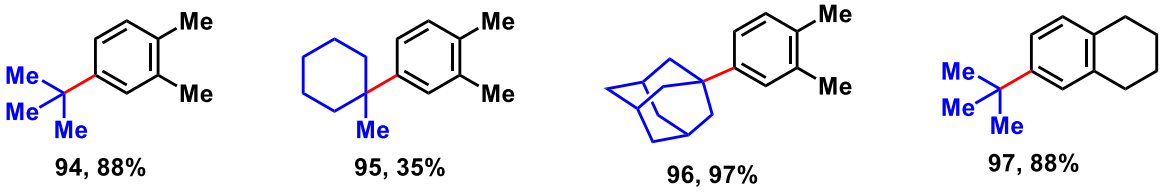

Figure 3.6 Scope of weakly donating arene substrates

3.2.3 *Mechanistic studies*

Mechanistic studies were conducted to understand how the alcohol was activated. When 1-adamantanol was subjected to the reaction conditions in the absence of 2-methyl-anisole, the corresponding alkyl bromide equivalent to the amount of the iron catalyst used

was isolated. Addition of 0.3 equivalent of TEMPO reduced the conversion to 12% and addition of 1 equivalent of TEMPO completely halted the reaction. These experiments initially supported a mechanism that involved radical intermediates (**Figure 3.7**).

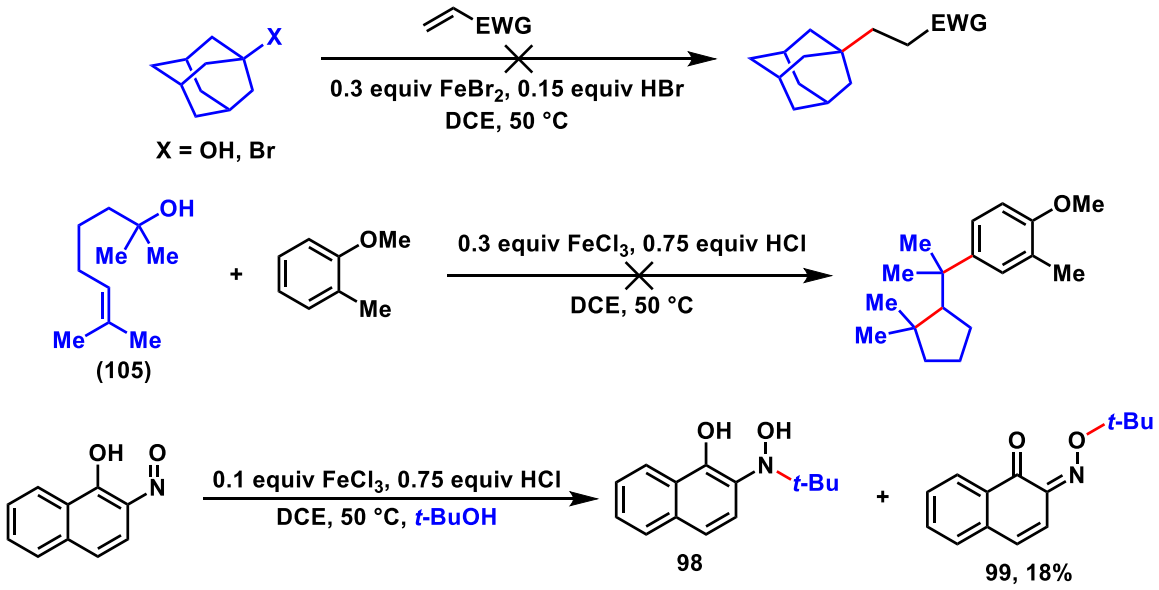

Figure 3.7 Mechanistic studies employed to investigate reaction's radical nature

To test for formation of radical intermediates, attempts were made to trap the reaction through a Michael addition.[11] A wide range of Michael acceptors were tested using both 1-adamantanol and 1-bromoadamantane (**Figure 3.8**). None of those experiments produced the anticipated Michael adducts. We then proceeded to examine radical clock **105**, but this method also proved ineffective. Finally, 2-nitroso-1-naphthol, another known radical trap compound,[12] was tested. Instead of the expected *N*-alkylation product **98**, the *O*-alkylation product **99** was isolated. All these factors came together to indicate that a polar mechanism is likely operative in this reaction, a conclusion that was substantiated later via computations and kinetics experiments.

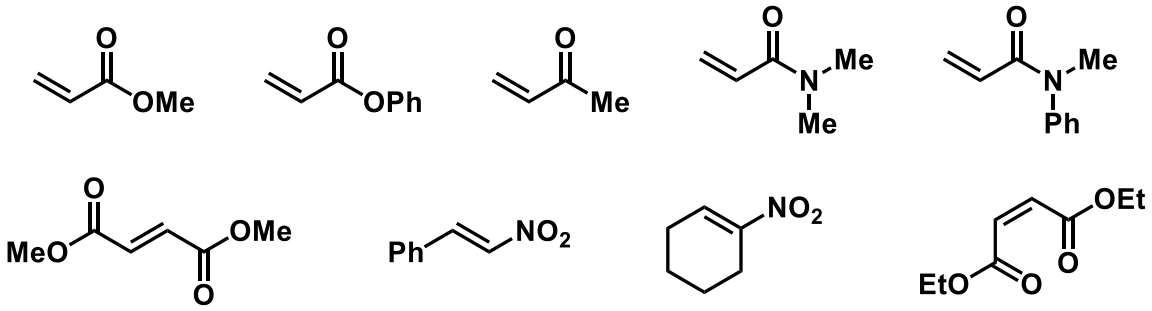

Figure 3.8 List of Michael acceptors tested in our reaction

3.2.4 *Asymmetric investigations*

While asymmetric Friedel-Crafts alkylations have been heavily studied, the examples are limited to the conjugate and carbonyl addition versions of the reaction.[13-14] For this reason, we sought to see if we could expand the enantioselectivity to our tertiary alcohol method. Our investigation began with identifying a chiral tertiary alcohol that could serve as the test substrate for the development of the method (**Figure 3.9**). Substrates **100**–**102** that contain a phenyl group were all found to be unable to alkylate, only returning unreacted starting material. Heptanol derivative **103** also was unreactive due to its poor solubility under the reaction conditions.

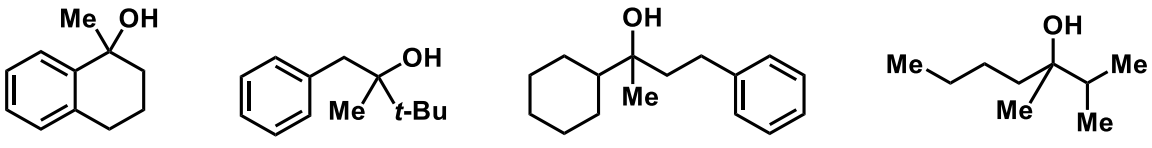

100 **101** **102** **103**

Figure 3.9 Unsuccessful alcohols for asymmetric catalysis

Undeterred, attention was turned to using a derivative of methyl cyclohexanol (**Figure 3.10**), whose parent compound was successful in our work. Subjecting 3,3-dimethyl

cyclohexanone to a Grignard reaction afforded tertiary alcohol **104**. This reagent combined with either 2-methylanisole or *ortho*-cresol to yield **105** and **106**, respectively. However, chiral HPLC and SFC assays could not be developed to resolve the enantiomers. This could possibly be due to the greasiness of the products; thus, chiral GC will be attempted to test this theory, and should that also be unsuccessful, additional alcohols will be tested.

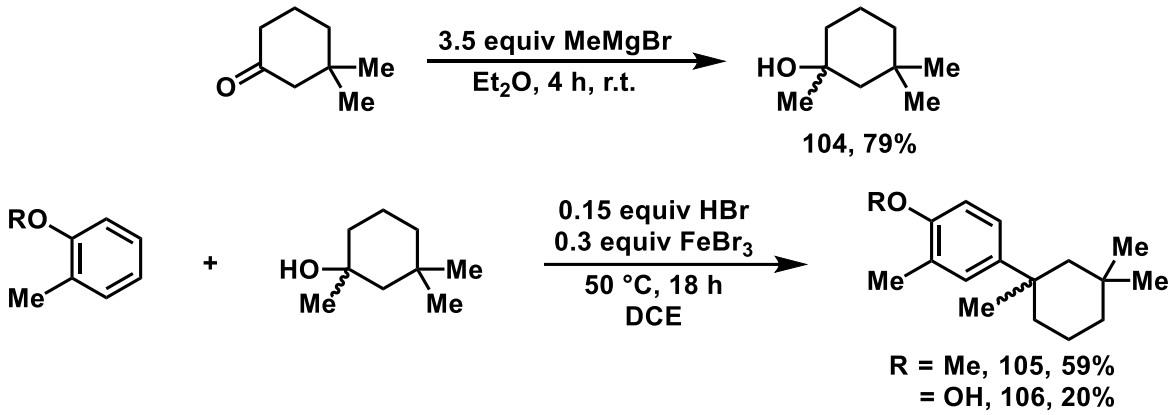

Figure 3.10 Substrate synthesis for asymmetric investigations

3.3 Discussion

When considering the reaction mechanism, the first question that needed to be addressed is whether the activation of the tertiary alcohol occurs through a radical or polar pathway. Radical intermediates could be intercepted by Michael acceptors, while carbocation intermediates could not. The lack of reactivity with Michael acceptors, as well as the failed radical clock experiment gave a strong indication that a radical mechanism is not at play. The inhibition of the reaction when TEMPO was added can likely be explained by an adverse reaction between TEMPO and the iron catalyst, an interaction that has been reported in the past.[15]

These observations, coupled with extensive kinetics and DFT calculations performed by Dr. Aaron Pan and our collaborator Dr. Brandon Haines, respectively, led to the following conclusion. $FeCl_3$ and aqueous HCl combine *in situ* to generate species **107** with enhanced acidity, which react with the tertiary alcohol to facilitate ionization to carbocation **108** that then reacts in a traditional EAS-type fashion (**Figure 3.11**).

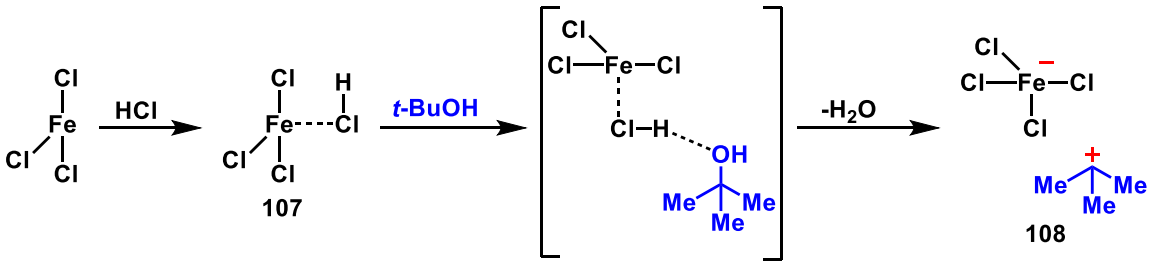

Figure 3.11 Proposed pathway for the activation of tertiary alcohols

Despite these setbacks, the method described in this chapter has practical utility for synthetic chemists. This method represents a significant improvement over the traditional Friedel–Crafts alkylation by allowing tertiary alcohols to be used directly as coupling partners. Prior to this development, an additional step would have been required to activate the alcohol, while generating additional waste. Furthermore, by utilizing an alcohol the major stoichiometric byproduct of this reaction is water, whereas the previously mentioned methods would generate a salt that would need to be disposed of. This would represent a significant boon to synthetic chemistry, as current methods to form chiral quaternary carbons generally require expensive, precious transition metal catalysts.[16]

3.4 Materials and methods

3.4.1 *Solvents and reagent*

Commercial reagents were purchased from MilliporeSigma, Acros Organics, Chem-Impex, TCI, Oakwood, and Alfa Aesar, and used without additional purification. Solvents were purchased from Fisher Scientific, Acros Organics, Alfa Aesar, and Sigma Aldrich. Tetrahydrofuran (THF), diethyl ether (Et_2O), acetonitrile (MeCN), dichloromethane (CH_2Cl2), benzene, 1,4-dioxane, and triethylamine (Et_3N) were sparged with argon and dried by passing through alumina columns using argon in a Glass Contour (Pure Process Technology) solvent purification system. Dimethylformamide (DMF), dimethyl sulfoxide (DMSO), and dichloroethane (DCE) were purchased in Sure/Seal or AcroSeal bottling and dispensed under N_2. Deuterated solvents were obtained from Cambridge Isotope Laboratories, Inc. or MilliporeSigma.

3.4.2 *Analytical instrumentation*

Melting points were measured with the MEL-TEMP melting point apparatus.

Proton nuclear magnetic resonance (^{1}H NMR) spectra, carbon nuclear magnetic resonance (^{13}C NMR) spectra and fluorine nuclear magnetic resonance (^{19}F NMR) spectra were recorded on Bruker Avance NEO 400 MHz or Bruker Avance 600 MHz spectrometers. Chemical shifts (δ) are reported in ppm relative to the residual solvent signal (δ 7.26 for ^{1}H NMR, δ 77.16 for ^{13}C NMR in $CDCl_3$).1 Data for ^{1}H NMR spectroscopy are reported as follows: chemical shift (δ ppm), multiplicity (s = singlet, d = doublet, t = triplet, q = quartet, m = multiplet, br = broad, dd = doublet of doublets, dt = doublet of triplets),

coupling constant (Hz), integration. Data for ^{13}C and ^{19}F NMR spectroscopy are reported in terms of chemical shift (δ ppm).

IR spectroscopic data were recorded on a NICOLET 6700 FT-IR spectrophotometer using a diamond attenuated total reflectance (ATR) accessory. Samples are loaded onto the diamond surface either neat or as a solution in organic solvent and the data acquired after the solvent had evaporated.

High resolution accurate mass (ESI) spectral data were obtained from the Analytical Chemistry Instrumentation Facility at the University of California, Riverside, on an Agilent 6545 Q-TOF LC/MS instrument (supported by NSF grant CHE-1828782). High resolution accurate mass (EI) spectral data were obtained from the Mass Spectrometry Facility at the University of California, Irvine, on a ThermoFinnegan TraceMS+ GC EI/CI instrument.

3.4.3 *Reaction setup, monitoring, and purification*

In general, the catalytic reactions are not air- or moisture-sensitive; however, the iron salts are hygroscopic and quickly change color when being weighed and added to the reaction vessel. This influences how much metal catalyst is being added because their molecular weights increase on hydration. For consistency and rigor, the iron salts were weighed and added to vials inside a nitrogen-filled glovebox. All other reagents, including the solvent were added outside the glovebox under open air. Reaction progresses were monitored using thin-layer chromatography (TLC) on EMD Silica Gel 60 F254 or Macherey-Nagel SIL HD (60 Å mean pore size, 0.75 mL/g specific pore volume, 5–17 μm particle size, with fluorescent indicator) silica gel plates. Visualization of the developed plates was performed

under UV light (254 nm). Purification and isolation of products were performed via silica gel chromatography (both column and preparative thin-layer chromatography). Organic solutions were concentrated under reduced pressure on IKA® temperature-controlled rotary evaporator equipped with an ethylene glycol/water condenser.

3.4.4 *General procedure*

3.4.4.a *General procedure A: alkylation with di-tert-butylperoxide*

A one-dram vial equipped with a stirring bar was sequentially added $FeCl_3$ (0.02–0.06 mmol, 10–30 mol%), anisole derivative (0.2 mmol, 1 equiv), DCE (0.8 mL, 0.25 M), DTBP (37 μL, 0.2 mmol,1 equiv), and TFA (11.5 μL, 0.15 mmol, 75 mol%). The reaction mixture was heated at 50 °C for 24 h, at which time the solution was filtered through a 5" pipette plug of silica gel (approximately half-filled) and eluted with hexanes/EtOAc (1:1) or hexanes/Et_2O (1:1). The solution was concentrated *in vacuo* and purified via silica gel chromatography to obtain the alkylation product.

3.4.4.a *General procedure B: alkylation with tertiary alcohols*

A one-dram vial equipped with a stirring bar was sequentially added iron salt (1–100 mol%), anisole (0.2 mmol, 1 equiv), DCE (0.8 mL, 0.25 M), tertiary alcohol (0.22 mmol, 1.1 equiv), and conc HCl (75 mol%). The reaction mixture was heated at 50 °C for 24 h, at which time the solution was filtered through a 5" pipette plug of silica gel (approximately half-filled) and eluted with hexanes/EtOAc (1:1). The solution was concentrated *in vacuo* and purified via silica gel chromatography to obtain the alkylation product.

3.4.6 *Tertiary alcohol preparation*

A 100 mL flame-dried flask equipped with a stirring bar under N_2 atmosphere was charged with anhydrous Et_2O (25 mL, 0.48 M) and cooled to 0 °C before the addition of the ketone (12 mmol, 1 equiv). The Grignard reagent (1–3.5 equiv) was added dropwise, then the reaction was warmed to room temperature. The reaction was allowed to run at room temperature for 4 h, with TLC monitoring, and once the TLC indicated completion, the solution was cooled to 0 °C before the addition of saturated NH_4Cl (10 mL) dropwise. The solution was extracted with ethyl acetate (3 x 15 mL) and the combined organic extract was washed with brine (2 x 10 mL), dried with anhydrous Na_2SO_4, and concentrated *in vacuo*.

3.4.7 *Characterization of reported compounds*

1,4-Di-*tert*-butyl-2-methoxybenzene (73)

Prepared using General Procedure B with 3-(*tert*-butyl)-1-methoxybenzene (32.8 mg, 0.200 mmol, 1 equiv), $FeCl_3$ (9.7 mg, 0.060 mmol, 0.3 equiv), DCE (0.8 mL, 0.25 M), *tert*-butanol (19 μL, 0.20 mmol, 1 equiv), and conc HBr (3 μL, 0.03 mmol, 0.15 equiv). Purification by preparative TLC (eluting with 19:1 hexanes/EtOAc) afforded **73** (33.1 mg, 75%) as a colorless oil. R_f: 0.77 (19:1 hexanes/EtOAc). ^1H NMR ($CDCl_3$, 600 MHz): δ 7.22–7.15 (m, 1H), 7.01–6.81 (m, 2H), 3.85 (s, 3H), 1.36 (s, 9H), 1.32 (s, 9H); ^{13}C NMR ($CDCl_3$, 101 MHz): δ 158.4, 150.2, 135.4, 126.2, 117.1, 109.3, 55.1, 34.6, 34.5, 31.5, 30.0. IR (ATR): 2955, 2830, 1611, 1563, 1462, 1399, 1360, 1268, 1228, 1158, 1079, 1039, 912,

853, 818, 734, 658 cm^{-1}. HRMS (ESI+): m/z $[M+H]^+$ calculated for $[C_{15}H_{25}O]^+$: 221.1900; found: 221.1892.

1,4-Di-*tert*-Butyl-2-ethoxybenzene (74)

Prepared using General Procedure B with 3-(tert-butyl)-1-ethoxybenzene (35.7 mg, 0.200 mmol, 1 equiv), $FeCl_3$ (9.7 mg, 0.060 mmol, 0.3 equiv), DCE (0.8 mL, 0.25 M), *tert*-butanol (19 μL, 0.20 mmol, 1 equiv), and conc HBr (3 μL, 0.03 mmol, 0.15 equiv). Purification by preparative TLC (eluting with hexanes) afforded **74** (40.3 mg, 86%) as a pale-yellow oil. R_f: 0.78 (19:1 hexanes/EtOAc). ^1H NMR ($CDCl_3$, 400 MHz): δ 7.19 (d, J = 8.6 Hz, 1H), 6.92–6.86 (m, 2H), 4.08 (q, J = 6.9 Hz, 2H), 1.47 (t, J = 7.0 Hz, 3H), 1.39 (s, 9H), 1.31 (s, 9H); ^{13}C NMR ($CDCl_3$, 101 MHz): δ 157.6, 150.1, 135.3, 126.2, 116.8, 109.8, 63.4, 34.6, 34.6, 31.8, 31.5, 30.0, 15.2. IR (ATR): 3454, 2978, 2858, 1736, 1503, 1369, 1310, 1255, 1159, 1131, 1097, 1071, 958, 836, 779 cm^{-1}. HRMS (ESI+): m/z $[M+H]^+$ calculated for $[C_{16}H_{27}O]^+$: 235.2056; found: 235.2052.

5-(*tert*-Butyl)benzo[d][1,3]dioxole (75)

Prepared using General Procedure B with 1,3-benzodioxole (24.4 mg, 0.200 mmol, 1 equiv), $FeCl_3$ (9.7 mg, 0.060 mmol, 0.3 equiv), DCE (0.8 mL, 0.25 M), *tert*-butanol (19 μL, 0.20 mmol, 1 equiv), and conc HBr (3 μL, 0.03 mmol, 0.15 equiv). Purification by preparative TLC (eluting with 19:1 hexanes/EtOAc) afforded **75** (12.1 mg, 34%) as a colorless oil. R_f: 0.46 (19:1 hexanes/EtOAc). ^1H NMR ($CDCl_3$, 400 MHz): δ 6.90 (d, J = 1.8 Hz, 1H), 6.83 (dd, J = 8.1, 1.8 Hz, 1H), 6.74 (d, J = 8.2 Hz, 1H), 5.92 (s, 2H), 1.28 (s, 9H); ^{13}C NMR ($CDCl_3$, 101 MHz): δ 147.5, 145.6, 145.2, 118.0, 107.8, 106.5, 100.9, 34.8, 31.7. IR (ATR): 2957, 2869, 1507, 1488, 1364, 1255, 1230, 1112, 1041, 939, 909, 859,

807, 640 cm^{-1}. HRMS (ESI+): m/z $[M+H]^+$ calculated for $[C_{11}H_{15}O_2]^+$: 179.1067; found: 179.1056.

1-(3-Bromopropoxy)-4-*tert*-butylbenzene (76)

Prepared using General Procedure B with 3-phenoxypropyl bromide (43.0 mg, 0.200 mmol, 1 equiv), $FeBr_3$ (5.9 mg, 0.020 mmol, 0.1 equiv), DCE (0.8 mL, 0.25 M), *tert*-butanol (19 μL, 0.20 mmol, 1 equiv), and conc HBr (3 μL, 0.03 mmol, 0.15 equiv). Purification by preparative TLC (eluting with 19:1 hexanes/EtOAc) afforded **76** (51.0 mg, 94%) as a colorless oil. R_f: 0.66 (hexanes). ^1H NMR ($CDCl_3$, 600 MHz): δ 7.31 (d, J = 9.0 Hz, 2H), 6.85 (d, J = 9.0 Hz, 2H), 4.12 (t, J = 6.0 Hz, 2H), 3.64 (t, J = 6.0 Hz, 2H), 2.31 (quint, J = 6.6 Hz, 2H), 1.30 (s, 9H); ^{13}C NMR ($CDCl_3$, 101 MHz): δ 157.1, 156.5, 143.7, 129.6, 126.4, 115.1, 114.1, 65.3, 34.2, 32.6, 31.7, 30.3. IR (ATR): 3041, 2960, 2868, 2369, 1609, 1582, 1512, 1469, 1435, 1420, 1389, 1363, 1294, 1240, 1183, 1117, 1032, 931, 827, 774, 753, 652, 552 cm^{-1}. HRMS (EI+): m/z $[M]^+$ calculated for $[C_{13}H_{19}BrO]^+$: 270.0619; found: 270.0619; $[M+2]^+$ calculated for $[C_{13}H_{19}BrO]^+$: 272.0600; found 272.0584; 1:1 intensity for $[M]^+/[M+2]^+$ signals.

1-Methoxy-2-methyl-4-(2-phenylpropan-2-yl)benzene (77)

Prepared using General Procedure B with 2-methylanisole (24.4 mg, 0.200 mmol, 1 equiv), $FeBr_3$ (17.7 mg, 0.060 mmol, 0.3 equiv), DCE (0.8 mL, 0.25 M), cumyl alcohol (28 μL, 0.2 mmol, 1 equiv), and conc HBr (3 μL, 0.03 mmol, 0.15 equiv). Purification by preparative TLC (eluting with 19:1 hexanes/EtOAc) afforded **77** (28.4 mg, 59%) as a pale-yellow oil. R_f: 0.63 (19:1 hexanes/EtOAc). ^1H NMR ($CDCl_3$, 400 MHz): δ 7.31–7.22 (m, 4H), 7.20–7.15 (m, 1H), 7.04 (dd, J = 8.4, 3.0 Hz, 1H), 7.00 (d, J = 2.5 Hz, 1H), 6.74 (d, J

= 8.4 Hz, 1H), 3.82 (s, 3H), 2.19 (s, 3H), 1.67 (s, 6H); ^{13}C NMR ($CDCl_3$, 101 MHz): δ 155.8, 151.2, 142.5, 129.5, 128.1, 126.9, 126.0, 125.6, 124.9, 109.4, 55.4, 42.3, 31.1, 16.6. IR (ATR): 2964, 2833, 1608, 1502, 1464, 1442, 1362, 1306, 1247, 1175, 1151, 1135, 1112, 1031, 995, 893, 809, 771, 154, 731, 617, 594, 560, 539 cm^{-1}. HRMS (ESI+): m/z $[M+H]^+$ calculated for $[C_{17}H_{21}O]^+$: 241.1587; found: 240.1524.

1-Methoxy-2-methyl-4-(1-methylcyclohexyl)benzene (78)

Prepared using General Procedure B with 2-methylanisole (24.4 mg, 0.200 mmol, 1 equiv), $FeBr_3$ (5.9 mg, 0.020 mmol, 0.1 equiv), DCE (0.8 mL, 0.25 M), 1-methylcyclohexanol (24.9 μL, 0.20 mmol, 1 equiv), and conc HBr (3 μL, 0.03 mmol, 0.15 equiv). Purification by preparative TLC (eluting with 19:1 hexanes/EtOAc) afforded **78** (43.2 mg, 99%) as a pale-yellow oil. R_f: 0.61 (19:1 hexanes/EtOAc). ^{1}H NMR ($CDCl_3$, 400 MHz): δ 7.22–7.12 (m, 2H), 6.85–6.78 (m, 1H), 3.85 (s, 3H), 2.27 (s, 3H), 2.07–1.92 (m, 2H), 1.65–1.52 (m, 4H), 1.52–1.37 (m, 4H), 1.20 (s, 3H); ^{13}C NMR ($CDCl_3$, 101 MHz): δ 155.5, 141.8, 128.5, 126.1, 124.0, 109.7, 55.4, 38.2, 37.3, 30.7, 26.6, 22.8, 16.7. IR (ATR): 2924, 2855, 1609, 1507, 1465, 1453, 1374, 1302, 1243, 1173, 1145, 1116, 1034, 996, 965, 883, 806, 755, 731, 650, 617, 608, 573, 564, 552, 529 cm^{-1}. HRMS (ESI+): m/z $[M+H]^+$ calculated for $[C_{15}H_{23}O]^+$: 219.1743; found: 219.1735.

1-Methoxy-2-methyl-4-(1-methylcyclopentyl)benzene (79)

Prepared using General Procedure B with 2-methylanisole (24.4 mg, 0.200 mmol, 1 equiv), $FeBr_3$ (17.7 mg, 0.060 mmol, 0.3 equiv), DCE (0.8 mL, 0.25 M), 1-methylcyclopentanol (25.2 μL, 0.20 mmol, 1 equiv), and conc HBr (3 μL, 0.03 mmol, 0.15 equiv). Purification by preparative TLC (eluting with 19:1 hexanes/EtOAc) afforded **79** (29.8 mg, 73%) as a

colorless oil. R_f: 0.66 (19:1 hexanes/EtOAc). ^{1}H NMR ($CDCl_3$, 400 MHz): δ 7.16–7.07 (m, 2H), 6.80–6.72 (m, 1H), 3.82 (s, 3H), 2.23 (s, 3H), 1.92–1.83 (m, 2H), 1.83–1.66 (m, 6H), 1.23 (s, 3H); ^{13}C NMR ($CDCl_3$, 101 MHz): δ 155.6, 143.4, 128.8, 126.0, 124.0, 109.6, 55.5, 46.5, 40.0, 29.7, 23.9, 16.6. IR (ATR): 2952, 2832, 1610, 1505, 1464, 1371, 1328, 1296, 1244, 1138, 1035, 994, 882, 806, 754, 714, 609, 575, 559, 547, 530 cm^{-1}. HRMS (ESI+): m/z $[M+H]^+$ calculated for $[C_{14}H_{21}O]^+$: 205.1587; found: 205.1579.

1-(4-Methoxy-3-methyl-phenyl)-adamantane (80)

Prepared using General Procedure B with 2-methylanisole (24.4 mg, 0.200 mmol, 1 equiv), $FeBr_3$ (5.9 mg, 0.020 mmol, 0.1 equiv), DCE (0.8 mL, 0.25 M), adamantanol (30.6 mg, 0.200 mmol, 1 equiv), and conc HBr (3 μL, 0.03 mmol, 0.75 equiv). Purification by preparative TLC (eluting with 19:1 hexanes/EtOAc) afforded **80** (50.8 mg, 99%) as a white solid. R_f: 0.49 (19:1 hexanes/EtOAc). M.p. 88–89°C. ^{1}H NMR ($CDCl_3$, 400 MHz): δ 7.17–7.11 (m, 2H), 6.81–6.76 (m, 1H), 3.81 (s, 3H), 2.23 (s, 3H), 2.08 (s, 3H), 1.94–1.86 (m, 6H), 1.81–1.70 (m, 6H). The spectral data recorded are consistent with those previously reported.[17]

4-(*tert*-Butyl)-1-methoxy-2-methylbenzene (81)

Prepared using General Procedure B with 2-methyl-anisole (24.4 mg, 0.200 mmol, 1 equiv), $FeCl_3$ (9.7 mg, 0.060 mmol, 0.3 equiv), DCE (0.8 mL, 0.25 M), *tert*-butanol (19 μL, 0.20 mmol, 1 equiv), and conc HBr (3 μL, 0.03 mmol, 0.15 equiv). Purification by preparative TLC (eluting with 19:1 hexanes/EtOAc) afforded **81** (33.5 mg, 94%) as a colorless oil. R_f: 0.62 (19:1 hexanes/EtOAc). ^{1}H NMR ($CDCl_3$, 600 MHz): δ 7.21–7.16

(m, 2H), 6.80–6.76 (m, 1H), 3.83 (s, 3H), 2.24 (s, 3H), 1.31 (s, 9H); The spectral data recorded are consistent with those previously reported.[18]

4-*tert*-Amyl-2-methylanisole (82)

Prepared using General Procedure B with 2-methylanisole (24.4 mg, 0.200 mmol, 1 equiv), $FeBr_3$ (0.59 mg, 0.0020 mmol, 0.01 equiv), DCE (0.8 mL, 0.25 M), *tert*-amyl alcohol (21.6 μL, 0.2 mmol, 1 equiv), and conc HBr (2 μL, 0.02 mmol, 0.1 equiv). Purification by preparative TLC (eluting with 19:1 hexanes/EtOAc) afforded **82** (36.9 mg, 96%) as a colorless oil. R_f: 0.69 (19:1 hexanes/EtOAc). ^{1}H NMR ($CDCl_3$, 400 MHz): δ 7.17–7.09 (m, 2H), 6.81–6.76 (m, 1H), 3.84 (s, 3H), 2.25 (s, 3H), 1.63 (q, J = 7.4 Hz, 2H), 1.28 (s, 6H), 0.71 (t, J = 7.4 Hz, 3H); ^{13}C NMR ($CDCl_3$, 400 MHz): δ 155.6, 141.3, 128.6, 125.8, 124.1, 109.4, 55.4, 37.0, 31.7, 28.8, 16.7, 9.3. IR (ATR): 2961, 2856, 1608, 1506, 1463, 1441, 1377, 1304, 1261, 1246, 1142, 1114, 1036, 994, 881, 807, 776, 775, 731, 654, 612, 573 cm^{-1}. HRMS (EI+): m/z $[M]^+$ calculated for $[C_{13}H_{20}O]^+$: 192.1514; found: 192.1516.

1-Methoxy-2-ethyl-4-(1-methylcyclohexyl)benzene (83)

Prepared using General Procedure B with 2-ethylanisole (27.2 mg, 0.200 mmol, 1 equiv), $FeBr_3$ (5.9 mg, 0.020 mmol, 0.1 equiv), DCE (0.8 mL, 0.25 M), 1-methylcyclohexanol (24.9 μL, 0.20 mmol, 1 equiv), and conc HBr (3 μL, 0.03 mmol, 0.75 equiv). Purification by preparative TLC (eluting with 19:1 hexanes/EtOAc) afforded **83** (46.0 mg, 99%) as a pale-yellow oil. R_f: 0.68 (19:1 hexanes/EtOAc). ^{1}H NMR ($CDCl_3$, 600 MHz): δ 7.16 (m, 2H), 6.79 (d, J = 9.0 Hz, 1H), 3.81 (s, 3H), 2.64 (q, J = 7.2 Hz, 2H), 1.96 (m, 2H), 1.55 (m, 5H), 1.45 (m, 3H), 1.20 (t, J = 7.2 Hz, 3H), 1.169 (s, 3H); ^{13}C NMR ($CDCl_3$, 150 MHz): δ 155.0, 141.9, 132.0, 126.8, 123.9, 109.8, 55.3, 38.1, 37.2, 26.5, 23.7, 22.7, 14.5. IR (ATR):

2926, 2856, 1607, 1503, 1453, 1373, 1306, 1245, 1147, 1134, 1117, 1052, 1030, 962, 891, 854, 807, 750, 650, 605, 553 cm^{-1}. HRMS (ESI+): m/z $[M+H]^+$ calculated for $[C_{16}H_{25}O]^+$: 233.1900; found: 233.1913.

2-Bromo-4-(*tert*-butyl)-1-methoxybenzene (84)

Prepared using General Procedure A with 2-bromo-methoxybenzene (37.4 mg, 0.200 mmol, 1 equiv), $FeCl_3$ (9.7 mg, 0.060 mmol, 0.3 equiv), DCE (0.8 mL, 0.25 M), DTBP (37 µL, 0.20 mmol, 1 equiv), and conc HCl (14 µL, 0.15 mmol, 0.75 equiv). Purification by preparative TLC (eluting with 19:1 hexanes/EtOAc) afforded **84** (25.8 mg, 53%) as a pale-yellow oil. R_f: 0.55 (19:1 hexanes/ EtOAc). ^1H NMR ($CDCl_3$, 600 MHz): δ 7.54 (d, J = 2.2 Hz, 1H), 7.27 (dd, J = 8.6, 2.2 Hz, 1H), 6.84 (d, J = 8.6 Hz, 1H), 3.88 (s, 3H), 1.29 (s, 9H); ^{13}C NMR ($CDCl_3$, 101 MHz): δ 153.7, 145.2, 130.6, 125.4, 111.7, 111.4, 56.4, 34.3, 31.5. IR (ATR): 2959, 2838, 1602, 1501, 1481, 1461, 1439, 1393, 1362, 1289, 1260, 1203, 1182, 1162, 1118, 1054, 1020, 909, 880, 862, 808, 748, 733, 719, 692 cm^{-1}. HRMS (EI+) m/z $[M]^+$ calculated for $[C_{11}H_{15}BrO]^+$: 242.0306; found: 242.0301.

4-(*tert*-Butyl)-3-methoxyanisole (85)

Prepared using General Procedure B with 1,3-dimethoxybenzene (27.6 mg, 0.200 mmol, 1 equiv), $FeBr_3$ (17.7 mg, 0.060 mmol, 0.3 equiv), DCE (0.8 mL, 0.25 M), *tert*-butanol (19 µL, 0.20 mmol, 1 equiv), and conc HBr (3 µL, 0.03 mmol, 0.15 equiv). Purification by preparative TLC (eluting with 19:1 hexanes/EtOAc) afforded **85** (23.3 mg, 60%) as a colorless oil. R_f: 0.47 (19:1 hexanes/EtOAc). ^1H NMR ($CDCl_3$, 600 MHz): δ 7.21 (d, J = 8.4 Hz, 1H), 6.51 (s, 1H), 6.45 (d, J = 8.4 Hz), 3.82 (s, 3H), 3.80 (s, 3H), 1.35 (s, 9H); ^{13}C NMR ($CDCl_3$, 101 MHz): δ 159.5, 159.1, 131.0, 126.9, 103.3, 99.8, 55.4, 55.1, 34.4, 30.0.

IR (ATR): 2996, 2953, 2834, 1611, 1581, 1502, 1484, 1461, 1438, 1412, 1389, 1358, 1305, 1274, 1257, 1210, 1151, 1145, 1096, 1035, 939, 925, 833, 795, 732, 659, 634, 601, 543 cm^{-1}. HRMS (ESI+): m/z $[M+H]^+$ calculated for $[C_{12}H_{19}O_2]^+$: 195.1380; found: 195.1371.

***N*-(4-(*tert*-Butyl)-3-methoxyphenyl)-2,2,2-trifluoroacetamide (86)**

Prepared using General Procedure B with *N*-(3-methoxyphenyl)-2,2,2-trifluoroacetamide (43.8 mg, 0.200 mmol, 1 equiv), $FeBr_3$ (17.7 mg, 0.060 mmol, 0.3 equiv), DCE (0.8 mL, 0.25 M), *tert*-butanol (19 μL, 0.20 mmol, 1 equiv), and conc HCl (14 μL, 0.15 mmol, 0.75 equiv). Purification by preparative TLC (eluting with 19:1 hexanes/EtOAc) afforded **86** (30.8 mg, 56%) as a light orange oil. R_f: 0.32 (19:1 hexanes/EtOAc). ^1H NMR ($CDCl_3$, 600 MHz): δ 7.86 (br s, 1H), 7.32 (d, J = 1.8 Hz, 1H), 7.25 (d, J = 8.4 Hz, 1H), 6.91 (dd, J = 8.4, 2.4 Hz, 1H), 3.85 (s, 3H), 1.35 (s, 9H); ^{13}C NMR ($CDCl_3$, 101 MHz): δ 159.1, 155.0 (q, J = 37.3 Hz), 136.9, 134.2, 127.1, 116.1 (q, J = 288.8 Hz), 111.9, 104.4, 55.3, 34.9, 29.7. IR (ATR): 3292, 3141, 2958, 2836, 1701, 1607, 1541, 1505, 1464, 1361, 1297, 1215, 1153, 1086, 1038, 968, 814, 716, 622 cm^{-1}. HRMS (ESI+): m/z $[M+H]^+$ calculated for $[C_{13}H_{17}F_3NO_2]^+$: 275.1206; found: 275.1219.

1-*tert*-Butyl-4-iodo-2-methoxybenzene (87)

Prepared using General Procedure B with 3-iodoanisole (46.8 mg, 0.200 mmol, 1 equiv), $FeBr_3$ (45.6 mg, 0.20 mmol, 1 equiv), DCE (0.8 mL, 0.25 M), *tert*-butanol (19 μL, 0.20 mmol, 1 equiv), and conc HBr (3 μL, 0.03 mmol, 0.15 equiv). Purification by preparative TLC (eluting with 19:1 hexanes/EtOAc) afforded **87** (11.6 mg, 20%) as an orange oil. R_f: 0.72 (19:1 hexanes/EtOAc). ^1H NMR ($CDCl_3$, 400 MHz): δ 7.15 (dd, J = 8.2, 1.8 Hz, 1H), 7.06 (d, J = 1.8 Hz, 1H), 6.90 (d, J = 8.2 Hz, 1H), 3.75 (s, 3H), 1.26 (s, 9H); ^{13}C NMR

($CDCl_3$, 101 MHz): δ 159.2, 138.3, 129.6, 128.4, 120.8, 91.4, 55.4, 34.9, 29.6. IR (ATR): 2997, 2866, 1579, 1558, 1485, 1461, 1382, 1359, 1290, 1233, 1201, 1180, 1142, 1105, 1075, 1027, 932, 849, 801, 611, 583, 548, 533 cm^{-1}. HRMS (EI+): m/z $[M]^+$ calculated for $[C_{11}H_{15}IO]^+$: 290.0168; found: 290.0170.

1-(5-Ethyl-2-methoxyphenyl)-adamantane (88)

Prepared using General Procedure B with 4-ethylanisole (27.2 mg, 0.200 mmol, 1 equiv), $FeBr_3$ (17.7 mg, 0.06 mmol, 0.3 equiv), DCE (0.8 mL, 0.25 M), adamantanol (30.6 mg, 0.200 mmol, 1 equiv), and conc HCl (14 μL, 0.15 mmol, 0.75 equiv). Purification by preparative TLC (eluting with 19:1 hexanes/EtOAc) afforded **88** (48.7 mg, 90%) as a cream-colored solid. R_f: 0.67 (19:1 hexanes/EtOAc). M.p. 58–59 °C. ^1H NMR ($CDCl_3$, 400 MHz): δ 7.05 (d, J = 2.3 Hz, 1H), 7.00 (dd, J = 8.2, 2.3 Hz, 1H), 6.80 (d, J = 8.2 Hz, 1H), 3.81 (s, 3H), 2.59 (q, J = 7.6 Hz, 2H), 2.11 (br d, J = 3.0 Hz, 6H), 2.08–2.03 (m, 3H), 1.77 (br t, J = 2.9 Hz, 6H), 1.22 (t, J = 7.6 Hz, 3H); ^{13}C NMR ($CDCl_3$, 101 MHz): δ 157.0, 138.4, 136.0, 126.4, 125.7, 111.8, 55.3, 40.8, 37.3, 29.3, 28.5, 16.0. IR (ATR): 2899, 2849, 1494, 1447, 1230, 1179, 1136, 1061, 1037, 1025, 990, 890, 818, 810, 718, 620, 602, 590, 579, 542 cm^{-1}. HRMS (EI+): m/z $[M]^+$ calculated for $[C_{19}H_{26}O]^+$: 270.1984; found: 270.1984.

1-(5-*tert*-Butyl-2-methoxyphenyl)-adamantane (89)

Prepared using General Procedure B with 4-*tert*-butylanisole (32.8 mg, 0.200 mmol, 1 equiv), $FeBr_3$ (17.7 mg, 0.06 mmol, 0.3 equiv), DCE (0.8 mL, 0.25 M), adamantanol (30.6 mg, 0.2 mmol, 1 equiv), and conc HBr (2 μL, 0.02 mmol, 0.1 equiv). Purification by preparative TLC (eluting with 19:1 hexanes/EtOAc) afforded **89** (31.0 mg, 52%) as a clear

oil. R_f: 0.82 (19:1 hexanes/EtOAc). ^{1}H NMR ($CDCl_3$, 400 MHz): δ 7.28 (d, J = 2.5 Hz, 1H), 7.19 (dd, J = 8.5, 2.5 Hz, 1H), 6.82 (d, J = 8.5 Hz, 1H), 3.83 (s, 3H), 2.13 (br d, J = 3.0 Hz, 6H), 2.11–2.05 (m, 3H), 1.79 (br t, J = 3.1 Hz, 5H), 1.75 (br t, J = 3.2 Hz, 1H), 1.33 (s, 9H); ^{13}C NMR ($CDCl_3$, 101 MHz): δ 156.5, 142.6, 137.7, 123.8, 123.1, 111.0, 55.0, 40.7, 37.2, 35.6, 34.3, 31.7, 29.2. IR (ATR): 2902, 2848, 2361, 1604, 1495, 1454, 1361, 1343, 1316, 1291, 1268, 1234, 1202, 1179, 1144, 1123, 1102, 1039, 1028, 978, 907, 884, 818, 809, 795, 731, 677, 666, 633, 574, 558, 547, 539, 530 cm^{-1}. HRMS (ESI+): m/z $[M+H]^+$ calculated for $[C_{21}H_{31}O]^+$: 299.2369; found: 298.2373.

Ethyl-3-(3-adamantyl-4-methoxyphenyl)propanoate (90)

Prepared using General Procedure B with ethyl-3-(4- methoxyphenyl)propanoate (41.7 mg, 0.200 mmol, 1 equiv), $FeBr_3$ (17.7 mg, 0.060 mmol, 0.3 equiv), DCE (0.8 mL, 0.25 M), adamantanol (30.6 mg, 0.20 mmol, 1 equiv), and conc HBr (3 μL, 0.03 mmol, 0.15 equiv). Purification by preparative TLC (eluting with 19:1 hexanes/EtOAc) afforded **90** (34.2 mg, 50%) as a waxy cream-colored solid. R_f: 0.41 (19:1 hexanes/EtOAc). M.p. 90–91 °C. ^{1}H NMR ($CDCl_3$, 400 MHz): δ 6.96 (d, J = 2.2 Hz, 1H), 6.92 (dd, J = 8.2, 2.3 Hz, 1H), 6.71 (d, J = 8.2 Hz, 1H), 4.06 (q, J = 7.1 Hz, 2H), 3.73 (s, 3H), 2.81 (t, J = 8.2 Hz, 2H), 2.51 (t, J = 8.2 Hz, 2H), 2.06–1.94 (m, 9H), 1.69 (br t, J = 3.0 Hz, 6H), 1.17 (t, J = 7.1 Hz, 3H); ^{13}C NMR ($CDCl_3$, 101 MHz): δ 173.3, 157.4, 138.6, 132.3, 126.8, 126.3, 111.8, 60.5, 55.2, 40.7, 37.3, 37.0, 36.5, 30.7, 29.2, 14.4. IR (ATR): 3010, 2972, 2901, 2888, 2843, 2366, 1735, 1604, 1491, 1454, 1414, 1368, 1298, 1260, 1200, 1181, 1162, 1147, 1035, 1024, 976, 865, 877, 816, 779, 718, 690, 638, 591, 568, 561, 543, 530 cm^{-1}. HRMS (ESI+): m/z $[M+H]^+$ calculated for $[C_{22}H_{31}O_3]^+$: 343.2268; found: 343.2242.

1-(5-Bromo-2-methoxyphenyl)-adamantane (91)

Prepared using General Procedure B with 4-bromoanisole (37.4 mg, 0.200 mmol, 1 equiv), $FeBr_3$ (17.7 mg, 0.060 mmol, 0.3 equiv), DCE (0.8 mL, 0.25 M), adamantanol (30.6 mg, 0.200 mmol, 1 equiv), and conc HBr (3 μL, 0.03 mmol, 0.15 equiv). Purification by preparative TLC (eluting with 19:1 hexanes/EtOAc) afforded **91** (63.6 mg, 99%) as a peach-colored solid. R_f: 0.42 (19:1 hexanes/EtOAc). M.p. 141–142 °C. ^{1}H NMR ($CDCl_3$, 600 MHz): δ 7.28 (d, J = 2.5 Hz, 1H), 7.26 (dd, J = 8.6, 2.5 Hz, 1H), 6.73 (d, J = 8.6 Hz, 1H), 3.81 (s, 3H), 2.05 (br s, 9H), 1.76 (br s, 6H); ^{13}C NMR ($CDCl_3$, 151 MHz): δ 157.9, 140.8, 129.8, 129.3, 113.3, 55.2, 40.3, 37.2, 37.0, 29.0. IR (ATR): 3007, 2898,2844, 2358, 1598, 1499, 1450, 1438, 1356, 1275, 1260, 1215, 1178, 1145, 1101, 1058, 1037, 1021, 975, 876, 785, 771, 719, 696, 673, 645, 589, 574, 556, 539, 530 cm^{-1}. HRMS (EI+): m/z $[M]^+$ calculated for $[C_{17}H_{21}BrO]^+$: 320.0776; found: 320.0761.

4-*tert*-Butyl-*o*-xylene (92)

Prepared using General Procedure B with *o*-xylene (21.2 mg, 0.200 mmol, 1 equiv), $FeCl_3$ (9.7 mg, 0.060 mmol, 0.3 equiv), DCE (0.8 mL, 0.25 M), *tert*-butanol (14.8 mg, 0.200 mmol, 1 equiv), and conc HCl (14 μL, 0.15 mmol, 0.75 equiv). Purification by preparative TLC (eluting with hexanes) afforded **92** (28.5 mg, 88%) as a colorless oil. R_f: 0.73 (hexanes). ^{1}H NMR ($CDCl_3$, 600 MHz): δ 7.19 (s, 1H), 7.16 (d, J = 7.8, 1H), 7.13 (d, J = 8.4 Hz, 1H), 2.29 (s, 3H), 2.26 (s, 3H), 1.33 (s, 9H); The spectral data recorded are consistent with those previously reported.[19]

1,2-Dimethyl-4-(1-methylcyclohexyl)benzene (93)

Prepared using General Procedure B with *o*-xylene (21.2 mg, 0.200 mmol, 1 equiv), $FeCl_3$ (9.7 mg, 0.060 mmol, 0.3 equiv), DCE (0.8 mL, 0.25 M), 1-methylcyclohexanol (22.8 mg, 0.200 mmol, 1 equiv), and conc HCl (14 μL, 0.15 mmol, 0.75 equiv). Purification by preparative TLC (eluting with hexanes) afforded **93** (14.3 mg, 35%) as a yellow oil. R_f: 0.62 (hexanes). ^{1}H NMR ($CDCl_3$, 600 MHz): δ 7.15 (s, 1H), 7.10 (q, J = 7.8 Hz, 2H), 2.27 (s, 3H), 2.24 (s, 3H), 1.98 (m, 2H), 1.54 (m, 5H), 1.45 (m, 3H), 1.17 (s, 3H); ^{13}C NMR ($CDCl_3$, 151 MHz): δ 147.7, 136.3, 133.5, 129.6, 127.4, 123.4, 38.1, 37.6, 26.6, 22.9, 20.3, 19.4. IR (ATR): 3020, 2922, 2855, 2361, 1611, 1507, 1467, 1450, 1374, 1306, 1133, 1110, 1020, 995, 964, 928, 910, 880, 733, 719, 610, 594, 547, 534 cm^{-1}. HRMS (EI+): m/z $[M]^+$ calculated for $[C_{15}H_{22}]^+$: 202.1722; found: 202.1713.

1-(1-Adamantyl)-3,4-dimethylbenzene (94)

Prepared using General Procedure B with *o*-xylene (21.2 mg, 0.200 mmol, 1 equiv), $FeCl_3$ (9.7 mg, 0.060 mmol, 0.3 equiv), DCE (0.8 mL, 0.25 M), 1-adamantanol (30.4 mg, 0.200 mmol, 1 equiv), and conc HCl (14 μL, 0.15 mmol, 0.75 equiv). Purification by preparative TLC (eluting with hexanes) afforded **94** (46.5 mg, 97%) as a white solid. R_f: 0.54 (hexanes). M.p. 108–109 °C. ^{1}H NMR ($CDCl_3$, 600 MHz): δ 7.14 (s, 1H), 7.10 (m, 2H), 2.27 (s, 3H), 2.23 (s, 3H), 2.08 (s, 3H), 1.91 (s, 6H), 1.76 (m, 6H); ^{13}C NMR ($CDCl_3$, 151 MHz): δ 149.2, 136.2, 133.7, 129.5, 126.4, 122.3, 43.4, 37.0, 29.1, 20.2, 19.4. IR (ATR): 2999, 2898, 2847, 1617, 1572, 1504, 1445, 1382, 1356, 1342, 1317, 1159, 1126, 1101, 1024, 993, 909, 889, 803, 731, 717, 688, 645, 563, 556, 546, 536 cm^{-1}. HRMS (EI+): m/z $[M]^+$ calculated for $[C_{18}H_{24}]^+$: 240.1878; found: 240.1880.

6-*tert*-Butyl-1,2,3,4-tetrahydronapthalene (95)

Prepared using General Procedure B with tetralin (26.4 mg, 0.200 mmol, 1 equiv), $FeCl_3$ (9.7 mg, 0.060 mmol, 0.3 equiv), DCE (0.8 mL, 0.25 M), *tert*-butanol (14.8 mg, 0.200 mmol, 1 equiv), and conc HCl (14 μL, 0.15 mmol, 0.75 equiv). Purification by preparative TLC (eluting with hexanes) afforded an inseparable mixture (30.9 mg, 51% 5ba + 20% tetralin) as a yellow oil. R_f: 0.72 (hexanes). ^{1}H NMR ($CDCl_3$, 600 MHz): δ 7.14 (d, J = 9.6 Hz, 1H), 7.09 (s, 1H), 7.02 (d, J = 9.6 Hz, 1H), 2.75 (m, 4H), 1.80 (s, 4H), 1.31 (s, 9H); ^{13}C NMR ($CDCl_3$, 151 MHz): δ 148.4, 136.7, 134.3, 129.0, 126.0, 122.7, 34.4, 31.6, 29.8, 29.0, 23.5. IR (ATR): 2932, 2859, 2836, 1503, 1477, 1459, 1437, 1411, 1392, 1362, 1270, 1245, 1201, 1189, 1136, 910, 893, 877, 827, 807, 714, 648, 615, 583, 550, 535 cm^{-1}. HRMS (EI+): m/z $[M]^+$ calculated for $[C_{14}H_{20}]^+$: 188.1565; found: 188.1564.

3-(*tert*-Butyl)-1H-indole (96)

Prepared using General Procedure B with indole (23.4 mg, 0.200 mmol, 1 equiv), $FeBr_3$ (17.7 mg, 0.060 mmol, 0.3 equiv), DCE (0.8 mL, 0.25 M), *tert*-butanol (14.8 mg, 0.200 mmol, 1 equiv), and conc HBr (3 μL, 0.03 mmol, 0.15 equiv). Purification via 2 cycles of preparative TLC (eluting with 19:1 hexanes/EtOAc) afforded **96** (12.9 mg, 37%) as a yellow oil. R_f: 0.58 (19:1 hexanes/EtOAc, then 7:3 hexanes/CH_2Cl_2). ^{1}H NMR ($CDCl_3$, 600 MHz): δ 7.83 (d, J = 7.8 Hz, 1H), 7.36 (d, J = 7.8 Hz 1H), 7.18 (t, J = 7.2 Hz, 1H), 7.10 (t, J = 7.2 Hz 1H), 6.94 (s, 1H), 1.47 (s, 9H); The spectral data recorded are consistent with those previously reported.[20]

3-(*tert*-Butyl)-1-methyl-1H-indole (97)

Prepared using General Procedure B with *N*-methylindole (26.2 mg, 0.200 mmol, 1 equiv), $FeBr_3$ (17.7 mg, 0.060 mmol, 0.3 equiv), DCE (0.8 mL, 0.25 M), *tert*-butanol (14.8 mg, 0.200 mmol, 1 equiv), and conc HBr (3 μL, 0.03 mmol, 0.15 equiv). Purification by preparative TLC (eluting with 19:1 hexanes/EtOAc) afforded a coeluted mixture (16.9 mg, 27%) **97** as a yellow oil. R_f: 0.26 (19:1 hexanes/EtOAc). ^1H NMR ($CDCl_3$, 500 MHz): δ 7.81 (d, J = 8.0 Hz, 1H), 7.30 (d, J = 8.2 Hz 1H), 7.21 (t, J = 7.5 Hz, 1H), 7.10 (t, J = 7.5 Hz 1H), 6.80 (s, 1H), 3.74 (s, 3H), 1.46 (s, 9H); ^{13}C NMR ($CDCl_3$, 151 MHz): δ 137.3, 126.9, 126.1, 121.6, 121.4, 119.4, 118.9, 111.4, 32.1, 31.7, 30.9. IR (ATR): 3145, 2952, 2865, 1546, 1482, 1464, 1423, 1390, 1375, 1360, 1327, 1259, 1233, 1202, 1153, 1135, 1110, 1053, 102, 987, 795, 723, 672, 573, 564 cm^{-1}. HRMS (ESI+): m/z $[M+H]^+$ calculated for $[C_{13}H_{18}N]^+$: 188.1439; found: 188.1437.

1-Bromoadamantane

A one-dram vial equipped with a stirring bar was sequentially added $FeBr_3$ (59.1 mg, 0.2 mmol, 1 equiv), 1-adamantanol (30.4 mg, 0.2 mmol, 1 equiv), DCE (0.8 mL, 0.25 M), HBr (10.0 μL, 0.09 mmol, 45 mol%). The reaction mixture was heated at 50 °C for 24 h, at which time the solution was filtered through a 5" pipette plug of silica gel (approximately half–filled) and eluted with DCM. The solution was concentrated in vacuo to yield the product (37.4 mg, 87%) as a white solid. 1H NMR ($CDCl_3$, 400 MHz): δ 2.36 (m, 6H), 2.10 (s, 3H), 1.73 (m, 6H). The spectroscopic data obtained are consistent with the previously reported literature.[21]

3.5 References

1. Warner, J. C.; Cannon, A. S.; Dye, K. M., Green chemistry. *Environmental Impact Assessment Review* **2004**, *24*(7–8), 775–779.

2. Yamauchi, T.; Hattori, K.; Mizutaki, S.; Tamaki, K.; Uemura, S., Selenium and tellurium tetrachlorides as reagents for the conversion of alcohols to alkyl chlorides and tellurium tetrachloride as a Lewis acid catalyst for aromatic alkylation. *Bulletin of the Chemical Society of Japan* **2006**, *59*(11), 3617–3620.

3. Tsuchimoto, T.; Tobita, K.; Hiyama, T.; Fukuzawa, S., Scandium(III) triflate-catalyzed Friedel-Crafts alkylation reactions. *The Journal of Organic Chemistry* **1997**, *62*(20), 6997–7005.

4. Sanz, R.; Miguel, D.; Álvarez–Gutiérrez, J. M.; Rodriguez, F., Brønsted-acid-catalyzed C3-selective propargylation and benzylation of indoles with tertiary alcohols. *Synlett* **2008**, *7*, 975–978.

5. Bras, J. L.; Muzart, J., Brønsted-acid-catalyzed coupling of electron-rich arenes with substituted allylic and secondary benzylic alcohols. *Tetrahedron* **2007**, *63*(33), 7942–7948.

6. Wang, B.; Xiang, S.; Sun, Z.; Guan, B.; Hu, P.; Zhao, K.; Shi, Z., Benzylation of arenes though $FeCl_3$-catalyzed Friedel-Crafts reaction via C–O activation of benzyl ether. *Tetrahedron Letters* **2008**, *49*(27), 4310–4312.

7. Mertins, K.; Iovel, I.; Kischel, J.; Zapf, A.; Beller, M., Gold-catalyzed benzylation of arenes and heteroarenes. *Advanced Synthesis & Catalysis* **2006**, *348*(6), 691–695.

8. Cozzi, P. G.; Zoli, L., A rational approach towards the nucleophilic substitutions of alcohols “on water”. *Angewandte Chemie International Edition* **2008**, *47*(22), 4162–4166.

9. Jefferies, L. R.; Cook, S. P., Iron-catalyzed arene alkylation reactions with unactivated secondary alcohols. *Organic Letters* **2014**, *16*(7), 2026–2029.

10. Zhang, S.; Vayer, M.; Noël, F.; Vukovic, V. D.; Golushko, A.; Rezajooei, N.; Rowley, C. N.; Lebœf, D.; Moran, J., Unlocking the Friedel-Crafts arylation of primary aliphatic alcohols and epoxides driven by hexafluoroisopropanol. *Chem* **2021**, *7*(12), 3425–3441.

12. Yamane, Y.; Yoshinaga, K.; Sumimoto, M.; Nishikata, T., Iron-enhanced reactivity of radicals enables C–H tertiary alkylations for construction of functionalized quaternary carbons. *ACS Catalysis* **2019**, *9*, 1757–1762.

13. Boer, T. J., Spin-trapping in early and some recent nitroso chemistry. *Canadian Journal of Chemistry* **1982**, *60*(12), 1602–1609.

14. Ahmad, T.; Khan, S.; Ullah, N., Recent advances in the catalytic asymmetric Friedel-Crafts reaction of indoles. *ACS Omega* **2022**, *7*(40), 35446–35485.

15. Humbeck, J. F. V.; Simonovich, S.; P.; Knowles, R. R.; MacMillan, D. W. C., Concerning the mechanism of the $FeCl_3$-catalyzed alpha-oxyamination of aldehydes: evidence for a non-SOMO activation pathway. *Journal of the American Chemical Society* **2010**, *132*(29), 10012–10014.

16. You, S.; Cai, Q.; Zeng, M., Chiral Brønsted acid catalyzed Friedel-Crafts alkylation reactions. *Chemical Society Reviews* **2009**, *38*, 2190–2201.

17. Maik, R.; Won, M.; Kim, B. K.; Xia, Y.; Choi, H. K.; Jin, G.; Jung, Y.; Kim, H. M.; Lee, K., Synthesis and structure–activity relationship of (*E*)-phenoxyacrylic amide derivatives as hypoxia-inducible factor (HIF) 1α inhibitors. *Journal of Medicinal Chemistry* **2012**, *55*(23), 10564–10571.

18. Tashiro, M.; Yamato, T., $AlCl_3$-CH_3NO_2 Catalyzed *t*–butylation of biphenyl, naphthalene and come phenol derivatives with 2,6-di(*t*-butyl)-*p*-cresol. *Organic Preparations and Procedures International* **1978**, *10*(3), 143–148.

19. Fischer, A.; Teo, K. C., Nitration of 4-*tert*-butyl-o-xylene in acetic anhydride. Formation and rearomatization of adducts. *Canadian Journal of Chemistry* **1978**, *56*(2), 258–266.

20. Arredondo, V.; Hiew, S. C.; Gutman, E. S.; Premachandra, I. D. U. A.; Vranken, D. L. V., Enantioselective palladium-catalyzed carbene insertion into the N–H bonds of aromatic heterocycles. *Angewandte Chemie International Edition* **2017**, *56*(15), 4156–4159.

21. Mizukami, Y.; Song, Z.; Takahashi, T., Halogen exchange reaction of aliphatic fluorine compounds with organic halides as halogen source. *Organic Letters* **2015**, *17*(24), 5942–5945.

Chapter 4: Cobalt-catalyzed C–H Functionalization of benzamides using electron-rich alkynes

4.1 Introduction

C–H activation represents a useful method to accomplish transformations similar to those previously discussed. One of the main limitations of this chemistry is the prevalence of palladium and rhodium catalysts, both of which are low in abundance and high in cost. For this reason, the utilization of cobalt as a catalyst has been extensively studied. The earliest reported example involved the carbonylation of azobenzene compounds to form 3-indazolines (**Figure 4.1**).[1]

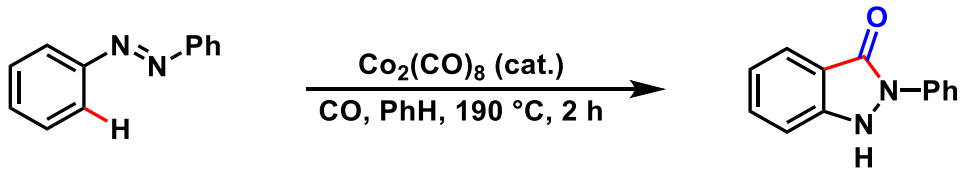

Figure 4.1 The first reported cobalt C–H activation

Similar to the rhodium and palladium catalyzed system, this chemistry works well for alkylation chemistry, adding in to alkenes and alkynes in a Heck type fashion. This has been demonstrated to work for a variety of directing groups, including azos, pyridines, and ketimines, as well as the insertion into C–H bonds on a multitude of heterocyclic starting materials.[2] When α,β-unsaturated imines are implemented, an annulation occurs similar to what was observed with rhodium (**Figure 1.31**), which can be used for the synthesis of highly substituted pyridines.[3]

Interestingly, when lower-valent cobalt systems are used, the traditional selectivity of the migratory insertion can be modulated, allowing for the formation of different regioisomeric products based on the ligand that is utilized (**Figure 4.2**).[4] When a chiral ligand is utilized, this transformation can be performed asymmetrically with good to moderate ee (58–86%).[5]

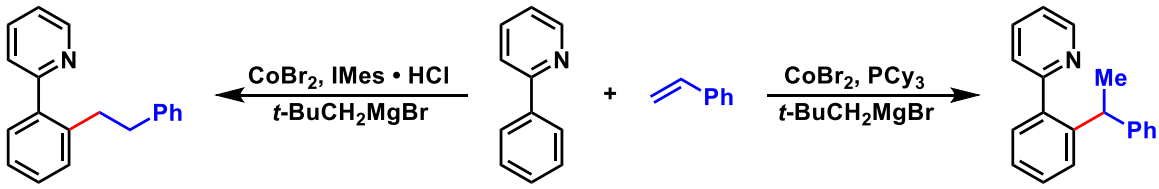

Figure 4.2 Ligand-induced regioselective C–H activation

In addition to standard alkenes, the addition of arenes to aziridines and aldimines to generate amine products has been reported.[6–7] When an aryl halide or pseudohalide is utilized, the reaction resembles a traditional cross-coupling, replacing the migratory insertion step with an oxidative addition/reductive elimination sequence to give the aryl–aryl coupling product, and is promoted by a variety of directing groups.[8–9]

The expansion of reactivity with cobalt is not limited to changes in regioselectivity. When *t*-BuONO is employed, the nitration of indoles was accomplished in a radical fashion (**Figure 4.3**).[10] While the utilization of other common C–H activation catalysts was employed, only cobalt was able to furnish the desired product in synthetically useful yields. This reaction has the added benefit of using a directing group that can be easily removed.

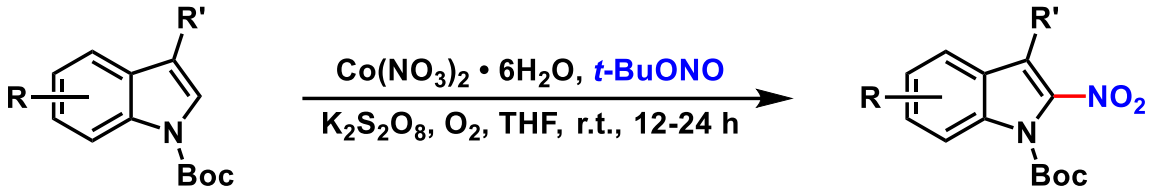

Figure 4.3 Site-selective nitration of indoles

One key transformation possible using cobalt C–H functionalization is the annulation of arenes with nitrogen-containing directing groups to synthesize isoquinolines. These transformations follow a similar pathway to the method for pyridine synthesis discussed in (**Chapter 1**, **Figure 1.29**), employing an alkyne to construct the pyridine component of the isoquinoline. Interestingly, when cobalt was utilized (**Figure 4.4**), a high degree of site-selectivity not seen with rhodium was observed.[11] This is attributed to the smaller ionic radius of cobalt causing more steric hinderance, which allows the cobalt to differentiate between the abstractable hydrogens more effectively than rhodium.

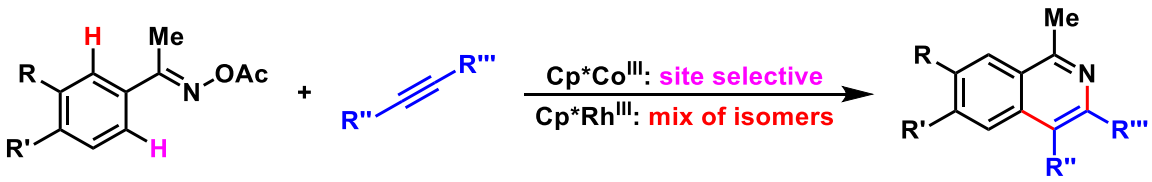

Figure 4.4 Cobalt-catalyzed site-selective isoquinoline synthesis

Of all the final products that can be targeted with cobalt C–H activation chemistry, the most relevant to the work described in the following chapter is the synthesis of isoquinolones. The earliest example (**Figure 4.5**) used a pyridine-*N*-oxide directing group, generating an equivalent of water in the process.[12] The *N*-oxide directing group has the benefit of being easily removed via treatment with alkoxide bases.

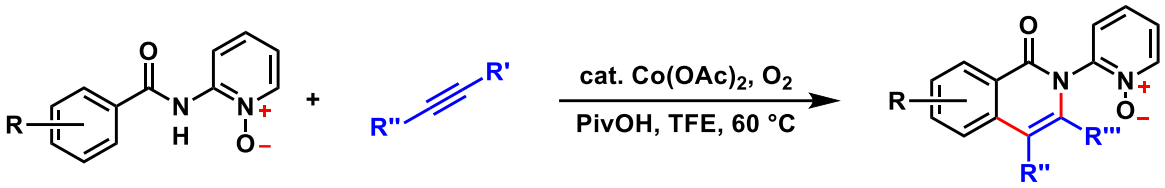

Figure 4.5 Pyridine-*N*-oxide synthesis of isoquinolones

This reaction also works well when alkenes[13] and allenes[14] are employed, generating the dihydroisoquinolone product. When the allene is used, treatment with base yields isoquinolone **109**. By tailoring the conditions and additives, product selectivity can be controlled, with potassium acetate favoring the isoquinolone **110** (**Figure 4.6**).

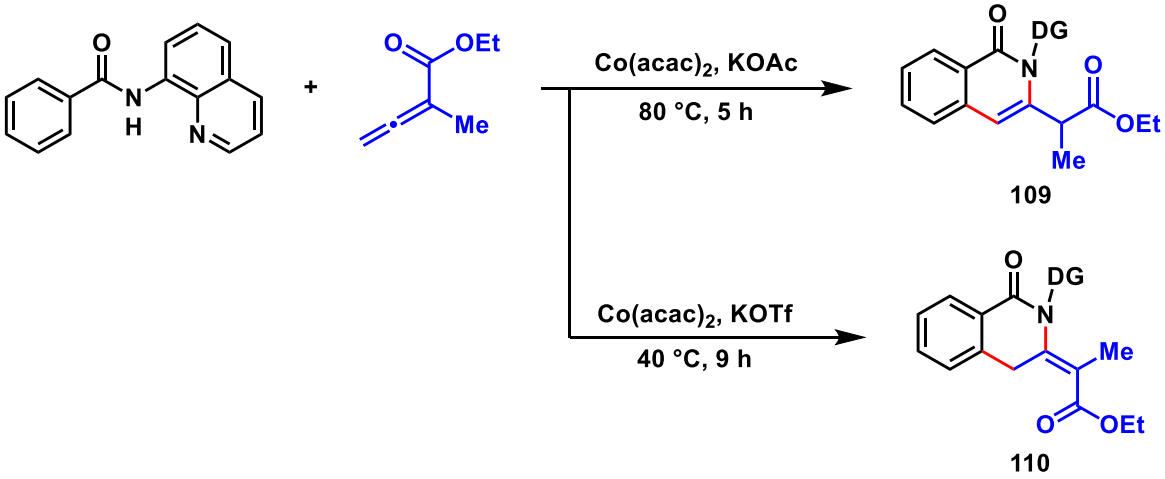

Figure 4.6 Effect of additives on observed tautomer

One of the main limitations of this chemistry is the minimal examples utilizing electron-rich alkenes.[15–16] Recently, our lab developed a method (**Figure 4.7**) using silyl enol ethers as a coupling partner.[17] The one thing all these methods have in common is the need to utilize a rhodium catalyst. In the following chapter work toward the utilization of cobalt for a C–H activation with an electron-rich alkyne will be described.

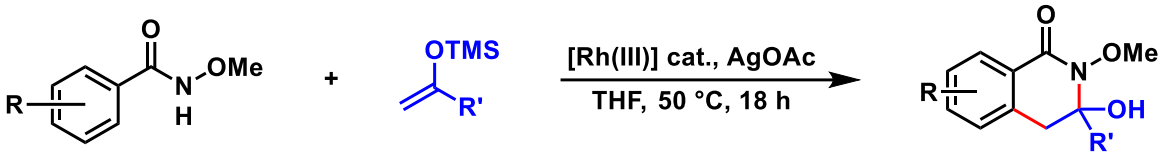

Figure 4.7 α-Arylation of silyl enol ethers using C–H activation

4.2 Results

The results that will be discussed in this chapter started as an effort to see if we could apply our conditions for silyl enol ethers to electron-rich alkynes, settling on ynamides as the substrates. Through minor modification of the reaction conditions, this did indeed prove to be possible, though the reliance on rhodium to catalyze the reaction presented a challenge on a sustainability front. For this reason, we turned our attention to the utilization of cobalt. Unlike with rhodium, this reaction functioned better when the silver and acetate sources are added separately. Under Cp*Co(III) catalysis with $AgSbF_6$ and CsOAc additives, a new regioisomer, that does not form under rhodium catalysis, was isolated.

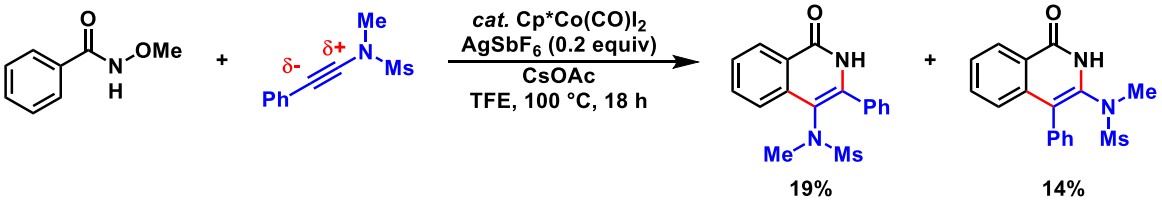

Figure 4.8 Distribution of observed products for cobalt-catalysis
Yields reported are isolated yields

This unexpected regioisomer is interesting from both steric and electronic perspectives. The traditional mechanism for transformations of this type involves a migratory insertion step, and the unexpected regioisomer would involve an unusual migratory insertion into

the electron-rich end of the alkyne. With this information in hand, we began swapping the additives to see if the selectivity could be pushed to exclusively form the non-traditional regioisomer (**Table 4.1**). Exploration of silver counter ion found that perchlorate, nitrate, and carbonate gave the best results. Sodium, potassium, and rubidium cations for the acetate were also tested, and it was found that rubidium gave the best overall yield, though the expected regioisomer dominated the mixtures.

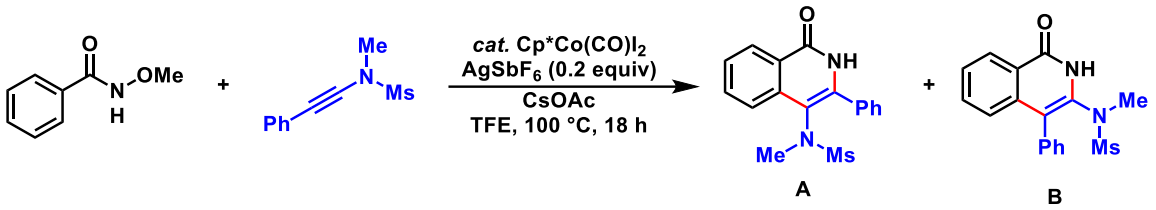

Table 4.1 Effect of additive on yield and selectivity

Entry	Silver Source	Acetate Source	Product A	Product B
1	$AgSbF_6$	CsOAc	19	14
2	$AgClO_4$	CsOAc	31	21
3	$AgNO_3$	CsOAc	35	23
4	Ag_2CO_3	CsOAc	39	27
5	$AgClO_4$	NaOAc	46	38
6	$AgClO_4$	KOAc	36	27
7	$AgClO_4$	RbOAc	50	35

Yields are based on NMR analysis with 1,3,5-trimethoxybenzene as an internal standard

One hypothesis as to why this new product is informed by the site-selectivity of the cobalt annulation chemistry that was discussed above. In that reaction, the change is attributed to the smaller atomic radius of cobalt introducing a steric effect that does not occur with rhodium. For this reason, we questioned whether reduction of the amount of steric hindrance generated from the cyclopentadiene ligand would affect the selectivity of this reaction. Fortunately, Kanai and coworkers reported a method that allows for the formation of cobalt complexes directly from unactivated cyclopentadiene.[18] In order to do

so, we sought to build a library of cyclopentadiene derivatives. Our first attempt began with a method reported by the Whittaker group starting from 2-methyl-5-acetylfuran (**Figure 4.9**).[19] From that starting material, a Wolff-Kishner reduction yielded 2-ethyl-5-methylfuran, which can be hydrolyzed to diketone **111**. Subsequent aldol condensation produced cyclopentenone **112**, which was primed for a Grignard reaction followed by elimination to generate 1,2,3-trimethylcyclopentadiene (**113**). Unfortunately, we were unable to observe elimination product due to loss of the in the rotary-evaporation step.

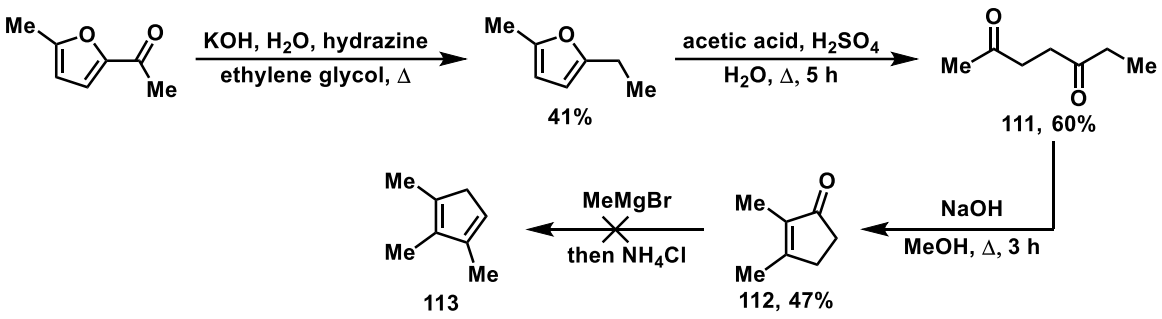

Figure 4.9 Proposed method for synthesis of trimethyl ligand

One of the main problems with the tandem Grignard addition-elimination method is the alcohol intermediate **114**. The highly reactive nature of this compound presents an opportunity for undesirable side reactions. The Harvey group showed that when the alcohol intermediate of the monomethyl cyclopentadiene was treated with aqueous acid (**Figure 4.10**), the major product of the reaction is primarily ether **115**, with no formation of the monomeric cyclopentadiene.[20] To circumvent this problem, a 1:1.3 ratio of aluminum phosphate and magnesium sulfate was used neat to effect dehydration, and when combined with vacuum distillation, yields the diene.

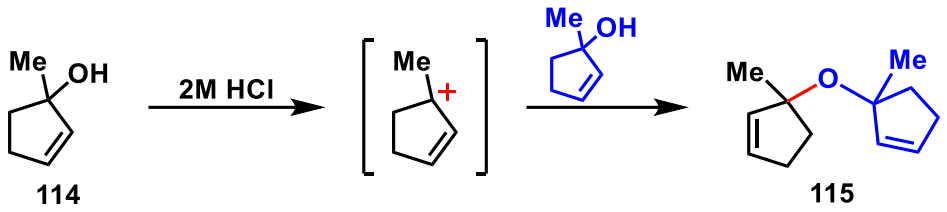

Figure 4.10 Acid catalyzed cyclopentene ether formation

While these studies are underway, we have begun exploring the reactivity of a collection of other ynamides to preliminarily probe where issues may arise in the scoping stage (**Figure 4.11**). When an *ortho*-bromophenyl group was installed (ynamide **116**), or the phenyl group was replaced with a naphthyl group (ynamide **117**), the crude yields were low, indicating that steric hinderance may be a limiting factor in this reaction. The ynamide with thiophene **118** also struggled, so the reaction time was extended, which did not improve the amount of product isolated, but saw change in the regioisomeric ratio in favor of the expected product.

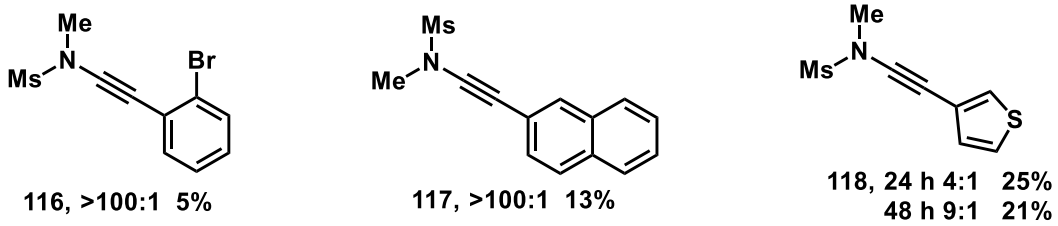

Figure 4.11 Initial probes into ynamide scope
Yields reported are recorded after initial preparatory TLC purification, are not fully pure. Ratios reported as product A: product B.

4.3 Discussion

As this chapter does not represent a completed project, the initial ground work has been laid to allow for publication. The first challenge that needs to be tackled is the testing

of new ligands on cobalt and seeing how they affect yield and selectivity. The buildup of sufficient alcohol starting material **114** to test the aluminum/magnesium dehydration conditions will be the priority. This coupling reaction was already tested with indene as the ligand, though the complex decomposed before it could be fully characterized. Before the decomposition, the product was tested in the C–H activation reaction, and it failed to produce either of the isoquinolone products, which may be due to the change in electronics caused by the benzannulation. In the meantime, all the benzamides and ynamides that will be used in the final substrate scope have been synthesized, meaning that the scoping process should proceed rapidly once the ideal conditions have been identified.

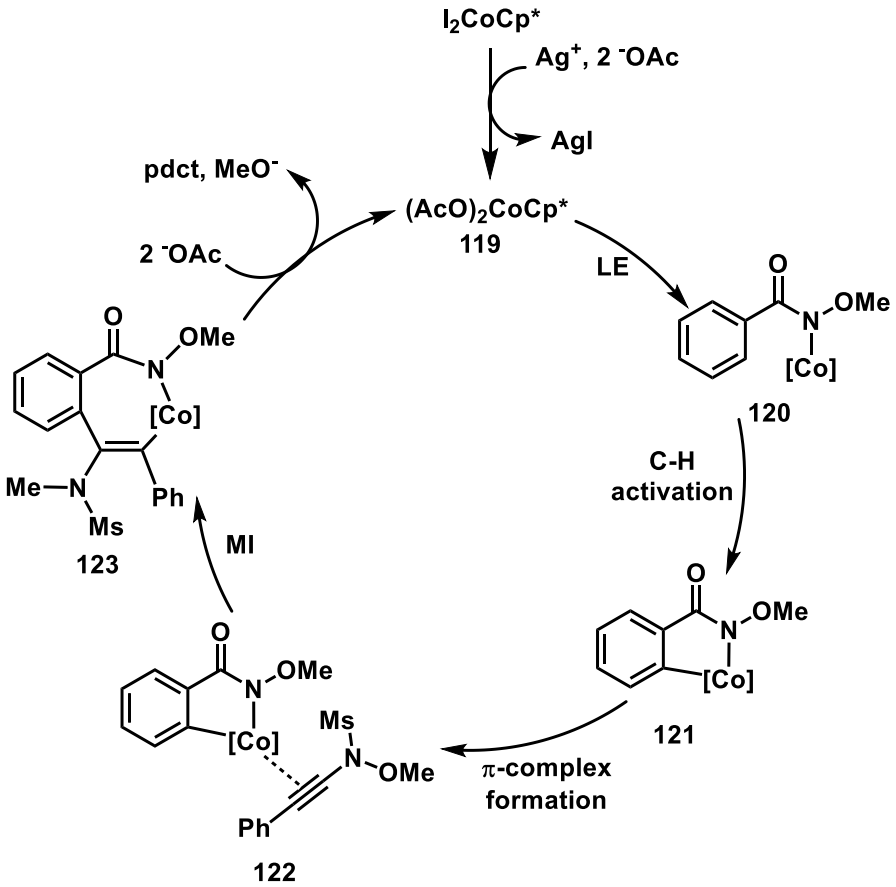

Figure 4.12 Proposed catalytic cycle

While we have not performed any mechanistic studies for this reaction, we have a theory on how it is proceeding (**Figure 4.12**). To begin, the precatalyst is converted into the active catalyst **119** in the presence of CsOAc. The silver sequesters the ejected halides to drive the equilibrium to the active catalyst. The cobalt complex then ligates the benzamide substrate, with the resultant complex **120** primed for C–H activation, giving five–membered cobaltacycle **121**. Following the formation of π-complex **122**, migratory insertion into the ynamide gives seven-membered cobaltacycle **123**, which then undergoes a concerted reductive elimination/*N–O* cleavage to generate the product, while turning over the Co(III) catalyst.

4.4 Materials and methods

4.4.1 *Solvents and reagents*

Commercial reagents were purchased from MilliporeSigma, Acros Organics, Chem-Impex, TCI, Oakwood, and Alfa Aesar, and used without additional purification. Solvents were purchased from Fisher Scientific, Acros Organics, Alfa Aesar, and MilliporeSigma. Tetrahydrofuran (THF), diethyl ether (Et_2O), acetonitrile (MeCN), dichloromethane (CH_2Cl_2), benzene, 1,4-dioxane, and triethylamine (Et_3N) were sparged with argon and dried by passing through alumina columns using argon in a Glass Contour (Pure Process Technology) solvent purification system. Dimethylformamide (DMF), dimethyl sulfoxide (DMSO), and dichloroethane (DCE) were purchased in Sure/Seal or AcroSeal bottling and dispensed under N_2. Deuterated solvents were obtained from Cambridge Isotope Laboratories, Inc. or MilliporeSigma.

4.4.2 *Analytical instrumentation*

Proton nuclear magnetic resonance (^{1}H NMR) spectra, carbon nuclear magnetic resonance (^{13}C NMR) spectra and fluorine nuclear magnetic resonance (^{19}F NMR) spectra were recorded on Bruker Avance NEO 400 MHz (not ^{1}H decoupled) or Bruker Avance 600 MHz spectrometers (^{1}H decoupled). Chemical shifts (δ) are reported in ppm relative to the residual solvent signal (δ 7.26 for ^{1}H NMR, δ 77.16 for ^{13}C NMR in $CDCl_3$).[1] Data for ^{1}H NMR spectroscopy are reported as follows: chemical shift (δ ppm), multiplicity (s = singlet, d = doublet, t = triplet, q = quartet, m = multiplet, br = broad, dd = doublet of doublets, dt = doublet of triplets), coupling constant (Hz), integration. Data for ^{13}C and ^{19}F NMR spectroscopy are reported in terms of chemical shift (δ ppm).

4.4.3 *Reaction setup, monitoring, and purification*

All reagents, including the solvent were added in the glovebox. Reaction progresses were monitored using thin-layer chromatography (TLC) on EMD Silica Gel 60 F254 or Macherey–Nagel SIL HD (60 Å mean pore size, 0.75 mL/g specific pore volume, 5–17 μm particle size, with fluorescent indicator) silica gel plates. Visualization of the developed plates was performed under UV light (254 nm). Purification and isolation of products were performed via silica gel chromatography (both column and preparative thin-layer chromatography). Organic solutions were concentrated under reduced pressure on IKA® temperature-controlled rotary evaporator equipped with an ethylene glycol/water condenser.

4.4.4 *General procedure*

In a 1–dram vial with a stirring bar, Cp*Co(CO)I_2 (4 mg, 0.01 mmol, 0.1 equiv), rubidium acetate (15 mg, 0.1 mmol, 1 equiv), silver perchlorate (4 mg, 0.02 mmol, 0.2 equiv), benzamide (15 mg, 0.1 mmol, 1 equiv), and ynamide (25 mg, 0.1 mmol, 1 equiv) were suspended in TFE (1 mL, 0.1 M) in the glovebox. The solution was capped, removed from the box, and heated at 100 °C for 18 h on a heating block. The reaction mixture was cooled to rt and directly filtered through silica with DCM and acetone as eluents. The resultant solution was concentrated *in vacuo* before purification via column chromatography with ethyl acetate/hexanes gradient (25→75% EtOAc) to yield the product as a mixture of regioisomers. The regioisomers were separated using preparatory TLC, eluting with methanol/DCM (3% MeOH).

4.4.5 *Ynamide synthesis*

4.4.5.a *Terminal alkyne halogenation*

A flame-dried round bottomed flask was charged with silver(I) nitrate (0.2 equiv), *N*–bromosuccinimide (1.2 equiv) and the corresponding alkyne (1 equiv). The mixture was suspended in acetone (0.33 M). The solution was wrapped in foil and allowed to stir at rt for 2–4 h after which it was vacuum-filtered. Water (10 mL) was added and the solution was extracted with hexanes (3 x 15 mL). The combined organic extract was washed with 10% HCl (1 x 15 mL), followed by brine (1 x 15 mL), and dried over anhydrous Na_2SO_4. The solution was concentrated *in vacuo* and purified via silica gel chromatography to obtain the bromination product.

4.4.5.b *Copper-catalyzed cross-coupling*

To a flame-dried round-bottomed flask was added copper(II) sulfate (0.1 equiv), 1,10–phenanthroline (0.2 equiv), K_2CO_3 (3 equiv), and *N*-methylmethanesulfonamide (1.2 equiv). The mixture was suspended in anhydrous toluene (0.93 M) and the alkynyl halide was added dropwise. The flask was flushed with nitrogen and allowed to stir at 80 °C overnight. The reaction was cooled to rt and filtered through celite, washing with DCM before concentration *in vacuo*. Purification by silica gel chromatography yielded the ynamide.

4.4.6 *Compound characterization*

3–(Bromoethynyl)thiophene

Prepared via the halogenation procedure with 3-(ethynyl)thiophene (0.20 mL, 2.0 mmol). Purification by flash chromatography (eluting with hexanes) afforded the product (0.253 g, 68%) as a yellow oil. R_f: 0.53 (hexanes). ^{1}H NMR ($CDCl_3$, 600 MHz): δ 7.48 (m, 1H), 7.26 (m, 1H), 7.12–7.11 (m, 1H); The spectral data is consistent with those previously reported in the literature.[21]

2–(Bromoethynyl)naphthalene

Prepared via the halogenation procedure with 2-(ethynyl)naphthalene (0.304 g, 2.0 mmol). Purification by flash chromatography (eluting with hexanes) afforded the product (0.205 g, 67%) as a yellow oil. R_f: 0.51 (hexanes). ^{1}H NMR ($CDCl_3$, 600 MHz): δ 7.99 (s, 1H), 7.81–7.77 (m, 3H), 7.50–7.48 (m, 3H); The spectral data is consistent with those previously reported in the literature.[22]

1-Bromohept-1-yne

Prepared via the halogenation procedure with 1-heptyne (0.26 mL, 2.0 mmol). Purification by flash chromatography (eluting with hexanes) afforded the product (0.213 g, 61%) as a yellow oil. R_f: 0.90 (hexanes). ^{1}H NMR ($CDCl_3$, 600 MHz): δ 2.20 (t, J = 6.6 Hz, 2H), 1.55–1.50 (m, 2 H), 1.36–1.31 (m, 4H), 0.90 (t, J = 7.2 Hz, 3H); The spectral data is consistent with those previously reported in the literature.[23]

***N*-methyl-*N*-(thiophen-3-ylethynyl)methanesulfonamide**

Prepared via the cross–coupling procedure with 3-(bromoethynyl)thiophene (0.253 g, 1.35 mmol). Purification by flash chromatography (0–40% EA/hexanes) afforded the product (0.223 g, 77%) as an orange oil. R_f: 0.23 (20% EA/hexanes). ^{1}H NMR ($CDCl_3$, 600 MHz): δ 7.44 (m, 1H), 7.26 (m, 1H), 7.10–7.09 (m, 1H), 3.29 (s, 3H), 3.12 (s, 3H); The spectral data is consistent with those previously reported in the literature.[24]

***N*-methyl-*N*-(naphthalen-2-ylethynyl)methanesulfonamide**

Prepared via the cross-coupling procedure with 2-(bromoethynyl)naphthalene (0.205 g, 0.89 mmol). Purification by flash chromatography (0–40%) afforded the product (0.2002 g, 87%) as an orange solid. R_f: 0.30 (20% EA/hexanes). ^{1}H NMR ($CDCl_3$, 600 MHz): δ 7.93 (s, 1H), 7.81–7.76 (m, 3H), 7.49–7.44 (m, 3H), 3.35 (s, 3H), 3.17 (s, 3H); The spectral data is consistent with those previously reported in the literature.[25]

***N*-(hept-1-yn-1-yl)-*N*-methylmethanesulfonamide**

Prepared via the cross–coupling procedure with 1-bromohept-1-yne (0.113 g, 0.65 mmol). Purification by flash chromatography (0–40%) afforded the product (0.046 g, 32%) as a yellow oil. R_f: 0.52 (20% EA/hexanes). ^{1}H NMR ($CDCl_3$, 600 MHz): δ 3.16 (s, 3H), 3.03

(s, 3H), 2.27 (t, J = 6.6 Hz, 2H), 1.51 (t, J = 6.6 Hz, 2H), 1.36-1.31 (m, 4H), 0.90 (t, J = 7.2 Hz); The spectral data is consistent with those previously reported in the literature.[26]

4.5 References

1. Murahashi, S., Synthesis of phthalimidines from Schiff bases and carbon monoxide. *Journal of the American Chemical Society* **1955**, *77*(23), 6403–6404.

2. Moselage, M.; Li, J.; Ackermann, L., Cobalt-catalyzed C–H activation. *ACS Catalysis* **2016**, *6*(2), 498–525.

3. Yamakawa, T.; Yoshikai, N., Annulation of α,β–unsaturated iminies and alkynes via cobalt-catalyzed olefinic C–H activation. *Organic Letters* **2013**, *15*(1), 196–199.

4. Gao, K.; Yoshikai, N., Low-valent cobalt catalysis: new opportunities for C–H functionalization. *Accounts of Chemical Research* **2014**, *47*(4), 1208–1219.

5. Lee, P.; Yoshikai, N., Cobalt-catalyzed enantioselective directed C–H alkylation of indole and styrenes. *Organic Letters* **2014**, *17*(1), 22–25.

6. Gao, K.; Paira, R.; Yoshikai, N., Cobalt-catalyzed *ortho*-C–H alkylation of 2-arylpiridines *via* ring-opening of aziridines. *Advanced Synthesis & Catalysis* **2014**, *356*(7), 1486–1490.

7. Gao, K.; Yoshikai, N., Cobalt-catalyzed arylation of aldimines *via* directed C–H bond functionalization: addition of 2-arylpiridines and self-coupling of aromatic aldimines. *Chemical Communication* **2012**, *48*, 4305–4307.

8. Li, B.; Wu, Z.; Gu, Y.; Sun, C.; Wang, B.; Shi, Z., Direct cross-coupling of C–H bonds with Grignard reagents through cobalt catalysis. *Angewandte Chemie International Edition* **2010**, *50*(5), 1109–1113.

9. Li, J.; Ackermann, L., Cobalt-catalyzed C–H arylations with weakly-coordinating amides and tetrazoles: expedient route to angiotensin-II-receptor blockers. *Chemistry a European Journal* **2015**, *21*(15), 5718–5722.

10. Saxena, P.; Kapur, M., Cobalt-catalyzed C–H nitration of indoles by employing a removable directing group. *Chemistry and Asian Journal* **2018**, *13*(7), 861–870.

11. Sun, B.; Yoshino, T.; Kanai, M.; Matsunaga, S., Cp^*Co^{III} catalyzed site-selective C–H activation of unsymmetrical *O*-acyl oximes: synthesis of multisubstituted isoquinolines from terminal and internal alkynes. *Angewandte Chemie International Edition* **2015**, *54*(44), 12968–12972.

12. Mei, R.; Wang, H.; Warratz, S.; Macgregor, S. A.; Ackermann, L., Cobalt-catalyzed oxidase C–/N–H alkyne annulation: mechanistic insights and access to anticancer agents. *Chemistry a European Journal* **2016**, *22*(20), 6759–6763.

13. Grigorjeva, L.; Daugulis, O., Cobalt-catalyzed, aminoquinoline-directed coupling of sp^2 C–H bonds with alkenes. *Organic Letters* **2014**, *16*(17), 4684–4687.

14. Li, T.; Zhang, C.; Tan, Y.; Pan, W.; Rao, Y., Cobalt-catalyzed C–H activation and regioselective intermolecular annulation with allenes. *Organic Chemistry Frontiers* **2016**, *4*, 204–209.

15. Guimond, N.; Gorelsky, S. I.; Fagnou, K., Rhodium(III)-catalyzed heterocycle synthesis using an internal oxidant: improved reactivity and mechanistic studies. *Journal of the American Chemical Society* **2011**, *133*(16), 6449–6457.

16. Webb, N. J.; Marsden, S. P.; Raw, S. A., Rhodium (III)-catalyzed C–H activation/annulation with vinyl esters as an acetylene equivalent. *Organic Letters* **2014**, *16*(18), 4718–4721.

17. Kou, X.; Kou, K. G. M., α-Arylation of silyl enol ethers via rhodium (III)-catalyzed C–H functionalization. *ACS Catalysis* **2020**, *10*(5), 3103–3109.

18. Sun, B.; Yoshino, T.; Matsunaga, S.; Kanai, M., Air-stable carbonyl(pentamethyl cyclopentadienyl)cobalt diiodide complex as a precursor for cationic(pentamethyl cyclopentadienyl)cobalt(III) catalysis: application for directed C–2 selective C–H amidation of indoles. *Advanced Synthesis & Catalysis* **2014**, *356*(7), 1491–1495.

19. Baig, M. A.; Banthorpe, D. V.; Derek, V.; Carr, G.; Whittaker, D., Reactions of some cyclic ethers in superacids. *Journal of the Chemical Society, Perkin Transactions II* **1989**, *12*, 1981–1986.

20. Meylemans, H. A.; Quintana, R. L.; Goldsmith, B. R.; Harvey, B. G., Solvent-free conversion of linalool to methylcyclopentadiene dimers: a route to renewable high-density fuels. *Chemistry-Sustainability-Energy-Materials* **2011**, *4*(4), 465–469.

21. Chuchmareva, M.; Strauch, C.; Schröder, S.; Collong, A.; Niggemann, M., Regio-and stereoselective *N*-addition to an open bromo vinyl cation. *Tetrahedron Letters* **2021**, *74*, 153173.

22. Beltran, F.; Miesch, L., Tertiary enamide-triggered S_EAr: domino allylation and enamine-type addition. *Organic Letters* **2019**, *21*(6), 1569–1573.

23. Bhupathiraju, D. K.; Sayeedi, M.; Rizvi, W.; Singh, S.; Batteas, J. D.; Drain, C. M., Practical, high-yield synthesis of thiol-terminated diacetylenes for formation of conductive monolayers. *Tetrahedron Letters* **2018**, *59*(40), 3629–3631.

24. Mukherjee, A.; Dateer, R. B.; Chaudhuri, R.; Bhunia, S.; Karad, S. N.; Liu, R., Gold-catalyzed 1,2-difunctionalizations of aminoalkynes using only *N*- and O- containing oxidants. *Journal of the American Chemical Society* **2011**, *133*(39), 15372–15375.

25. Yoo, H. J.; Youn, S. W., Zn(II)-catalyzed one-pot synthesis of coumarins from ynamides and salicylaldehydes. *Organic Letters* **2019**, *21*(9), 3422–3426.

26. Zhou, S.; Ye, J.; Zheng, X., Copper-catalyzed room-temperature cross-dehydrogenative coupling of secondary amides with terminal alkynes: a chemoselective synthesis of ynamides. *Organic & Biomolecular Chemistry* **2024**, *22*, 1299–1309.